IWARA 2020
VIDEO CONFERENCE

9th International Workshop on
Astronomy and Relativistic Astrophysics
Mexico, 6 - 12 September, 2020

Can gravitation waves prove the existence of the quark-gluon plasma?

MATTHIAS HANAUSKE
FRANKFURT INSTITUTE FOR ADVANCED STUDIES
JOHANN WOLFGANG GOETHE UNIVERSITÄT
INSTITUT FÜR THEORETISCHE PHYSIK
ARBEITSGRUPPE RELATIVISTISCHE ASTROPHYSIK
D-60438 FRANKFURT AM MAIN

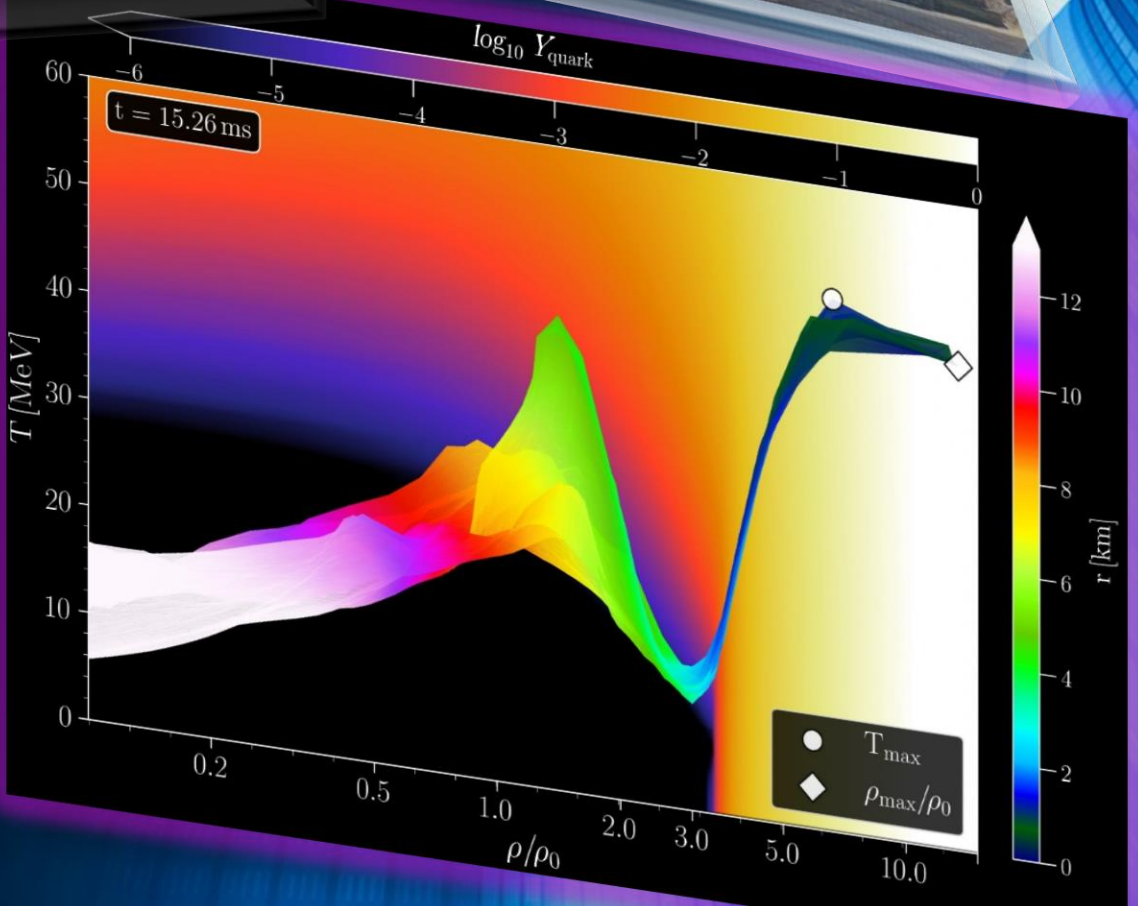

In collaboration with Lukas Weih, Elias R. Most, Jens Papenfort, Luke Bovard, Gloria Montana, Laura Tolos, Jan Steinheimer, Anton Motornenko, Veronica Dexheimer, Horst Stöcker, and Luciano Rezzolla

Can we detect the quark-gluon plasma with gravitational waves?

- Introduction
- Gravitational-wave signatures of the hadron-quark ph
  compact star mergers
  - *Signatures within the late inspiral phase (premerger signals)*
    - Constraining twin stars with GW170817; G Montana, L Tolós, M Han
      99 (10), 103009 (2019)
  - *Signatures within the post-merger phase evolution*
    - **Prompt phase transition scenario**
      Identifying a first-order phase transition in neutron-star mergers through gr
      Bastian, DB Blaschke, K Chatziioannou, JA Clark, JA Clark, T Fischer, M Oerte
      (2019)
    - **Delayed phase transition scenario**
      Postmerger Gravitational-Wave Signatures of Phase Transitions in Binar
      Rezzolla; Physical Review Letters 124 (17), 171103 (2020)
    - **Phase-transition triggered collapse scenario**
      Signatures of quark-hadron phase transitions in general-relativistic neu
      Papenfort, V Dexheimer, M Hanauske, S Schramm, H Stöcker, L. Rezzol ...122 (6), 061101
      (2019)

YES
WE
CAN

The long awaited event GW170817

	Low-spin priors ($\|\chi\| \leq 0.05$)	High-spin priors ($\|\chi\| \leq 0.89$)
Primary mass m_1	1.36–$1.60\ M_\odot$	1.36–$2.26\ M_\odot$
Secondary mass m_2	1.17–$1.36\ M_\odot$	0.86–$1.36\ M_\odot$
Chirp mass $\mathcal{M}$	$1.188^{+0.004}_{-0.002} M_\odot$	$1.188^{+0.004}_{-0.002} M_\odot$
Mass ratio m_2/m_1	0.7–1.0	0.4–1.0
Total mass $m_{\rm tot}$	$2.74^{+0.04}_{-0.01} M_\odot$	$2.82^{+0.47}_{-0.09} M_\odot$
Radiated energy $E_{\rm rad}$	$> 0.025 M_\odot c^2$	$> 0.025 M_\odot c^2$
Luminosity distance $D_{\rm L}$	40^{+8}_{-14} Mpc	40^{+8}_{-14} Mpc
Viewing angle Θ	$\lesssim 55°$	$\lesssim 56°$
Using NGC 4993 location	$\lesssim 28°$	$\lesssim 28°$
Combined dimensionless tidal deformability $\tilde{\Lambda}$	$\lesssim 800$	$\lesssim 700$
Dimensionless tidal deformability $\Lambda(1.4 M_\odot)$	$\lesssim 800$	$\lesssim 1400$

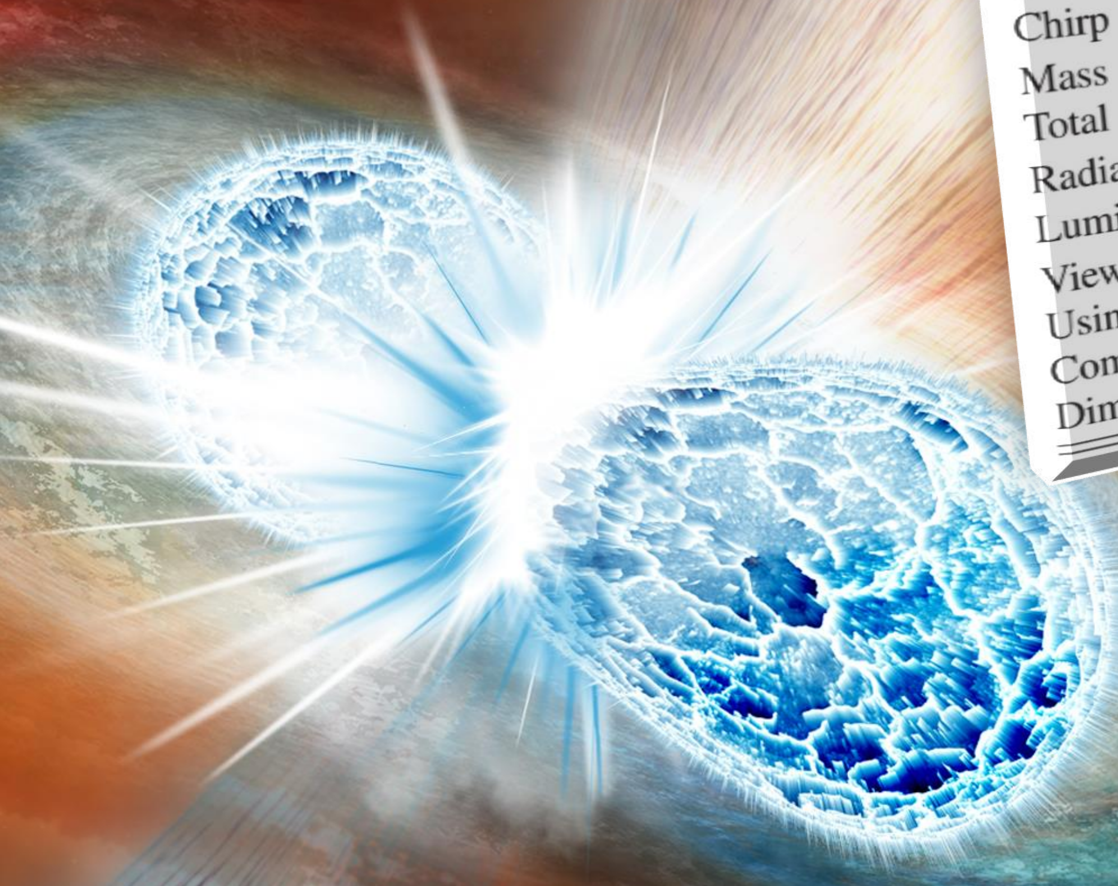

17. August 2017

First detection of a gravitational wave from a binary neutron star merger event!

Gravitational Wave GW170817 and Gamma-Ray Emission GRB170817A

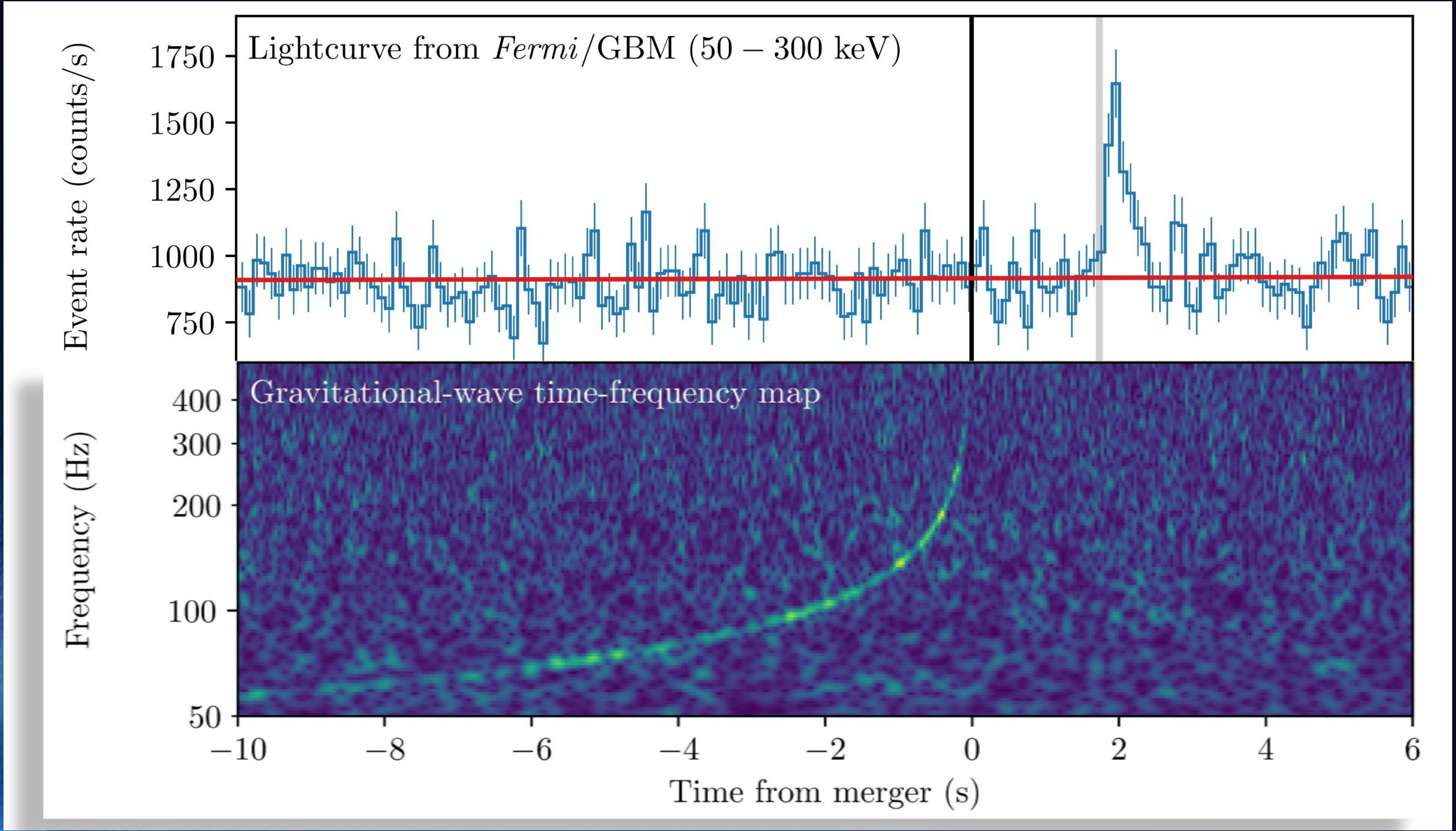

The second event: GW190425

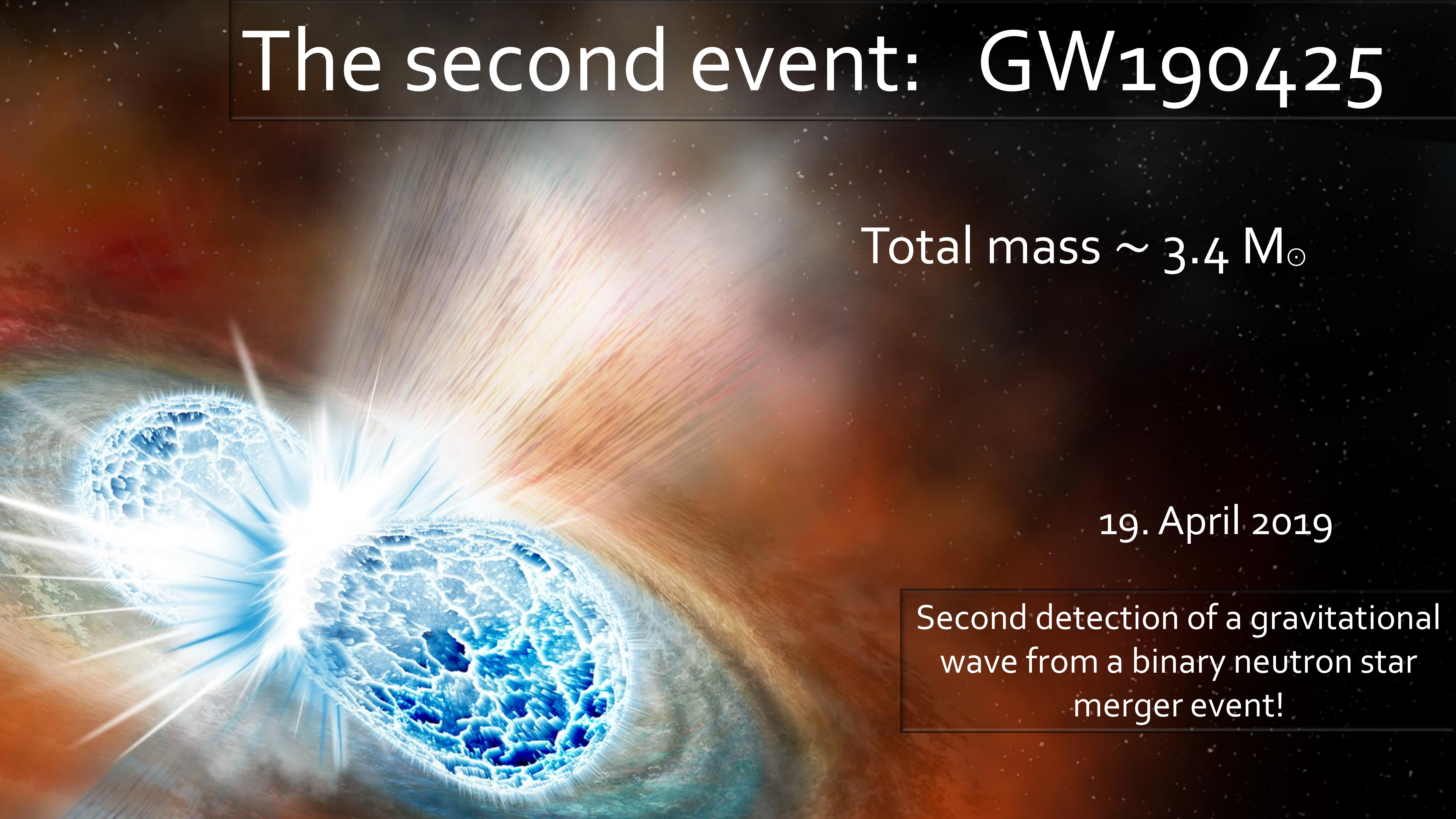

Total mass ~ 3.4 $M_\odot$

19. April 2019

Second detection of a gravitational wave from a binary neutron star merger event!

GW190814 The third event ???

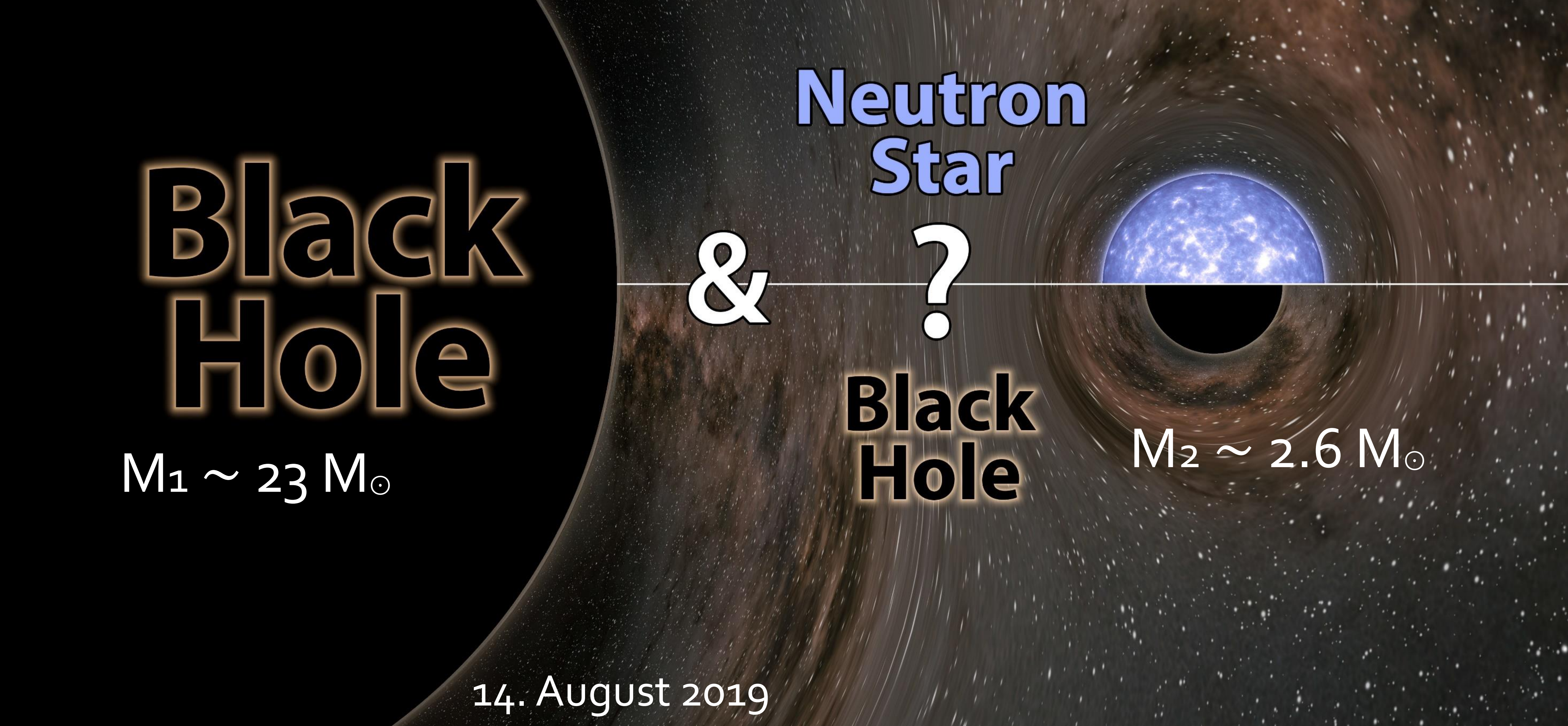

$M_1 \sim 23\ M_\odot$

$M_2 \sim 2.6\ M_\odot$

14. August 2019

Broadbrush picture

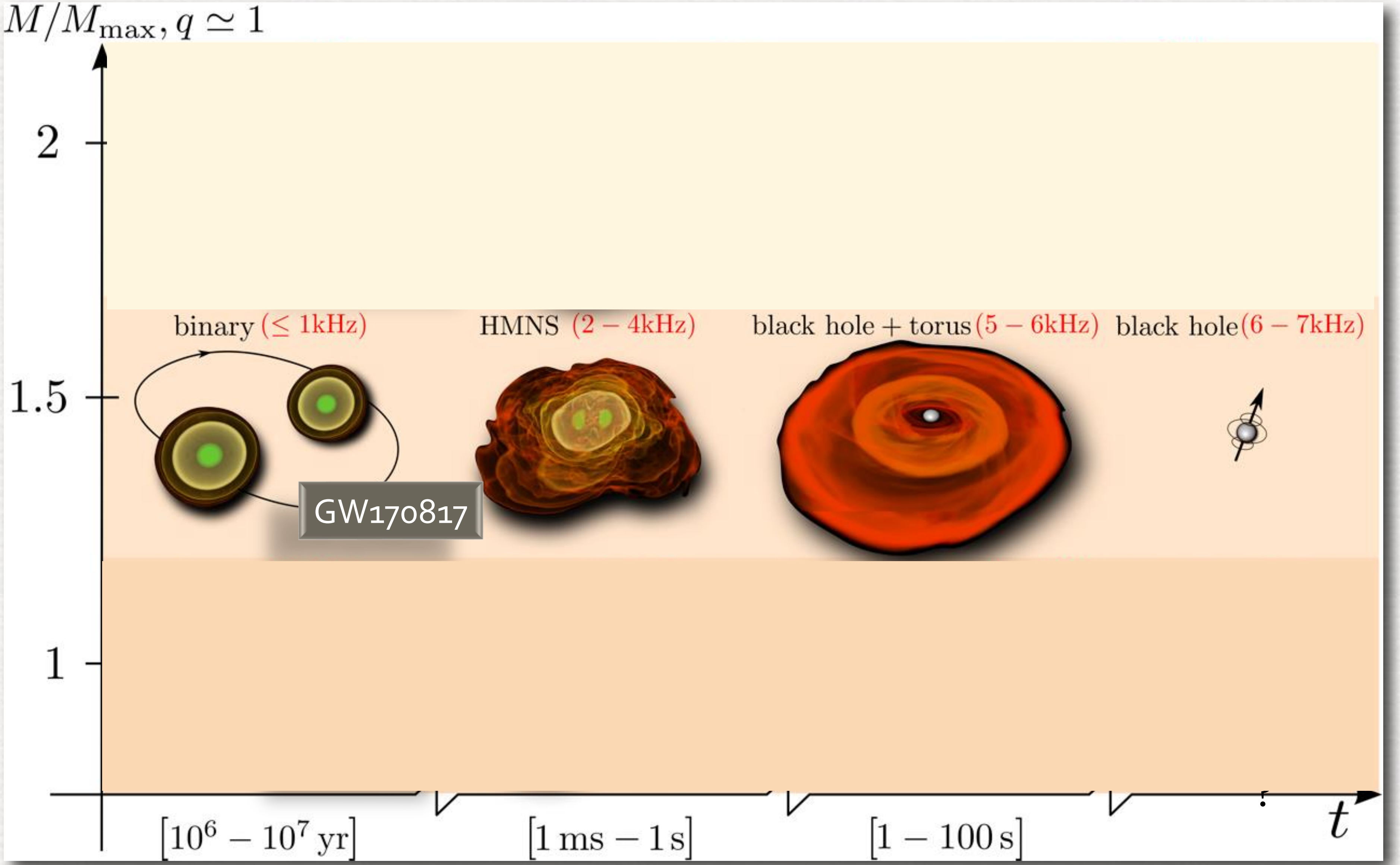

Numerical Relativity and Relativistic Hydrodynamics of Binary Neutron Star Mergers

Einstein's theory of general relativity and the resulting general relativistic conservation laws for energy-momentum in connection with the rest-mass conservation are the theoretical groundings of neutron star binary mergers:

$$R_{\mu\nu} - \frac{1}{2} g_{\mu\nu} R = 8\pi T_{\mu\nu}$$

$$\nabla_\mu (\rho u^\mu) = 0\,, \qquad \nabla_\nu T^{\mu\nu} = 0\,.$$

(3+1) decomposition of spacetime

$$g_{\mu\nu} = \begin{pmatrix} -\alpha^2 + \beta_i \beta^i & \beta_i \\ \beta_i & \gamma_{ij} \end{pmatrix}$$

$$d\tau^2 = \alpha^2(t, x^j) dt^2 \qquad x^i_{t+dt} = x^i_t - \beta^i(t, x^j) dt$$

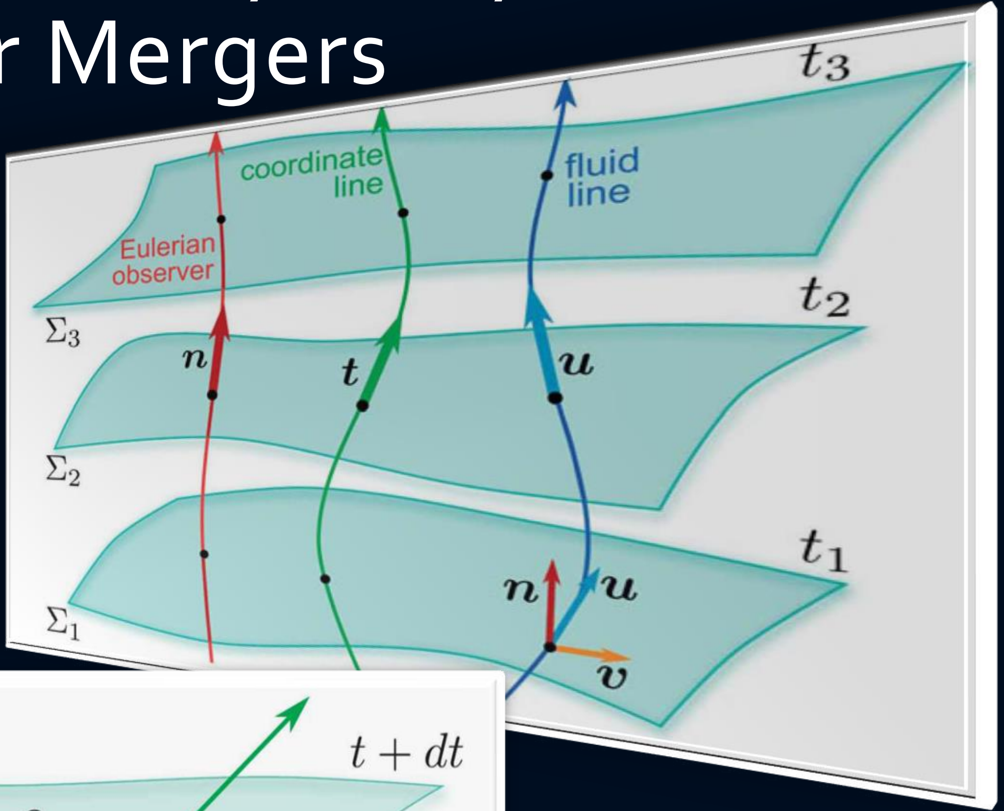

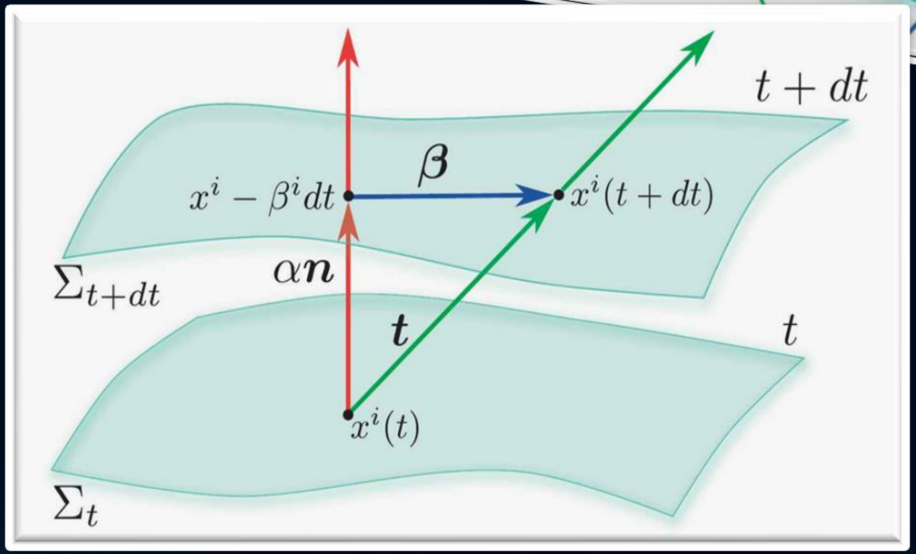

All figures and equations from: Luciano Rezzolla, Olindo Zanotti: Relativistic Hydrodynamics, Oxford Univ. Press, Oxford (2013)

The QCD – Phase Transition and the Interior of a Hybrid Star

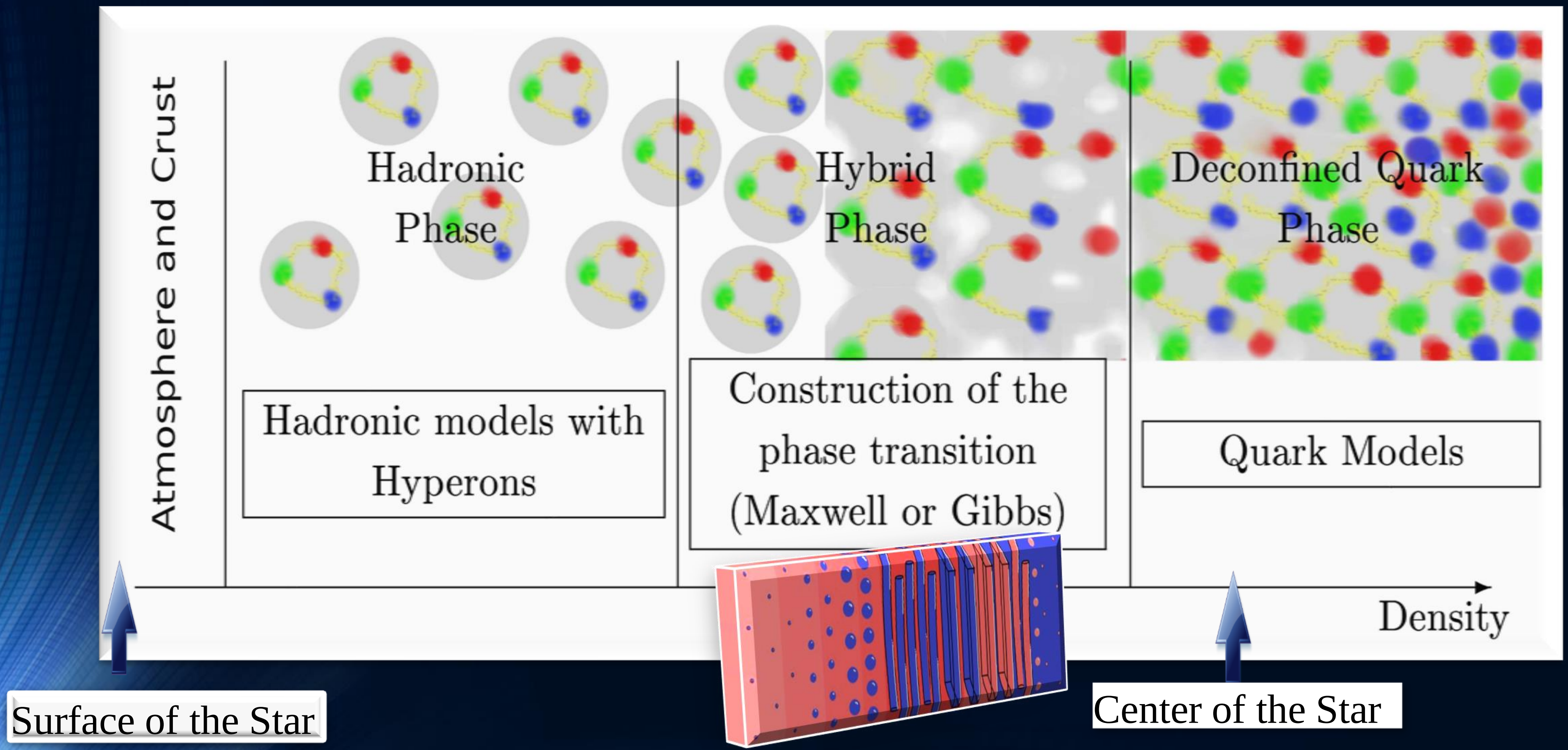

Matthias Hanauske; Doctoral Thesis:
Properties of Compact Stars within QCD-motivated Models; University Library Publication Frankfurt (2004)

Gravitational-wave signatures within the late inspiral phase

Construction of the EOS with a hadron-quark phase transition

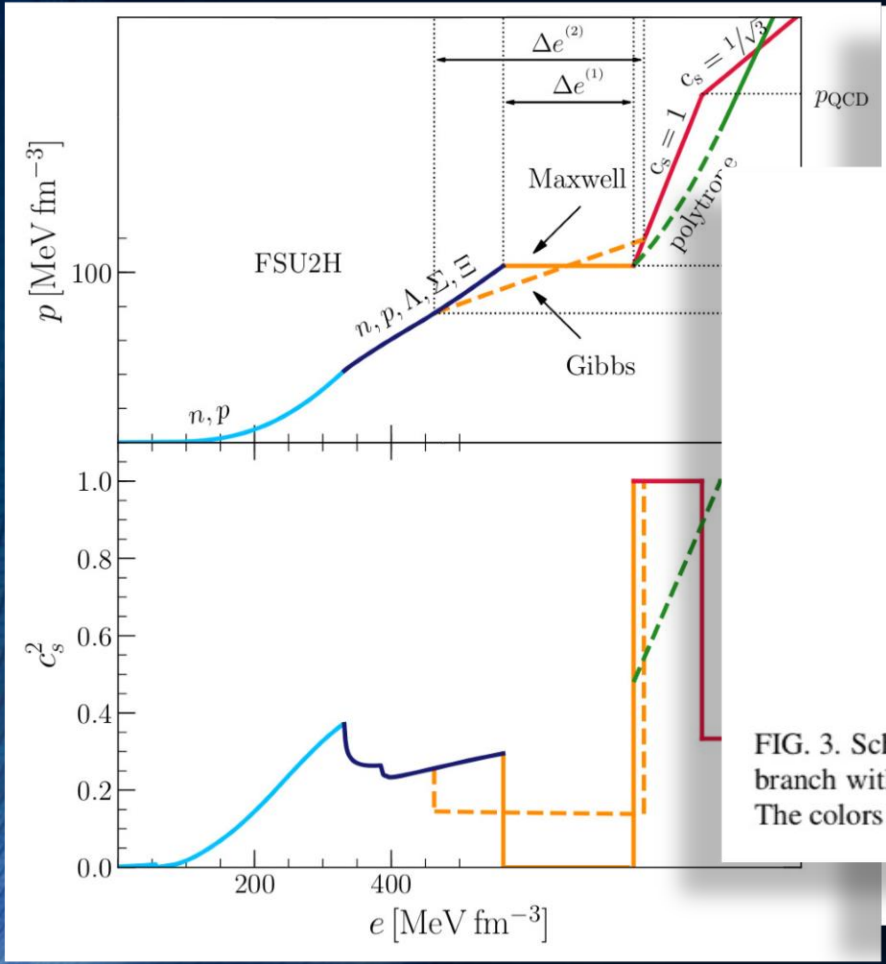

The Mass-Radius relation and the twin star property

Maxwell Construction Gibbs Construction

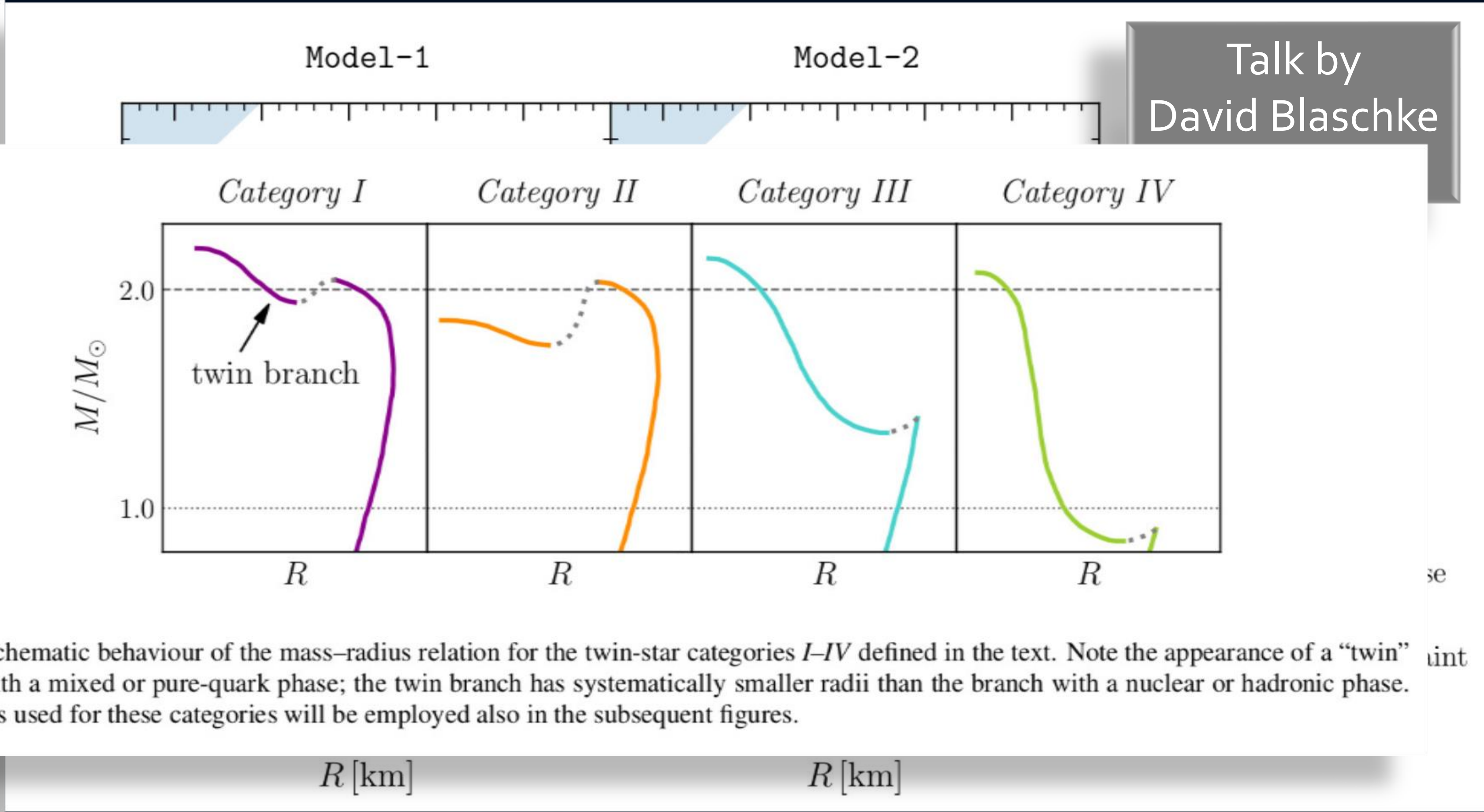

FIG. 3. Schematic behaviour of the mass–radius relation for the twin-star categories *I–IV* defined in the text. Note the appearance of a "twin" branch with a mixed or pure-quark phase; the twin branch has systematically smaller radii than the branch with a nuclear or hadronic phase. The colors used for these categories will be employed also in the subsequent figures.

G. Montana, L.Tolos, M.Hanauske and L.Rezzolla
„Constraining twin stars with GW170817", PRD 99(10), 2019

G. Montana, L.Tolos, M.Hanauske

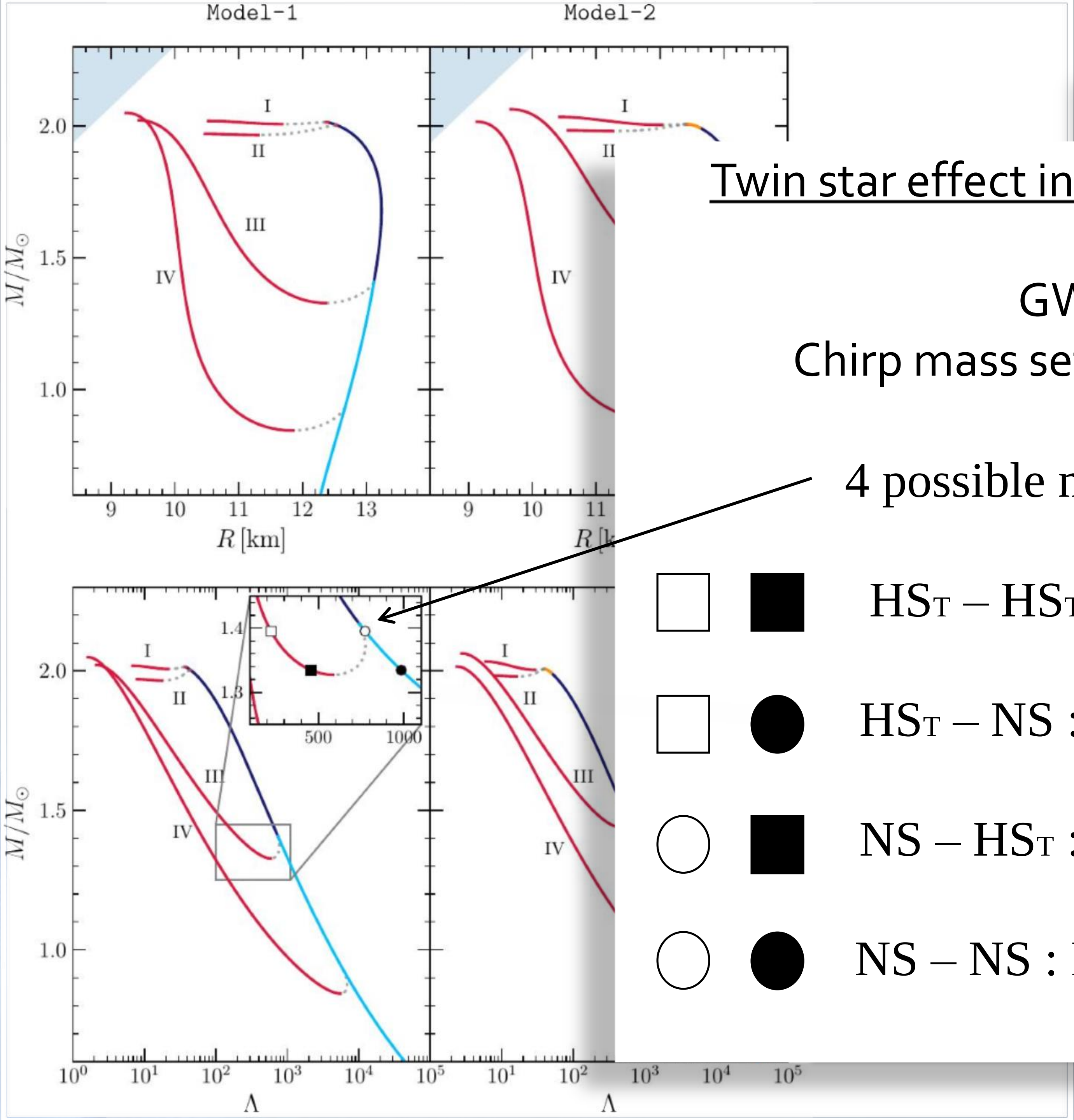

Twin star effect in the tidal deformability

GW170817:
Chirp mass set to $M_{ch} = 1.188\ M_\odot$

4 possible merger scenarios:

- □ ■ $HS_T – HS_T$: Hybrid star – Hybrid Star
- □ ● HS_T – NS : Hybrid star – Neutron Star
- ○ ■ NS – HS_T : Neutron star – Hybrid Star
- ○ ● NS – NS : Neutron star – Neutron Star

tars
9
bility
Λ of a
f its mass

Constraining the hadron-quark phase transition with GW170817

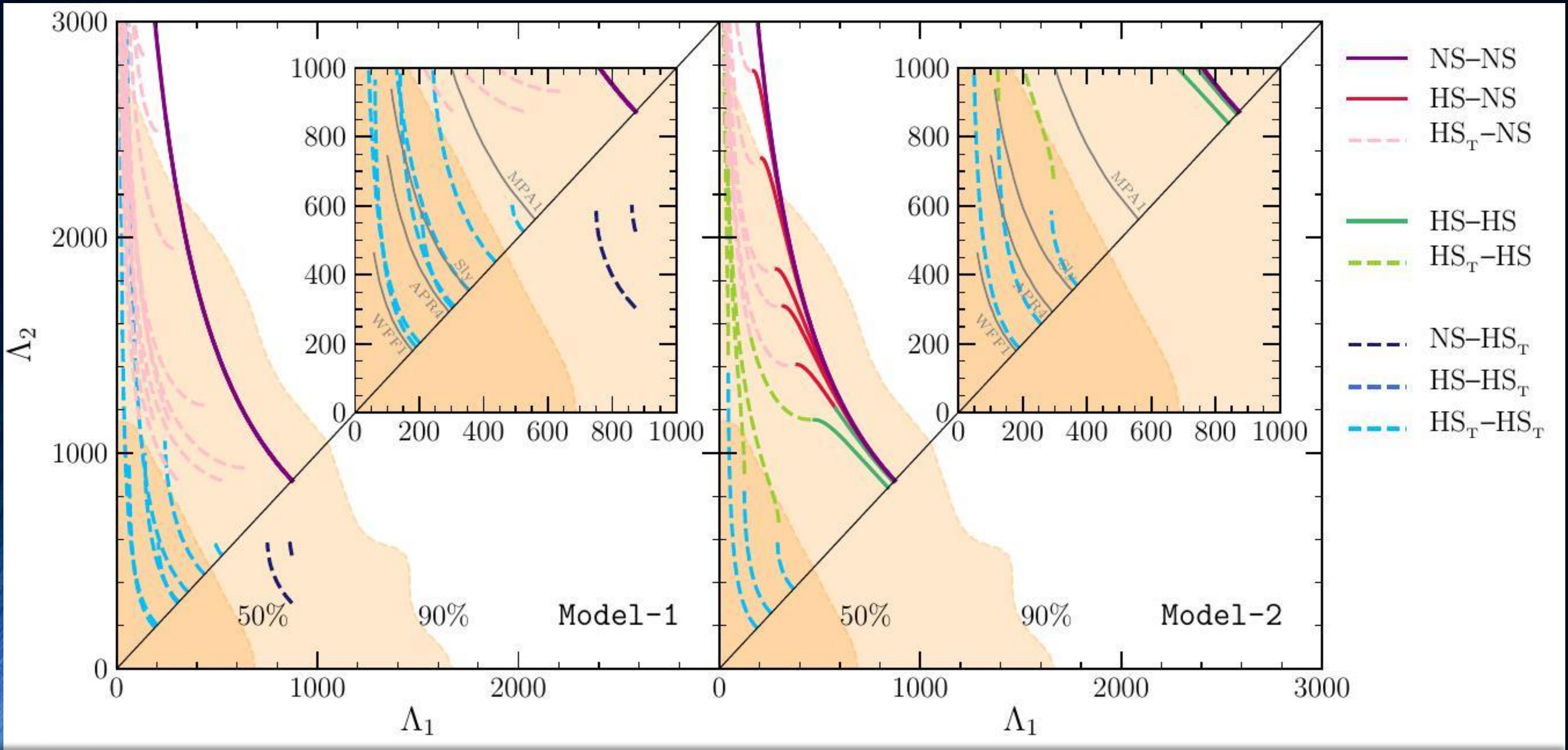

Assuming that the hadronic part of the EOS is given by the FSU2H model, the phase transition takes place already in the inspiral phase -> GW170817 was a hybrid star merger

Pre-merger signatures of the hadron-quark phase transition

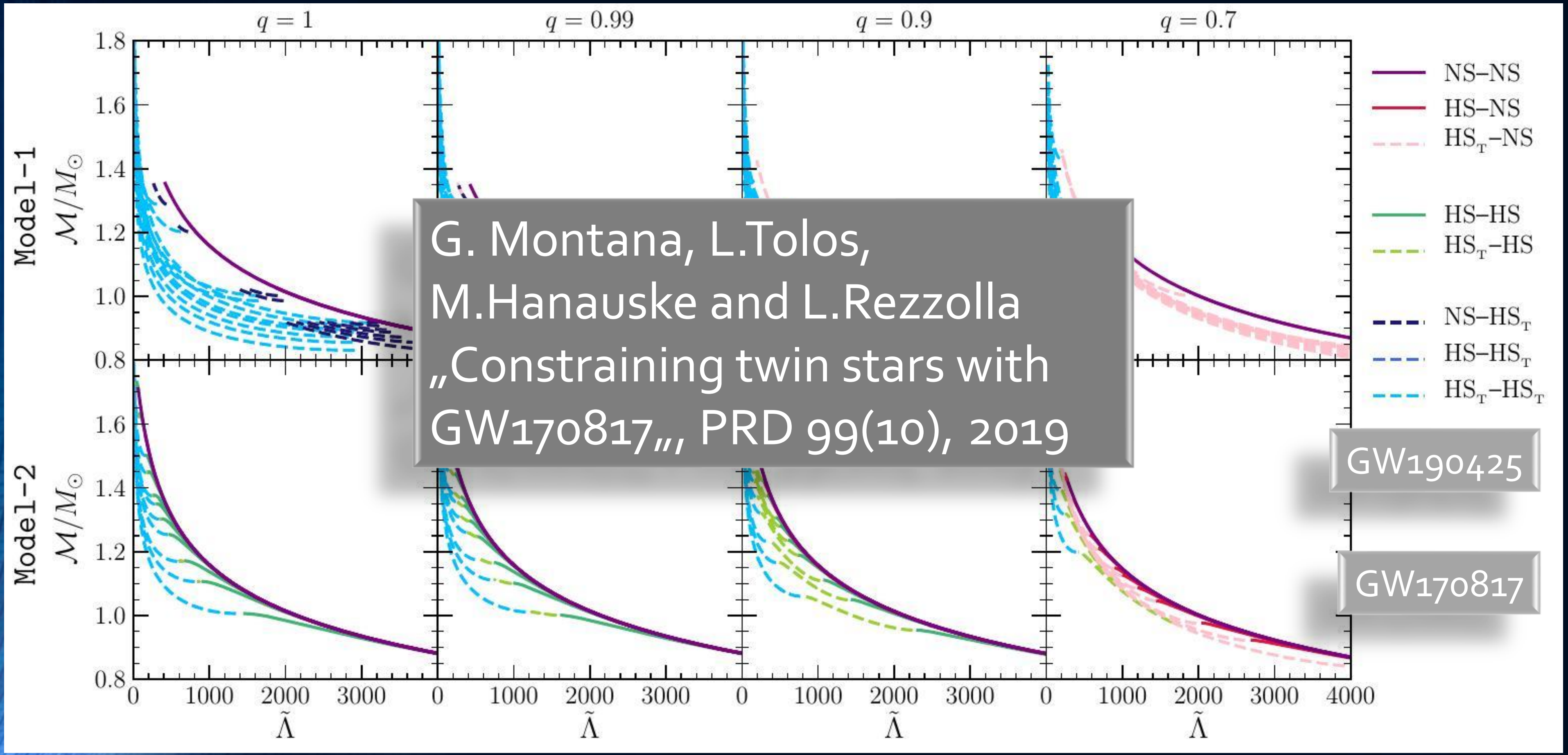

Chirp mass set to M_{ch} as a function of the weighted dimensionless tidal deformability $\tilde{\Lambda} = \tilde{\Lambda}(M_1, M_2, \Lambda_1, \Lambda_2)$ for different mass ratios q

In the next few years, further gravitational waves from binary neutron star collisions with different chirp masses and mass ratios will be detected and thus the equation of state will be further restricted.

GW170817 (only the late inspiral GW was detected!)
Constraining the maximum mass and radius of neutron stars

L.Rezzolla, E.Most, L.Weih, “Using Gravitational Wave Observations and Quasi-Universal Relations to constrain the maximum Mass of Neutron Stars”,The Astrophysical Journal Letters 852, L25 (2018): 2.01 +/-0.04 < M_{TOV} < 2.16 +/-0.17

Constraining M_{TOV} , see also: S.Lawrence et al. ,APJ808,186, 2015, Margalit & Metzger, The Astrophysical Journal Letters 850, L19 (2017): M_{TOV} < 2.17 (90%) Zhou, Zhou, Li, PRD 97, 083015 (2018) Ruiz, Shapiro, Tsokaros, PRD 97,021501 (2018)

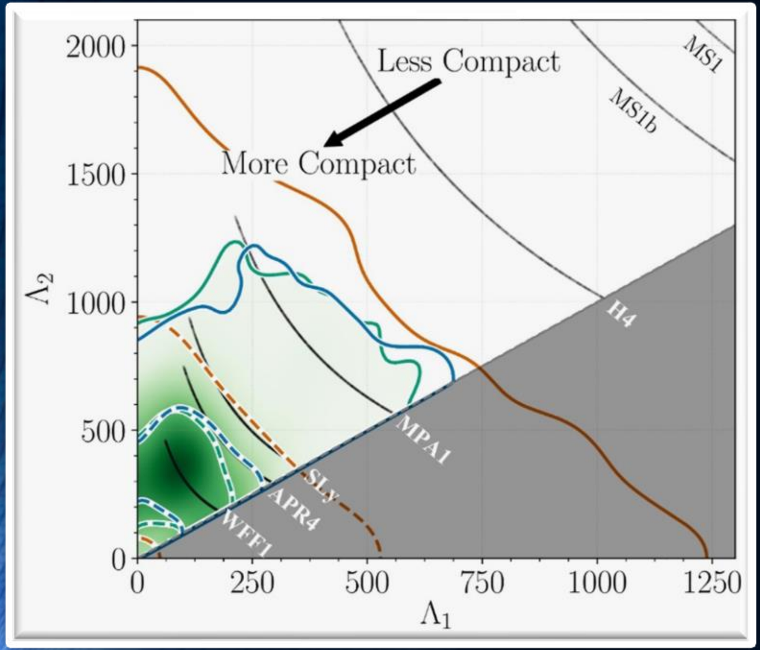

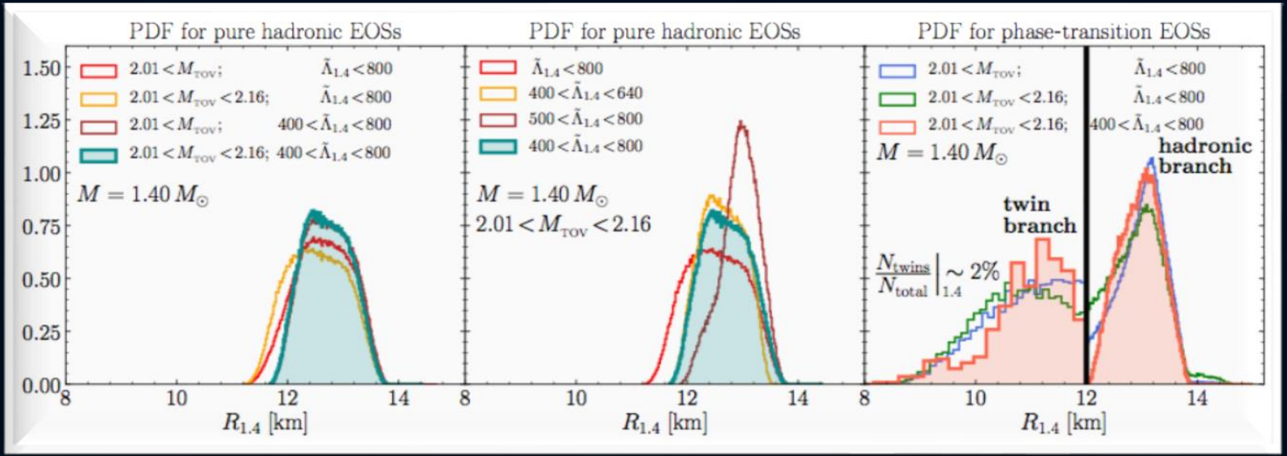

E.Most, L.Weih, L.Rezzolla, J. Schaffner-Bielich “New constraints on radii and tidal deformabilities of neutron stars from GW170817”, PRL 120, 261103 (2018)

GW170817: Measurements of neutron star radii and equation of state, *The LIGO /Virgo Collaboration*, arXiv:1805.11581v1

See also: De, Finstad, Lattimer, Brown, Berger, Biwer, (2018), arXiv:1804.08583 ; Bauswein, Just, Janka, N. Stergioulas, APJL 850, L34 (2017) ; Fattoyev, Piekarewicz, Horowitz, PRL 120, 172702 (2018) ; Nandi & Char, Astrophys. J. 857, 12 (2018) ; Paschalidis, Yagi, Alvarez-Castillo, Blaschke, Sedrakian, PRD 97, 084038 ; Ruiz, Shapiro, Tsokaros, PRD 97, 021501 (2018) ; Annala, Gorda, Kurkela, Vuorinen, PRL 120, 172703 (2018) ; Raithel, Özel, Psaltis, (2018) arXiv:1803.07687

Signatures within the post-merger phase evolution
Prompt phase transition scenario

Talk by David Blaschke
yesterday

Identifying a first-order phase transition in neutron-star mergers through gravitational waves; A Bauswein, NUF Bastian, DB Blaschke, K Chatziioannou, JA Clark, JA Clark, T Fischer, M Oertel; Physical review letters 122 (6), 061102 (2019)

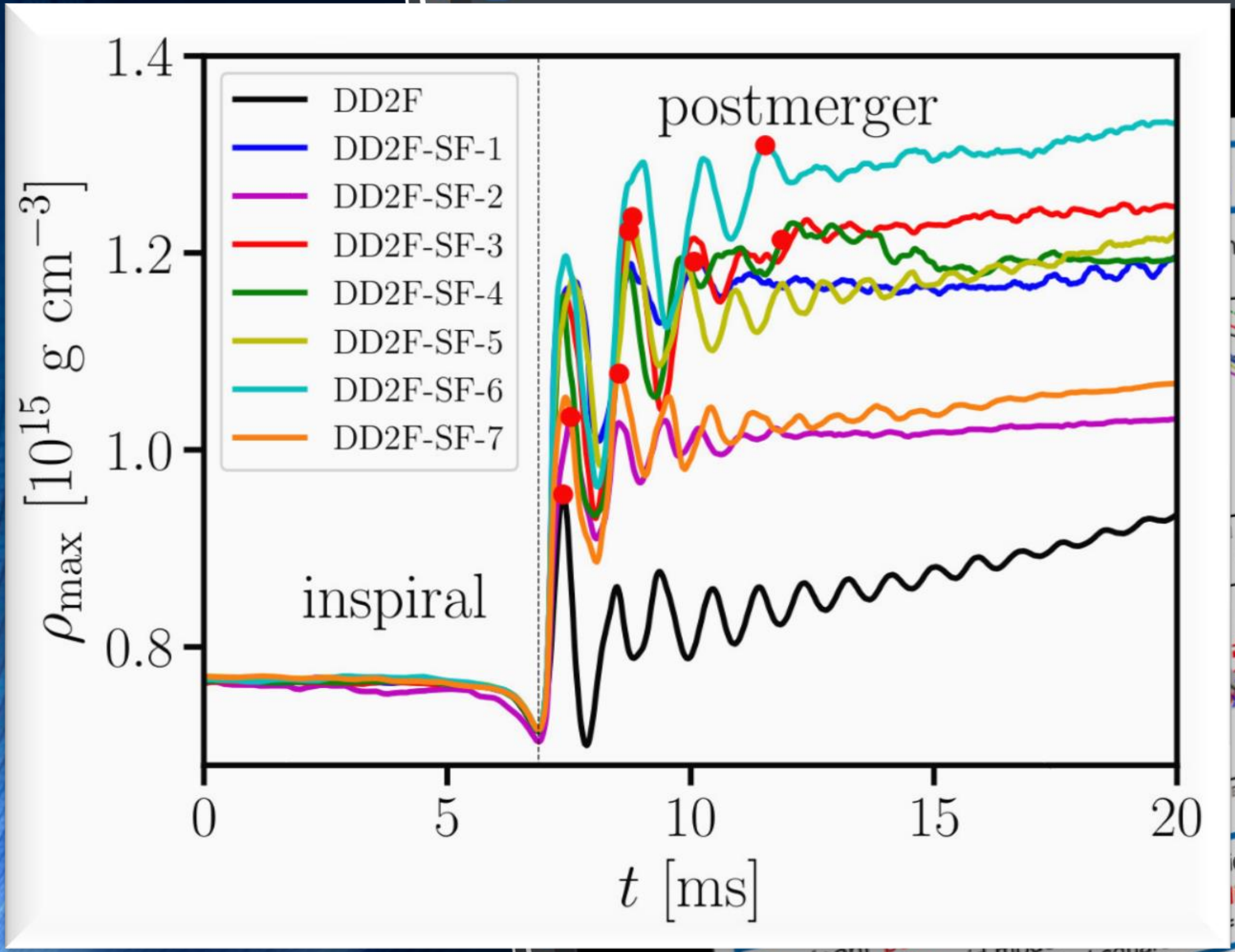

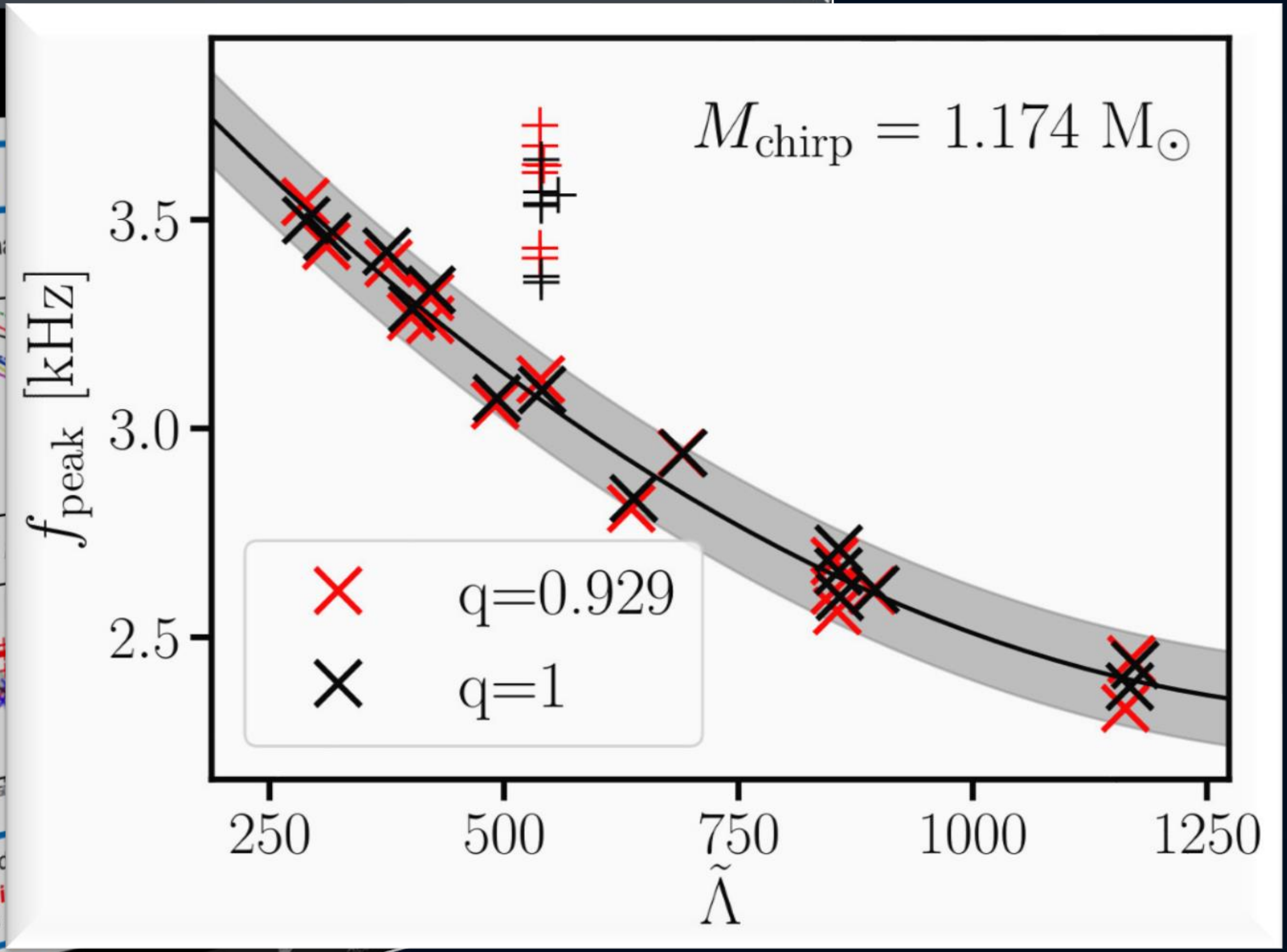

Evolution of the density in the post merger phase

ALF2-EOS: Mixed phase region starts at $3\rho_0$ (see red curve), initial NS mass: 1.35 $M_\odot$

Hanauske, et.al. PRD, 96(4), 043004 (2017)

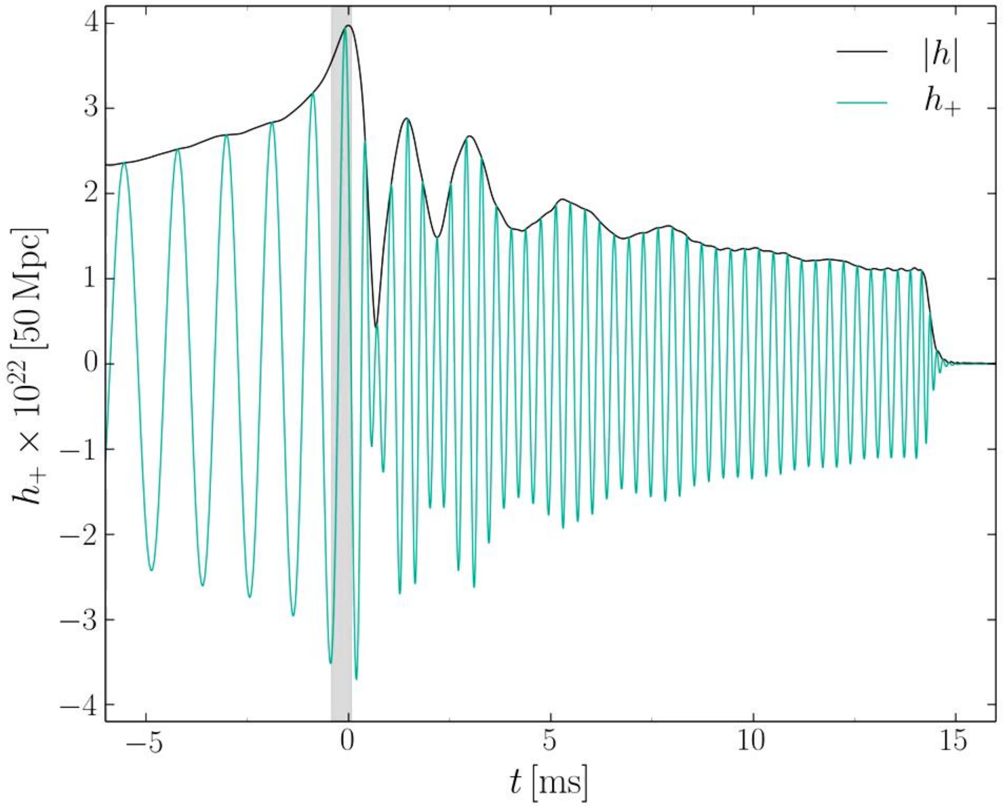

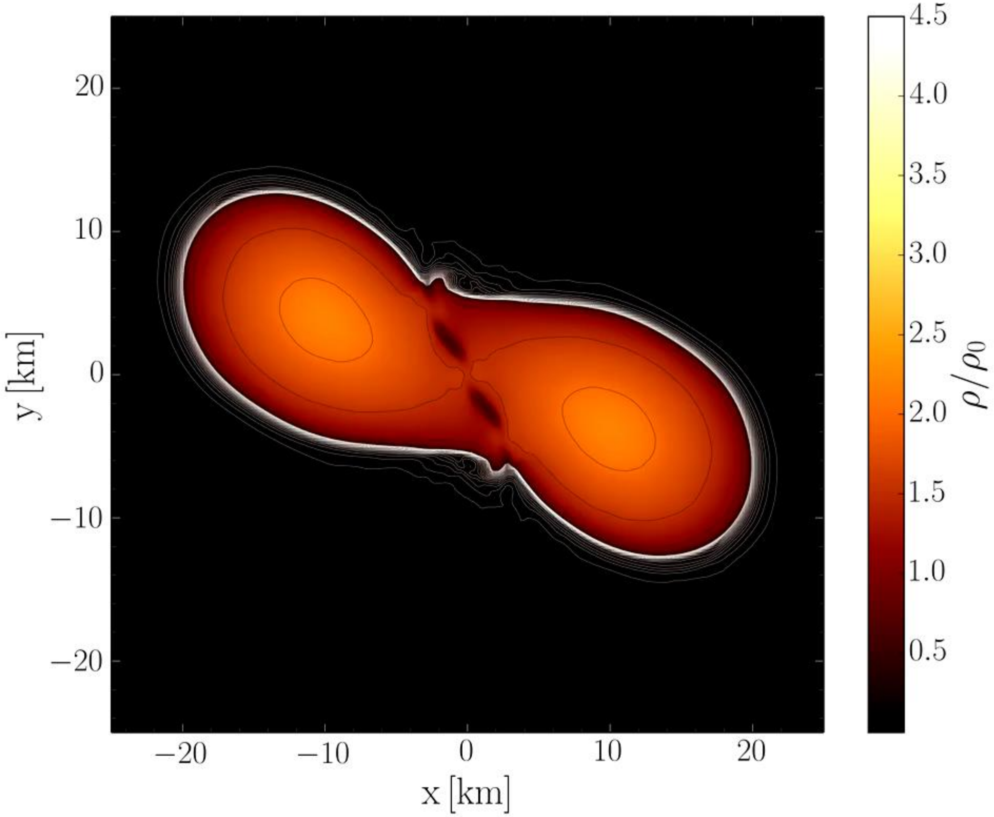

Gravitational wave amplitude
at a distance of 50 Mpc

Rest mass density distribution ρ(x,y)
in the equatorial plane
in units of the nuclear matter density ρ_0

The different Phases of a Binary Compact Star Merger Event

Late inspiral and merger phase

Transient early postmerger phase

Postmerger phase

Collapse to the Kerr black hole and ringdown phase

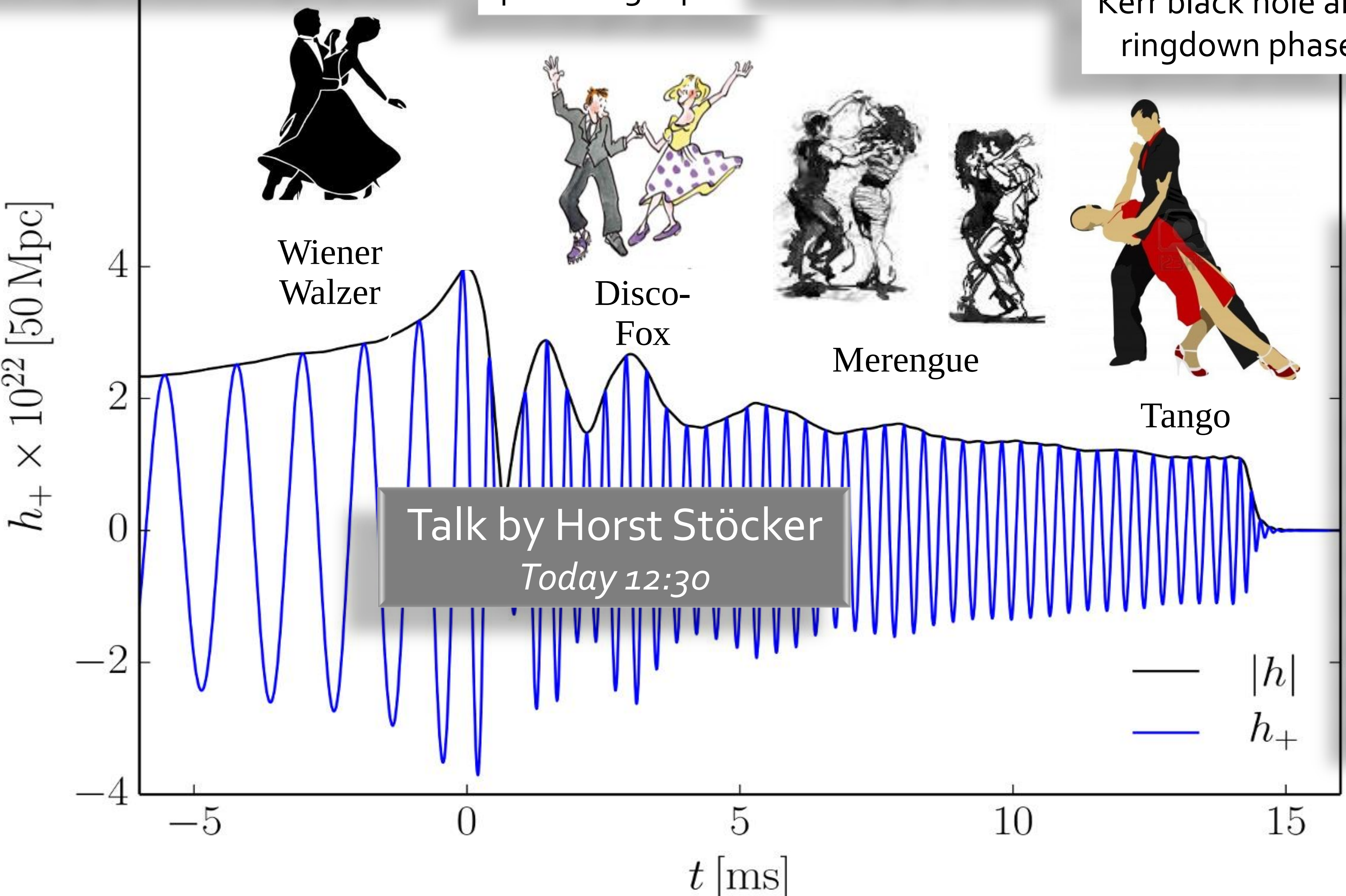

Talk by Horst Stöcker

Today 12:30

Wy exactly these dances? Details in

"Binary Compact Star Mergers and the Phase Diagram of Quantum Chromodynamics", Matthias Hanauske and Horst Stöcker, Discoveries at the Frontiers of Science, 107-132; Springer, Cham (2020)

Density and Temperature Evolution inside the HMNS

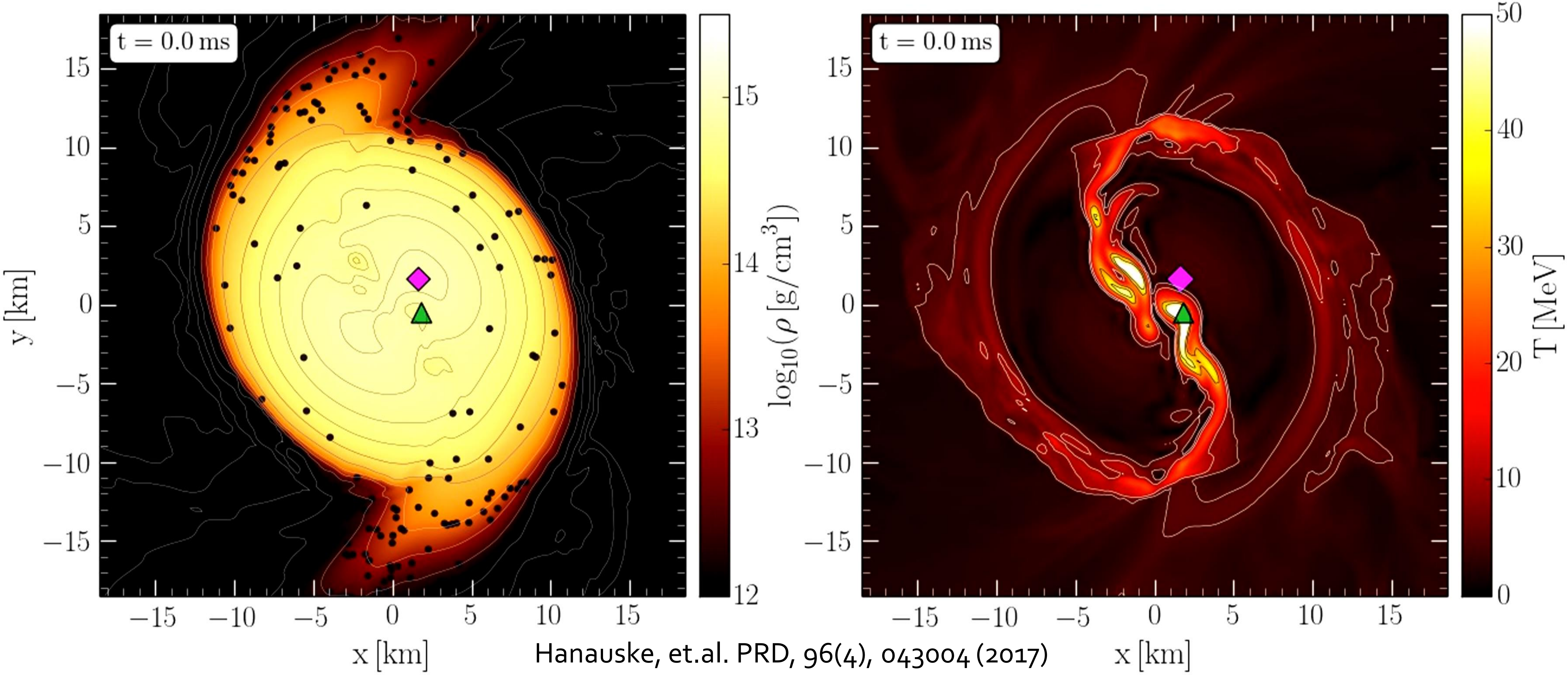

Hanauske, et.al. PRD, 96(4), 043004 (2017)

Rest mass density on the equatorial plane

Temperature on the equatorial plane

Binary Neutron Star Mergers in the QCD Phase Diagram

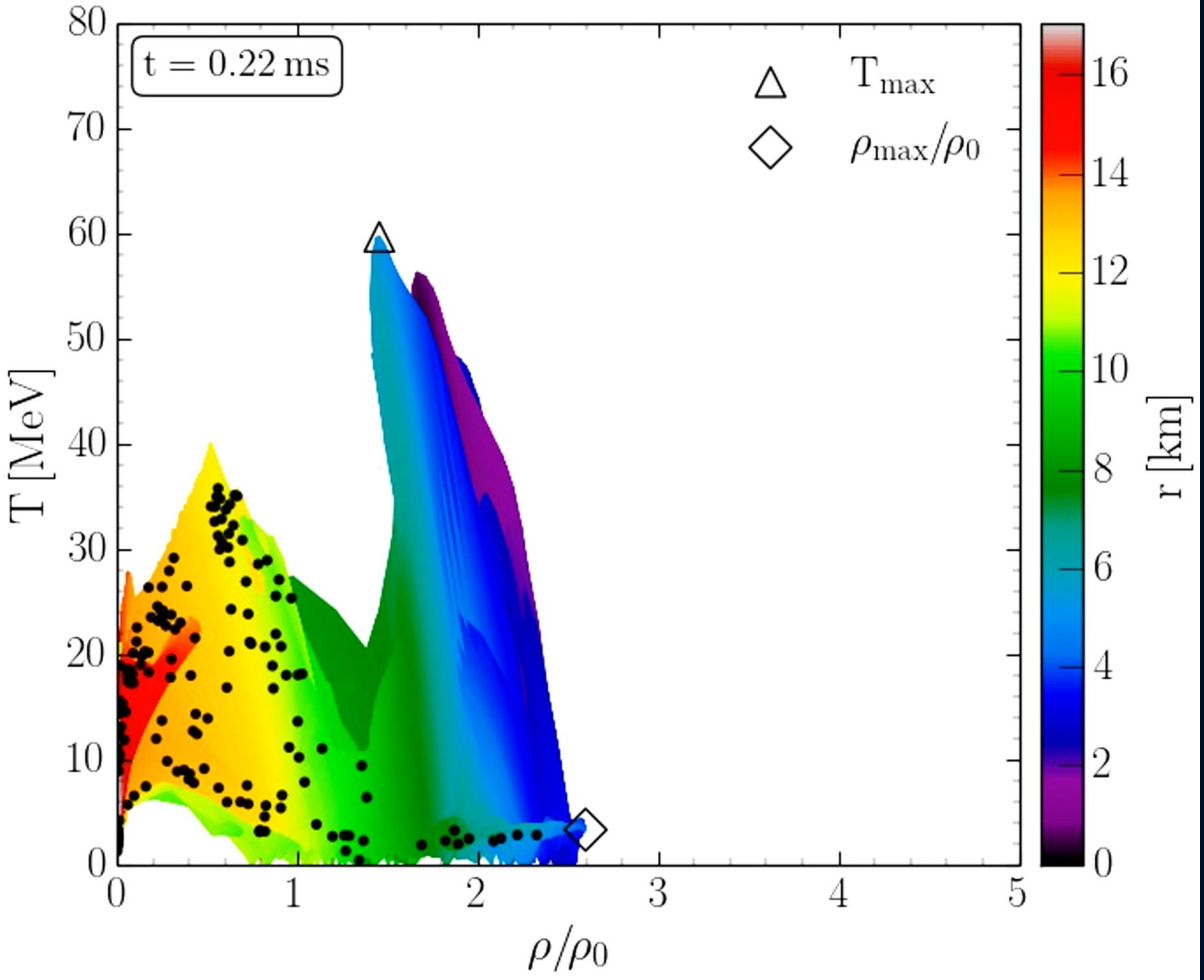

Evolution of hot and dense matter inside the inner area of a hypermassive neutron star simulated within the LS220 EOS with a total mass of $M_{total}=2.7\ M_\odot$ in the style of a (T- ρ) QCD phase diagram plot

The color-coding indicate the radial position r of the corresponding (T- ρ) fluid element measured from the origin of the simulation (x , y) = (0 , 0) on the equatorial plane at z = 0.

The open triangle marks the maximum value of the temperature while the open diamond indicates the maximum of the density.

Signatures within the post-merger phase evolution

Delayed phase transition scenario

Postmerger Gravitational-Wave Signatures of Phase Transitions in Binary Mergers; LR Weih, M Hanauske, L Rezzolla; Physical Review Letters 124 (17), 171103 (2020)

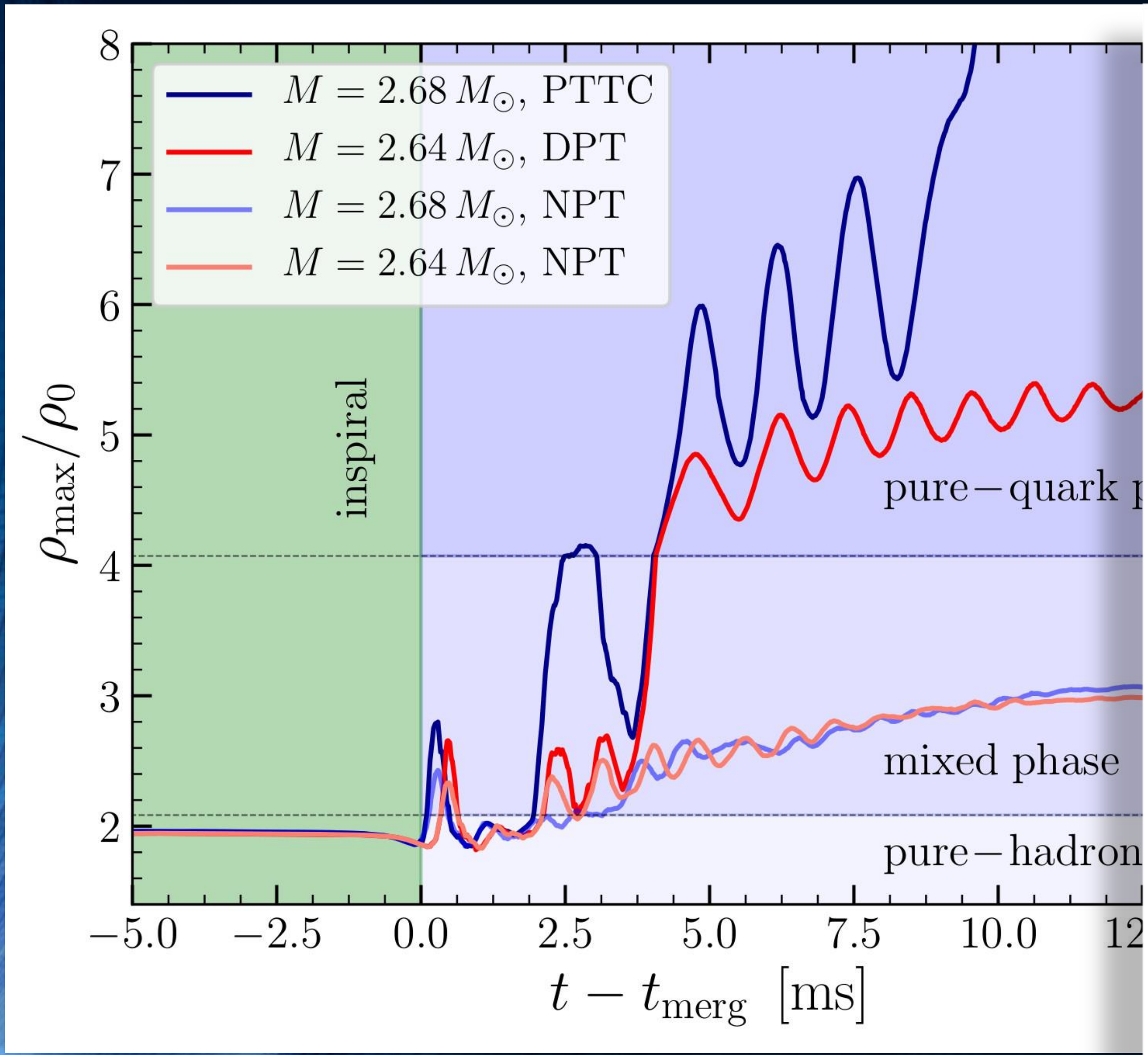

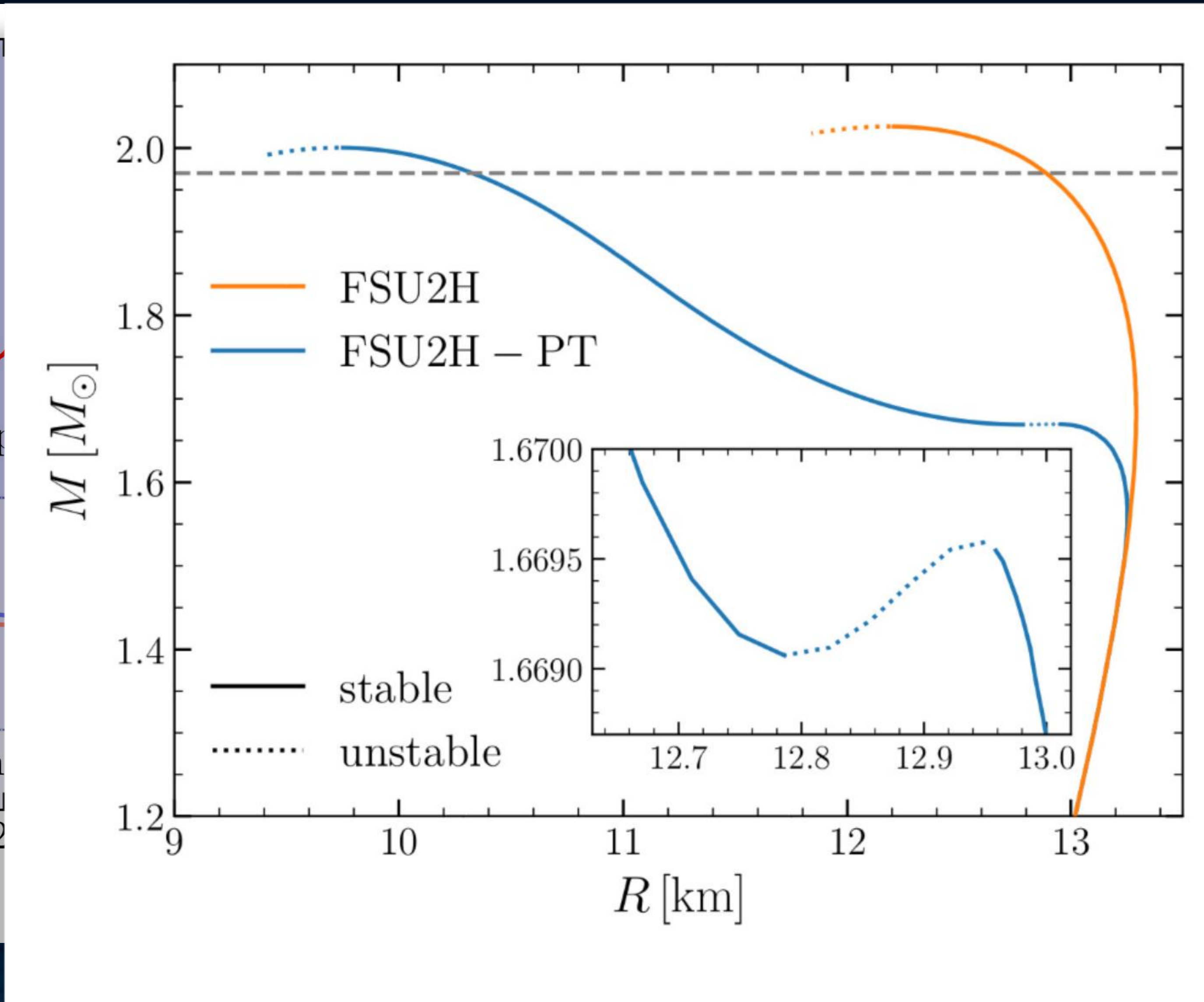

Density and temperature evolution inside the HMHS

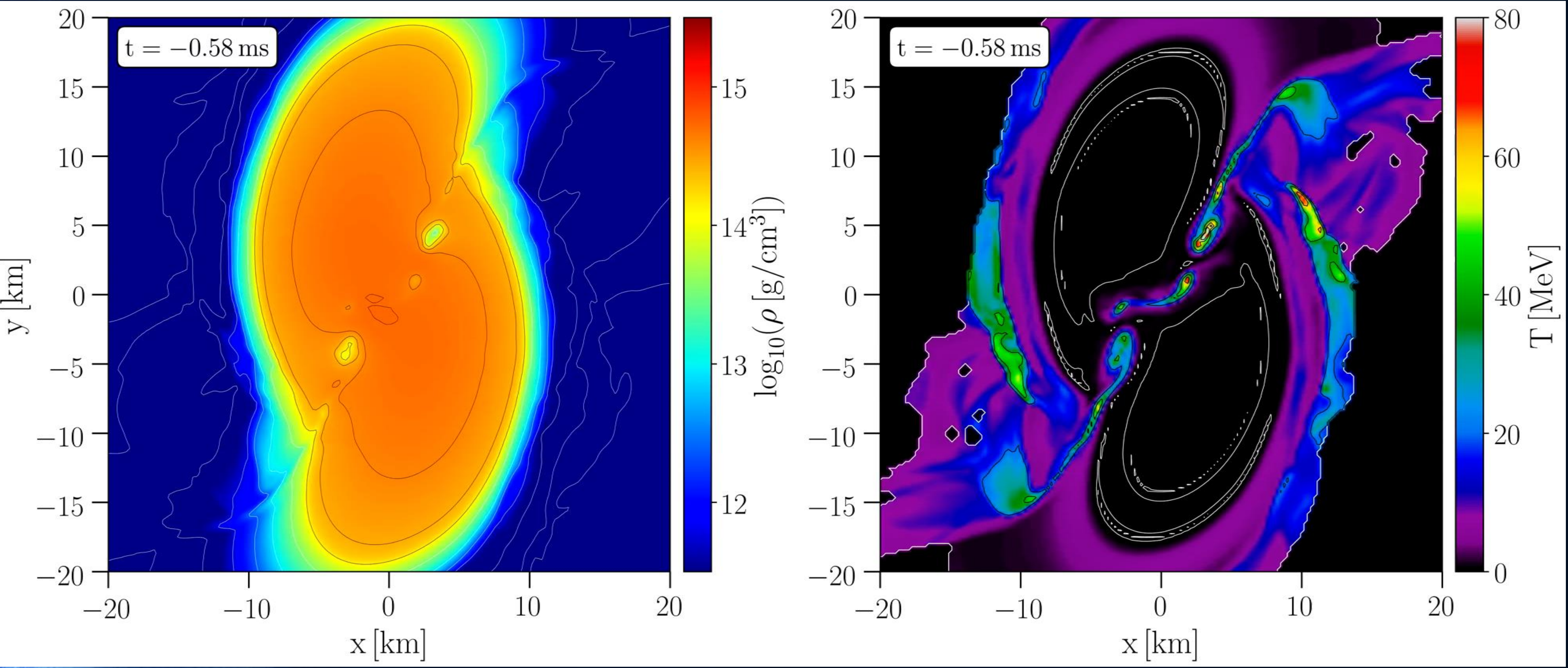

EOS: FSU2H-PT + thermal ideal fluid, Mass: 1.32 M☉

Binary Neutron Star Mergers in the QCD Phase Diagram

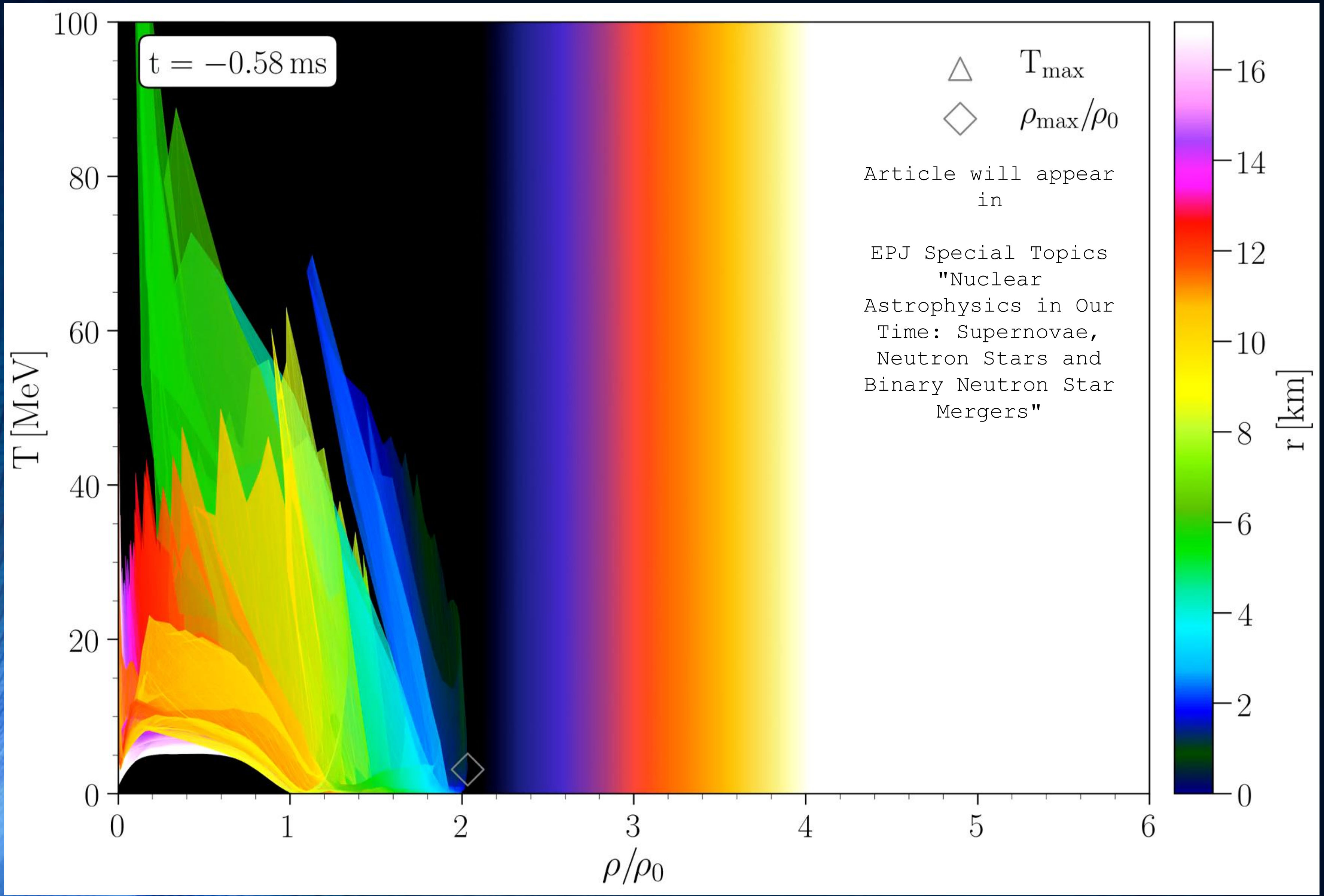

Evolution of hot and dense matter inside the inner area of a hypermassive hybrid star simulated within the (FSU2H-PT + thermal ideal fluid) EOS with a total mass of M_{total}=2.64 $M_\odot$ in the style of a (T- ρ) QCD phase diagram plot

The color-coding indicate the radial position r of the corresponding (T- ρ) fluid element measured from the origin of the simulation (x , y) = (0 , 0) on the equatorial plane at z = 0.

The open triangle marks the maximum value of the temperature while the open diamond indicates the maximum of the density.

These figures show the configuration of the HMHS at a time right before the collapse to the more compact star. The small asymmetry in the density profile and especially the double-core structure is amplified by the collapse resulting in a large one-sided asymmetry (i.e., an m = 1 asymmetry in a spherical-harmonics decomposition), which triggers a sizeable h21 GW strain.

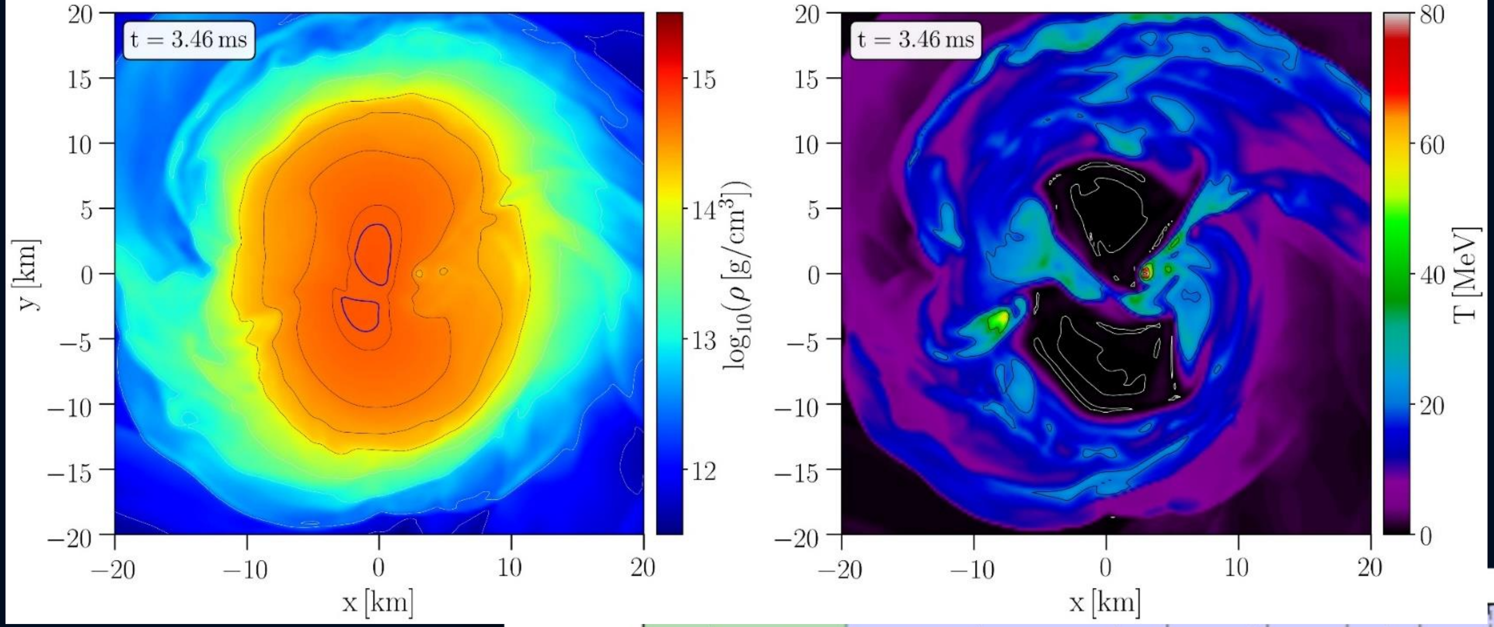

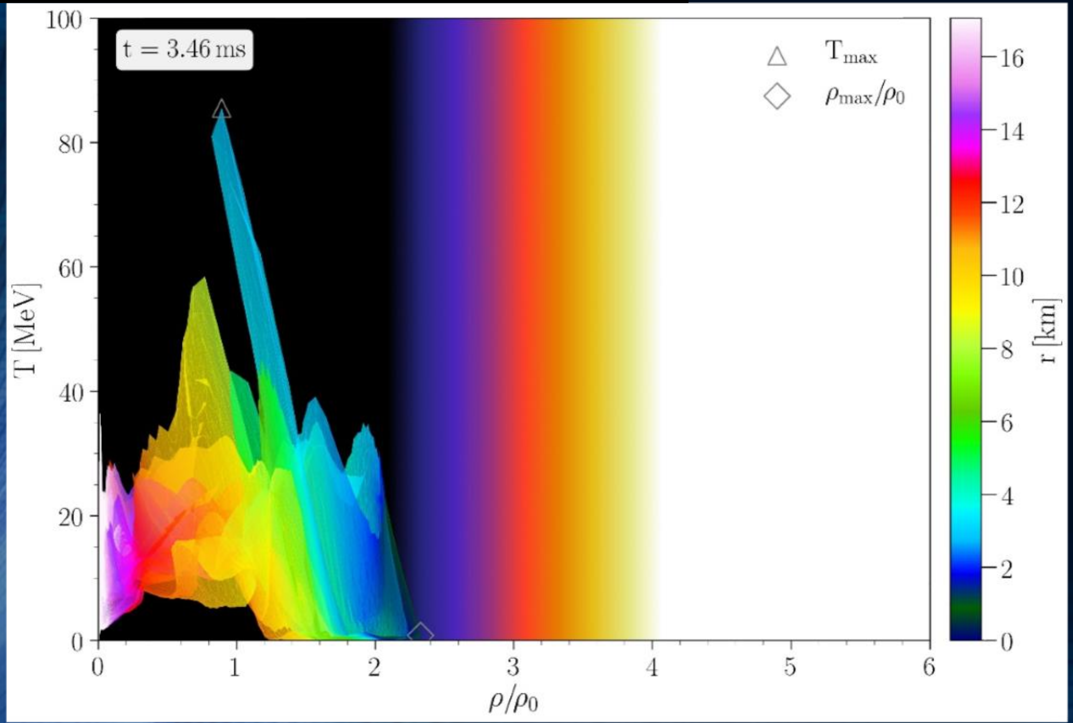

Density maximum

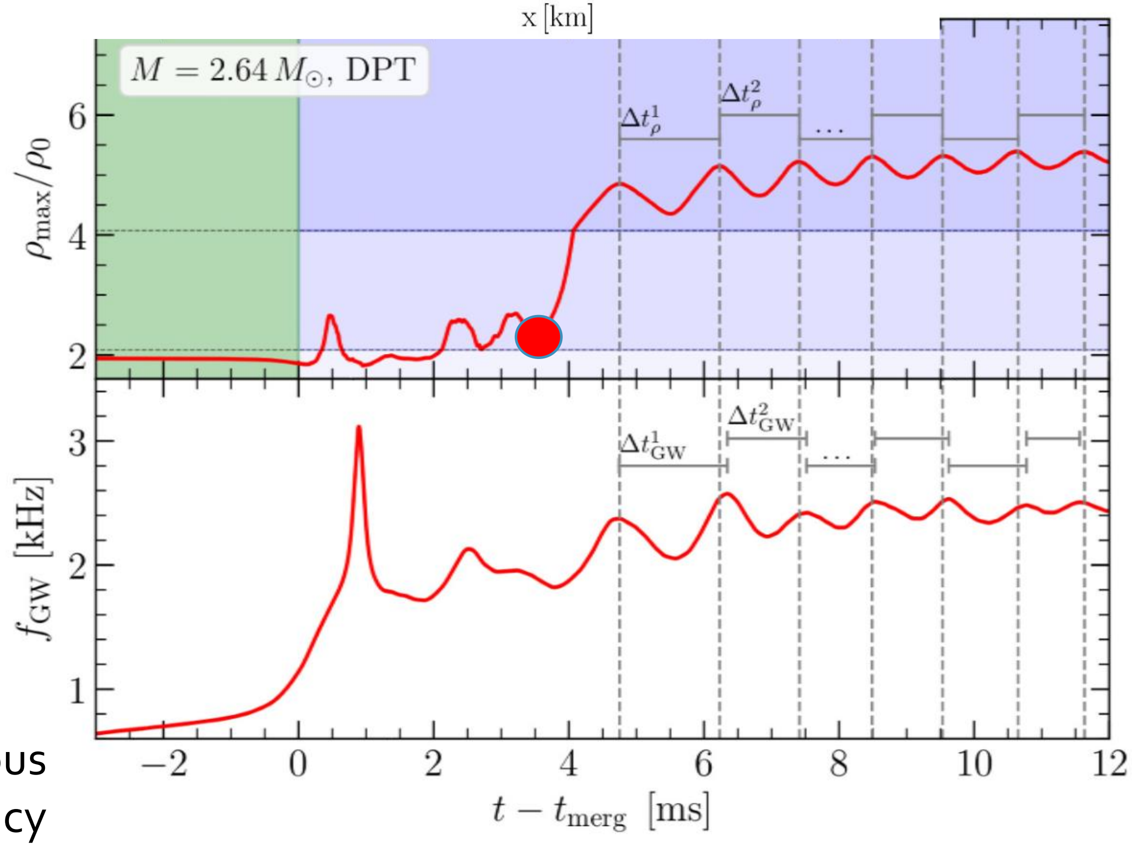

Instantaneous GW frequency

The figures correspond to a time near the first density maximum at t = 4.8ms (see red marker). The large m = 1 contribution can be seen by looking at the asymmetry of the spatial location of the quark core, which is marked with the second blue contour line. As a result of this asymmetry, the location of the two temperature are at different radial distances from the grid center.

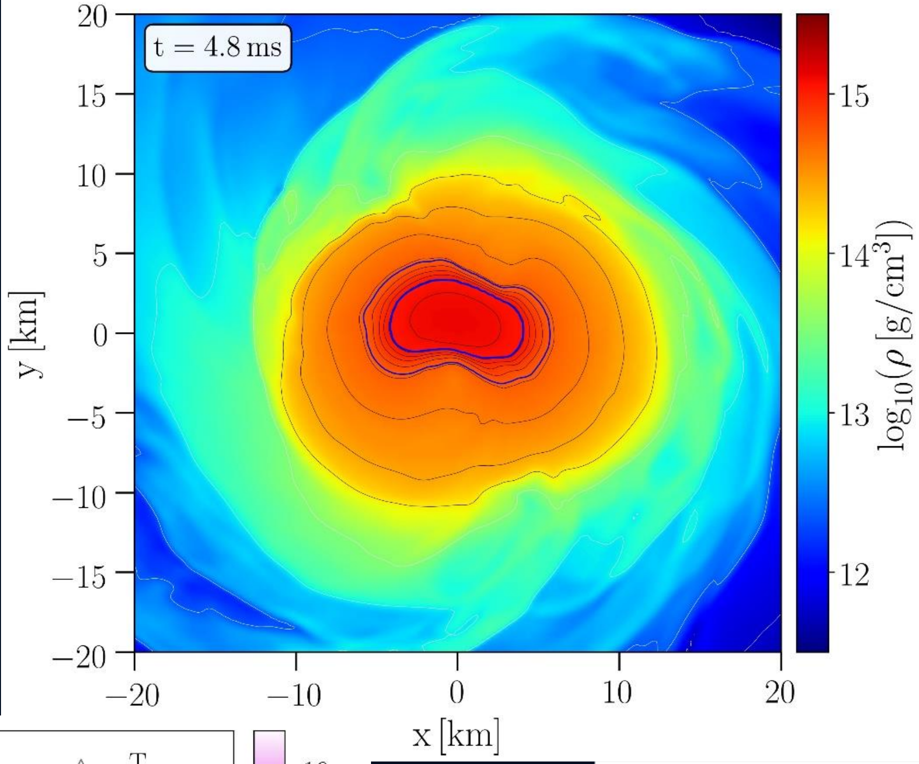

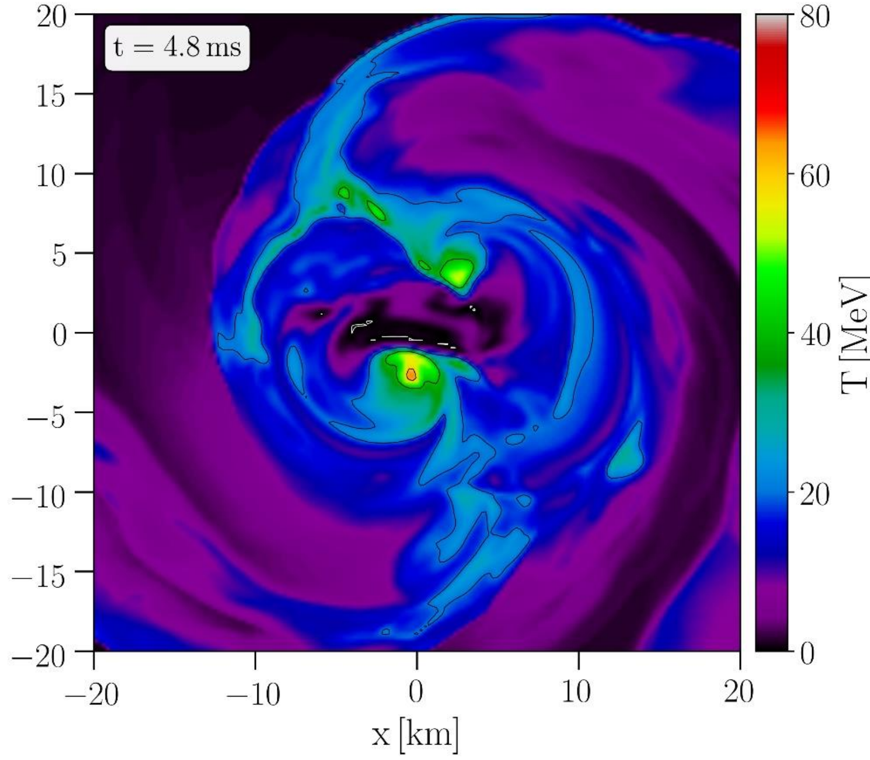

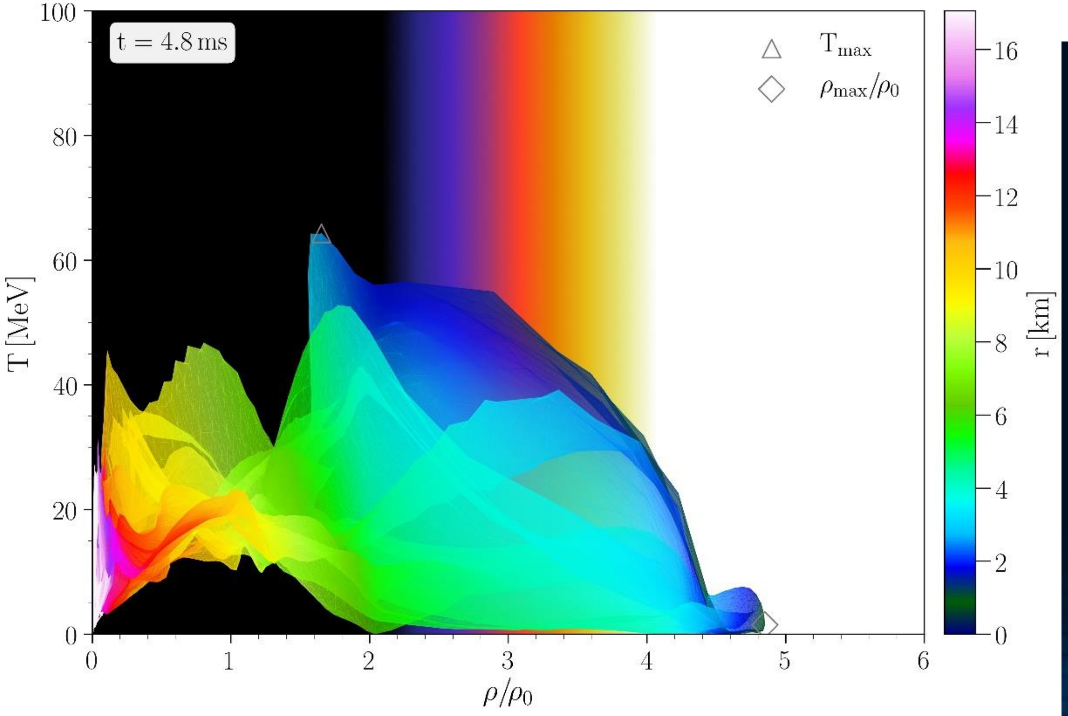

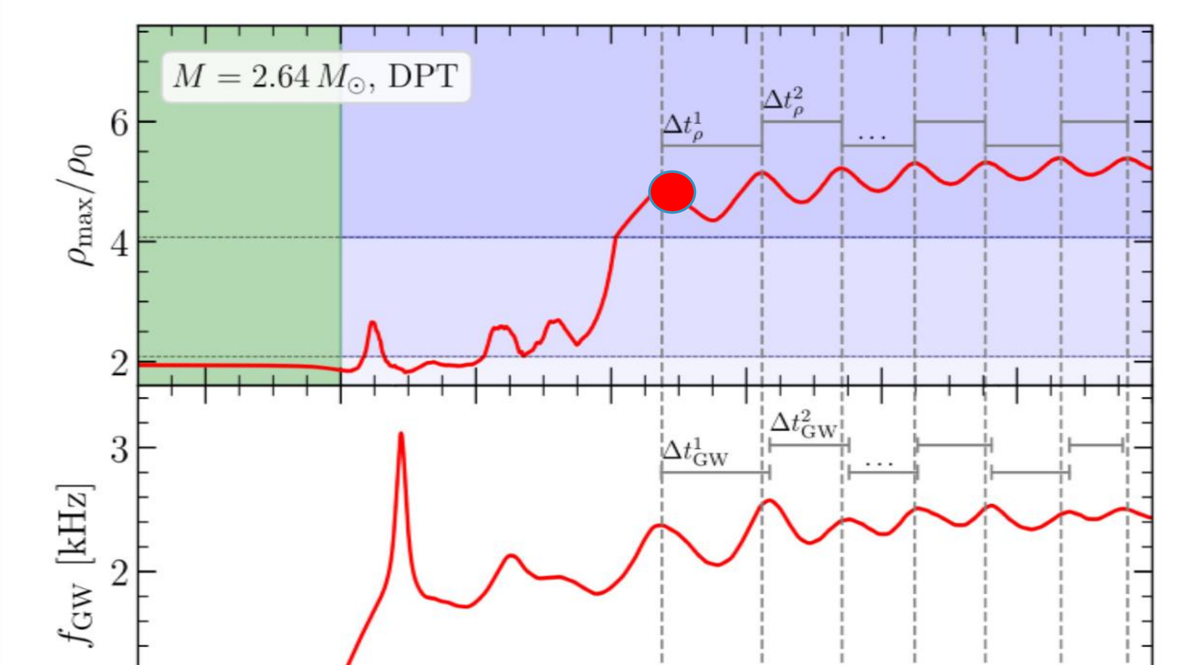

The figures correspond to a time near the first density minimum at t = 5.52ms (see red marker). The large m = 1 contribution can be seen by looking at the asymmetry of the spatial location of the quark core, which is marked with the second blue contour line. As a result of this asymmetry, the location of the two temperature are at different radial distances from the grid center.

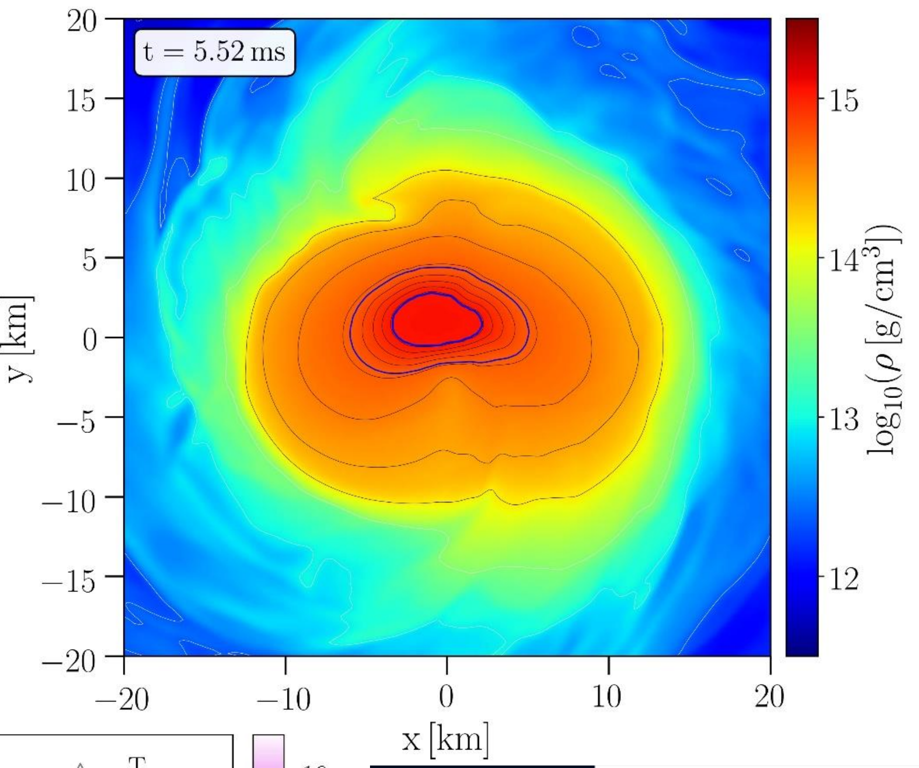

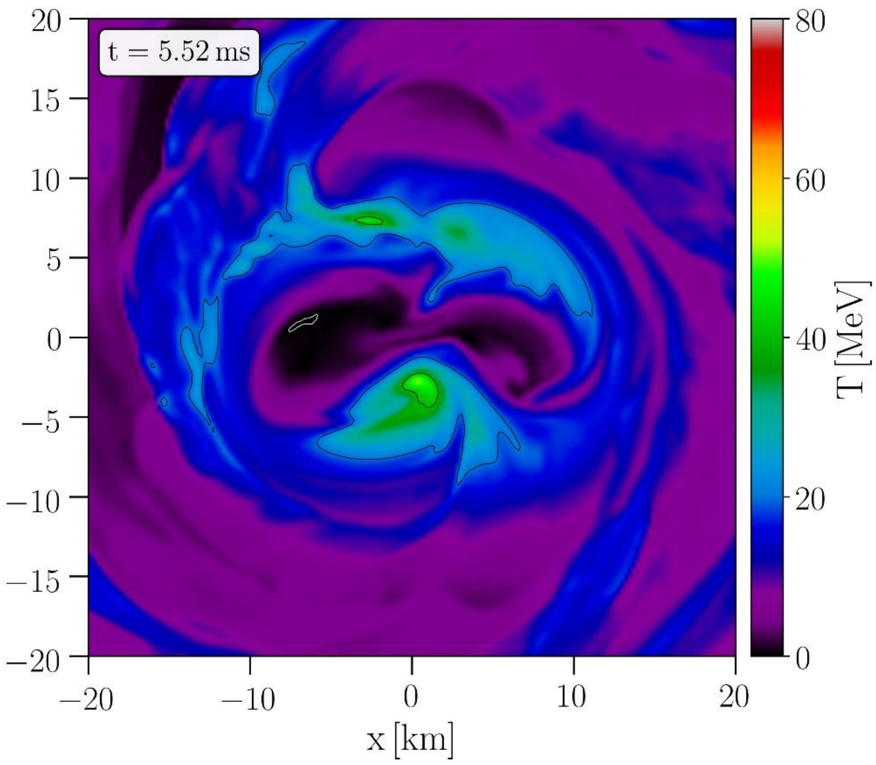

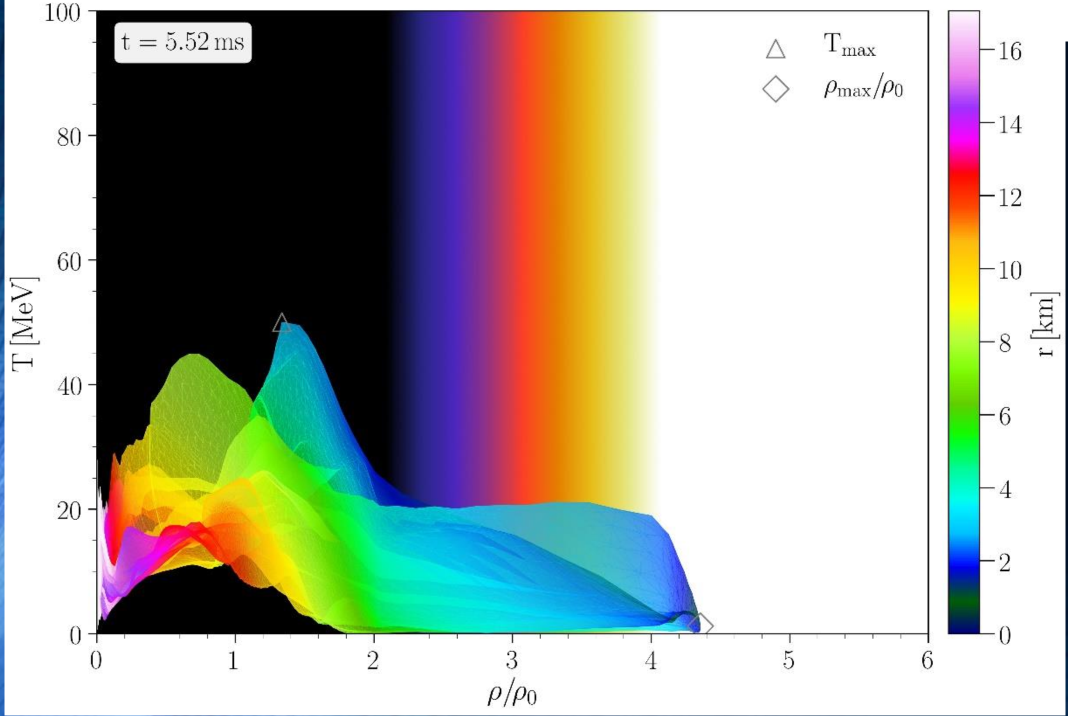

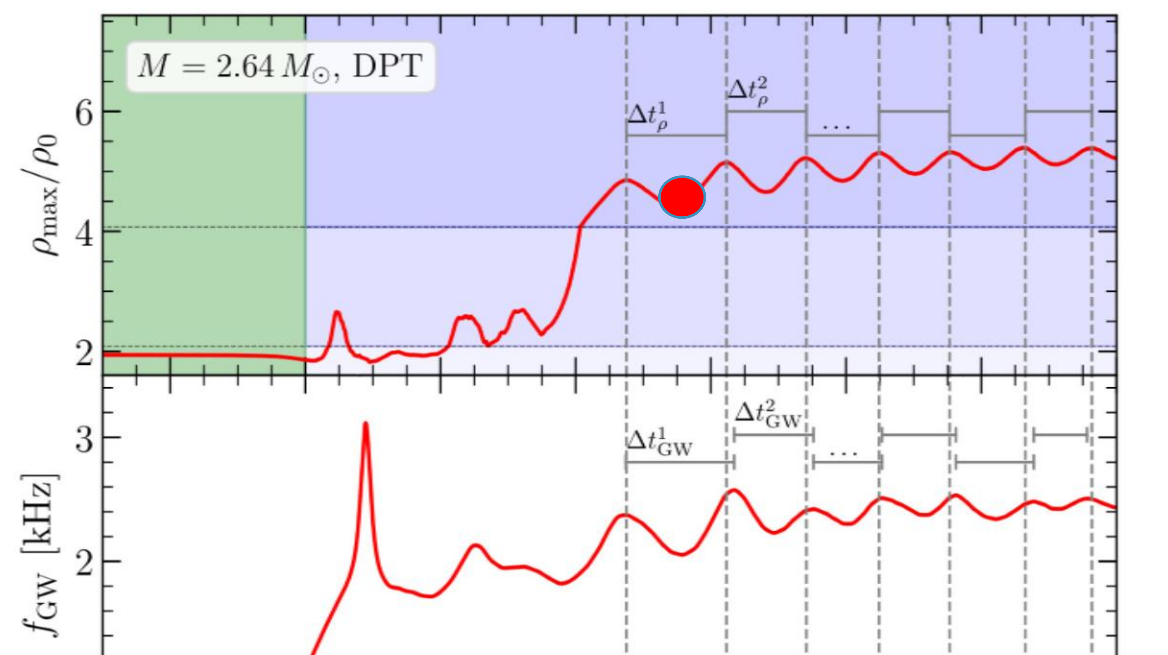

The collapse of the HMNS to the HMHS causes the system to vibrate. At the times when the maximum of the central density is reached, the pure quark core with its stiffer equation of state presses violently against the gravitational pressure and the star expands again and, as a result, its central density decreases.

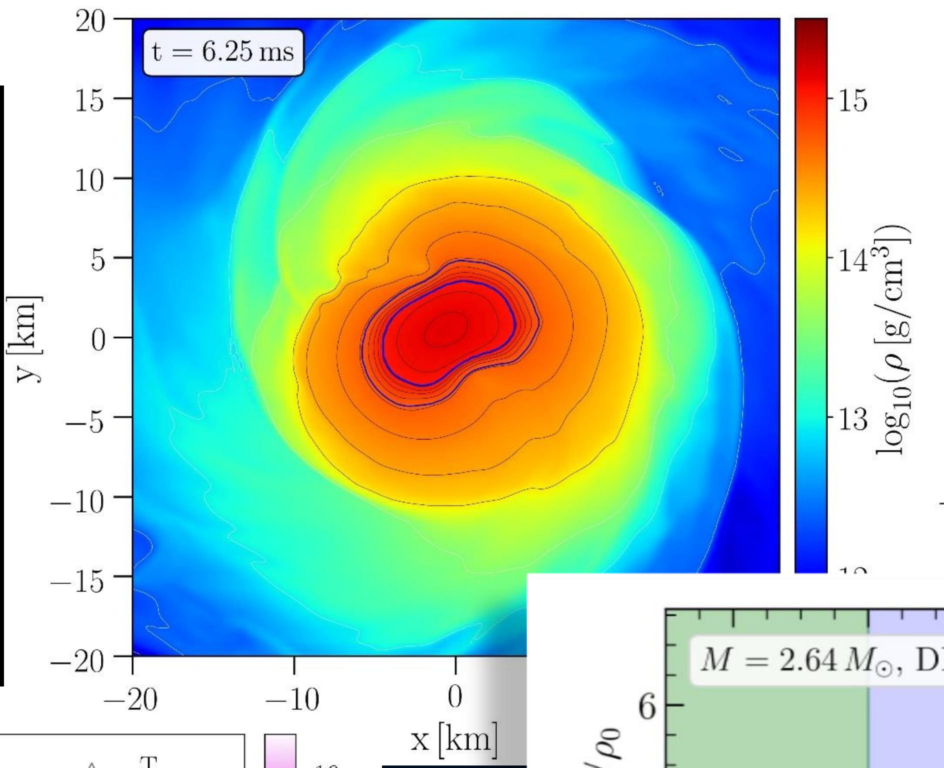

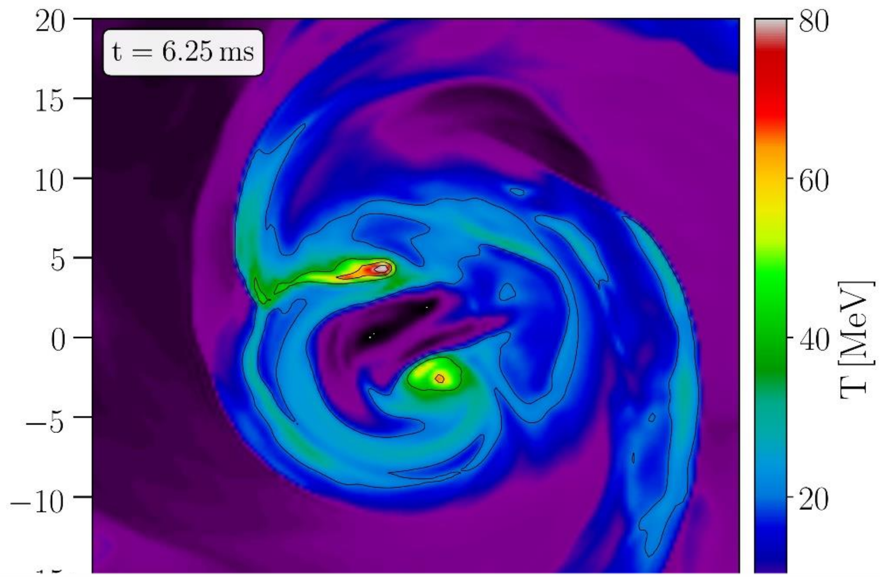

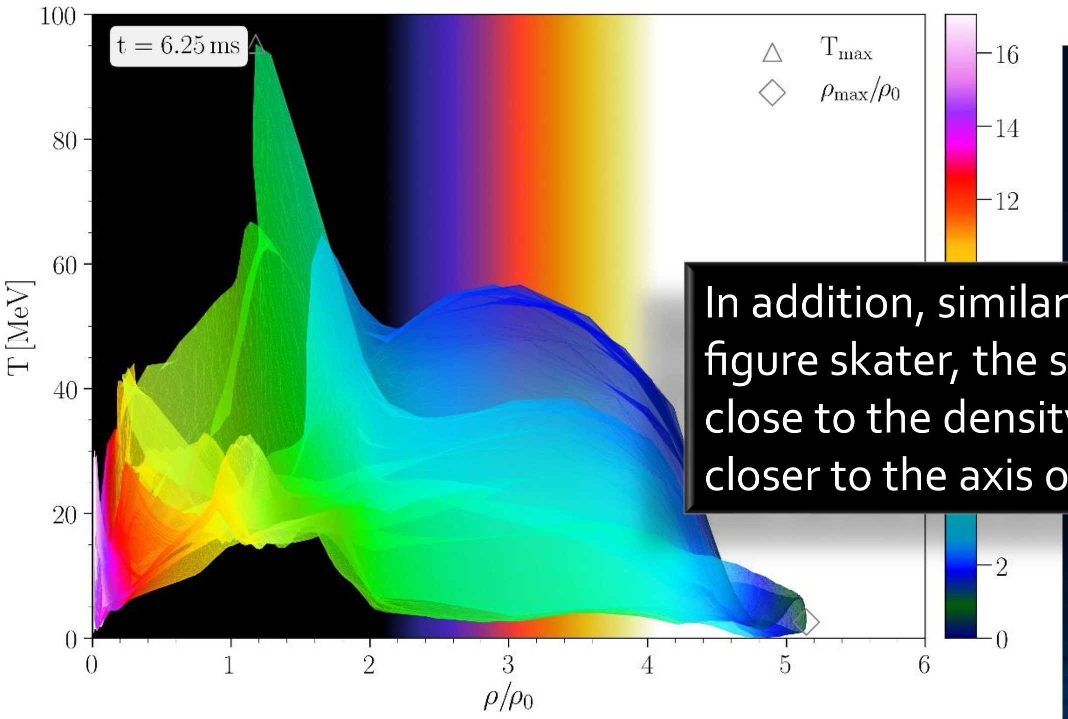

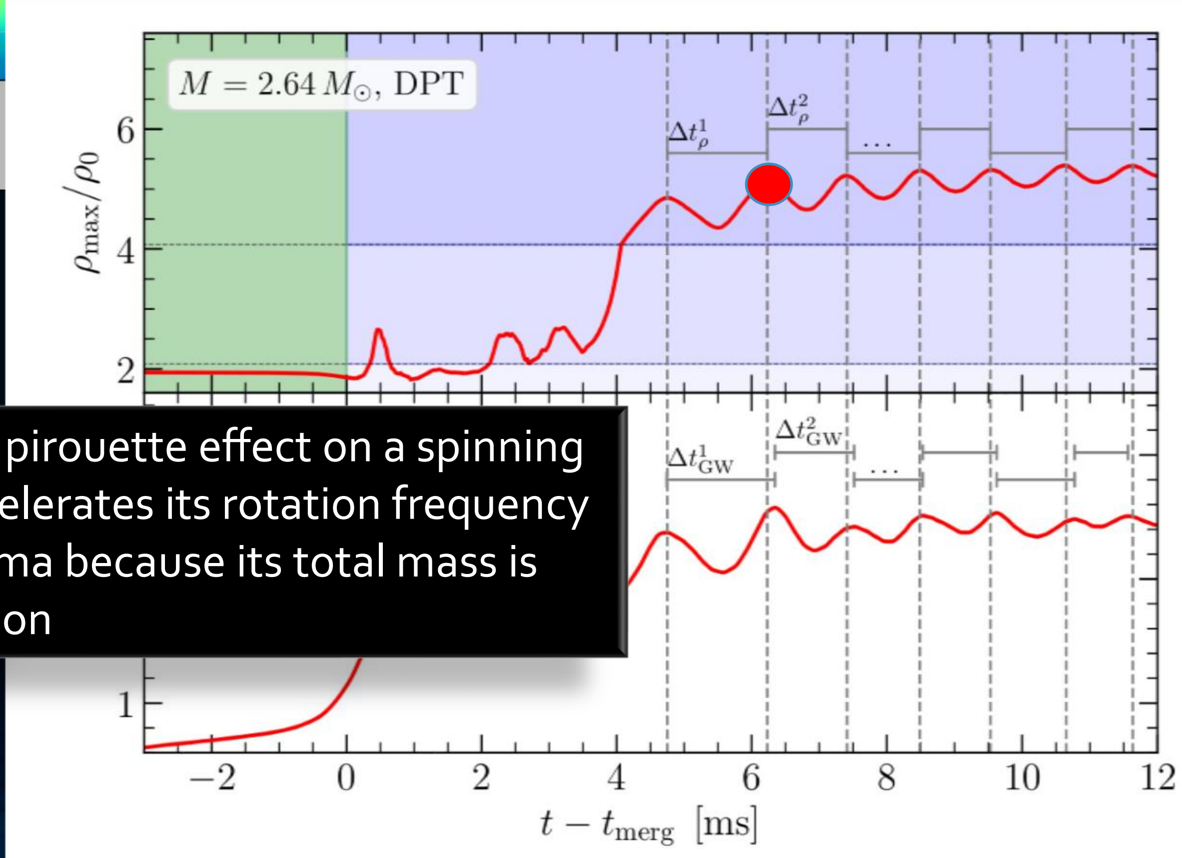

In addition, similar to the pirouette effect on a spinning figure skater, the star accelerates its rotation frequency close to the density maxima because its total mass is closer to the axis of rotation

These figures report the HMHS properties at t = 13.15 ms and shows that in addition to the two temperature hot-spots, a new high temperature shell surrounding a cold core appears within the mixed phase region of the remnant . For subsequent post-merger times, the two temperature hot-spots will be smeared out to become a ring like structure on the equatorial plane

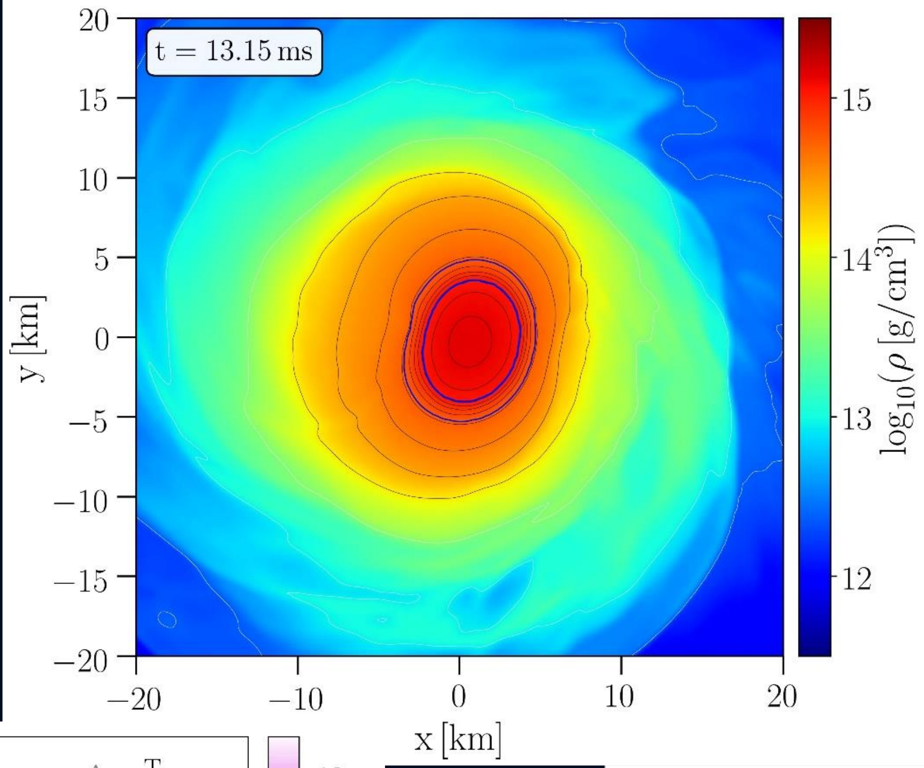

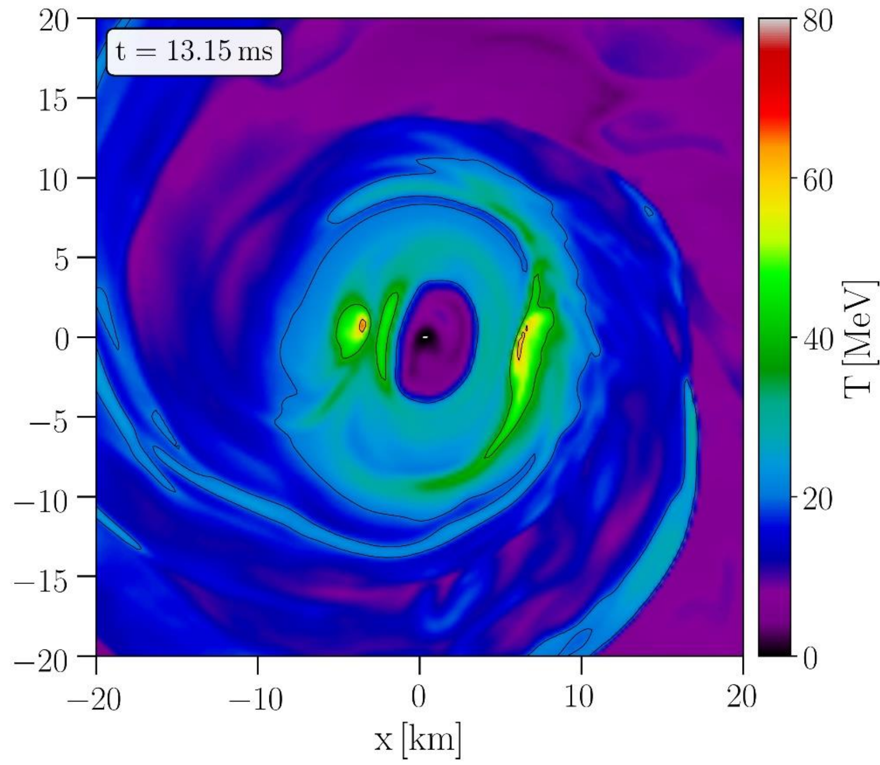

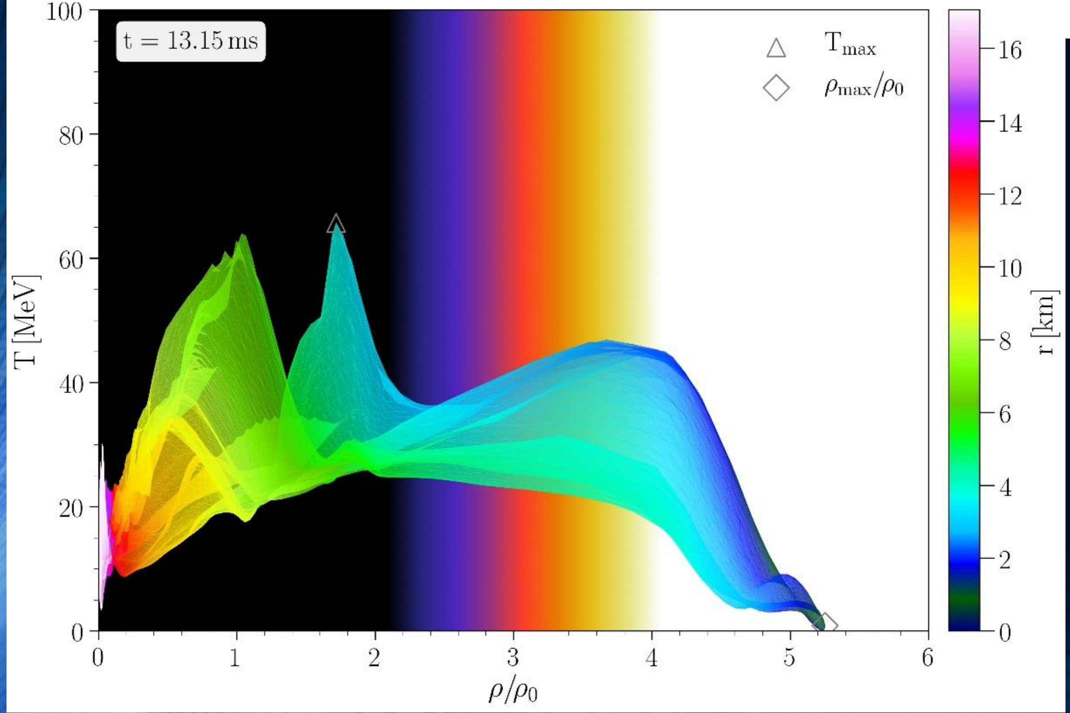

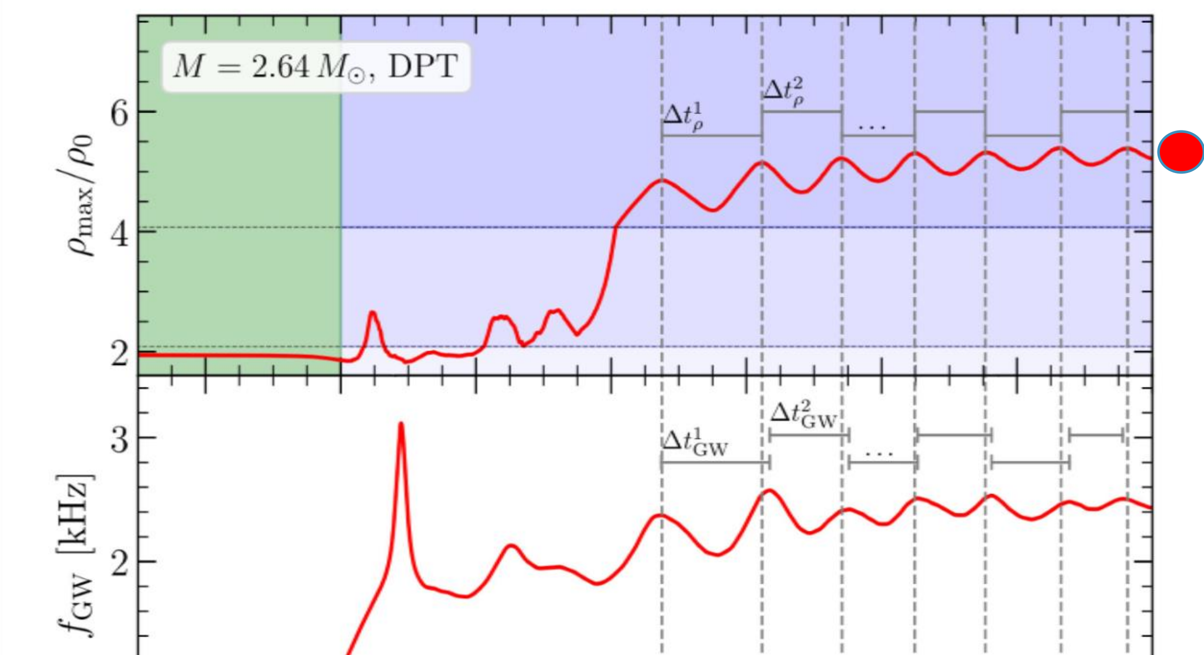

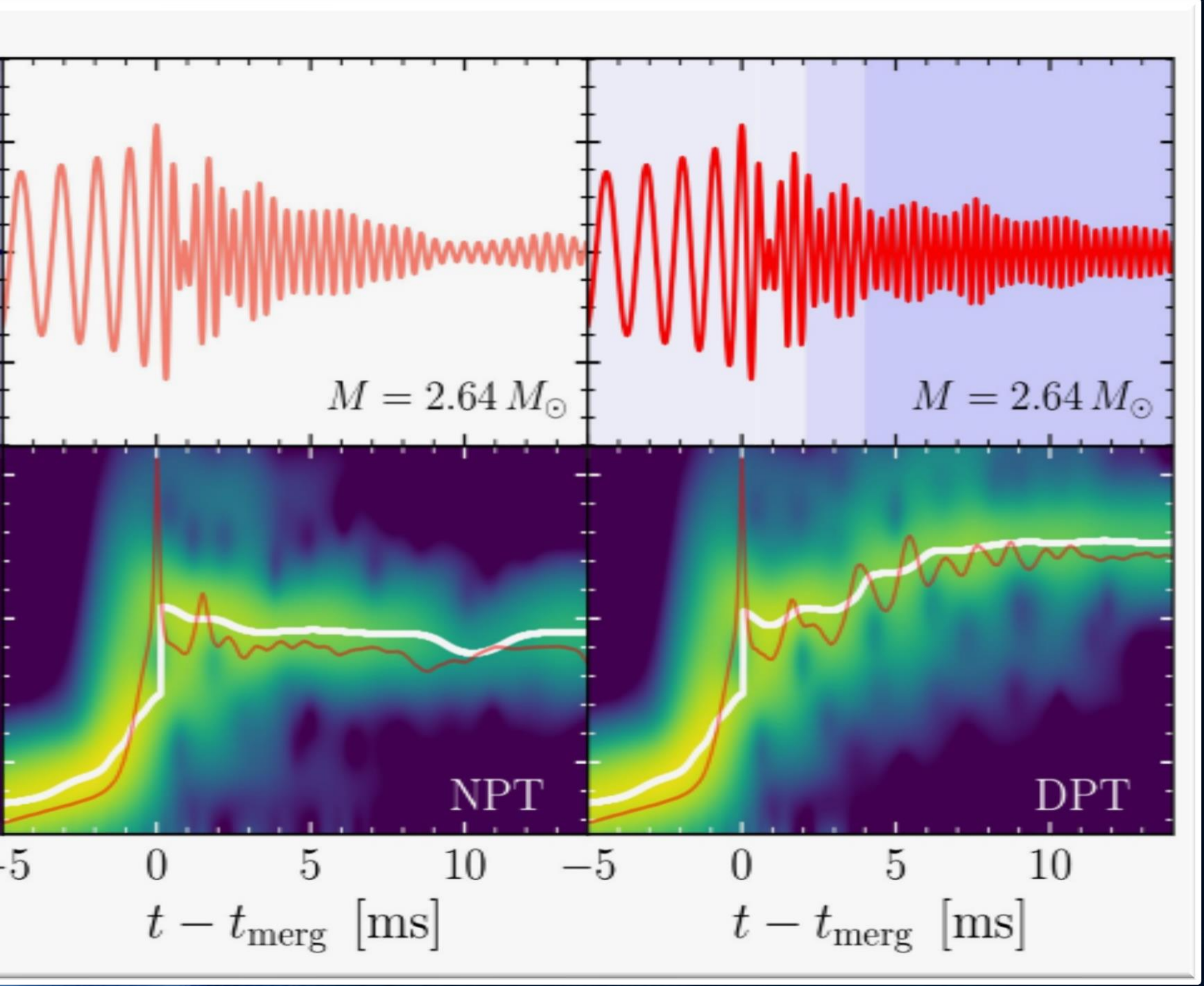

Strain h+ (top) and its spectrogram (bottom) for the binary neutron star simulation of the delayed phase transition scenario. In the top panel the different shadings mark the times when the HMNS core enters the mixed and pure quark phases.. In the bottom panels, the white lines trace the maximum of the spectrograms, while the red lines show the instantaneous gravitational-wave frequency.

Differnce in the h_+^{12} − gravitational wave mode

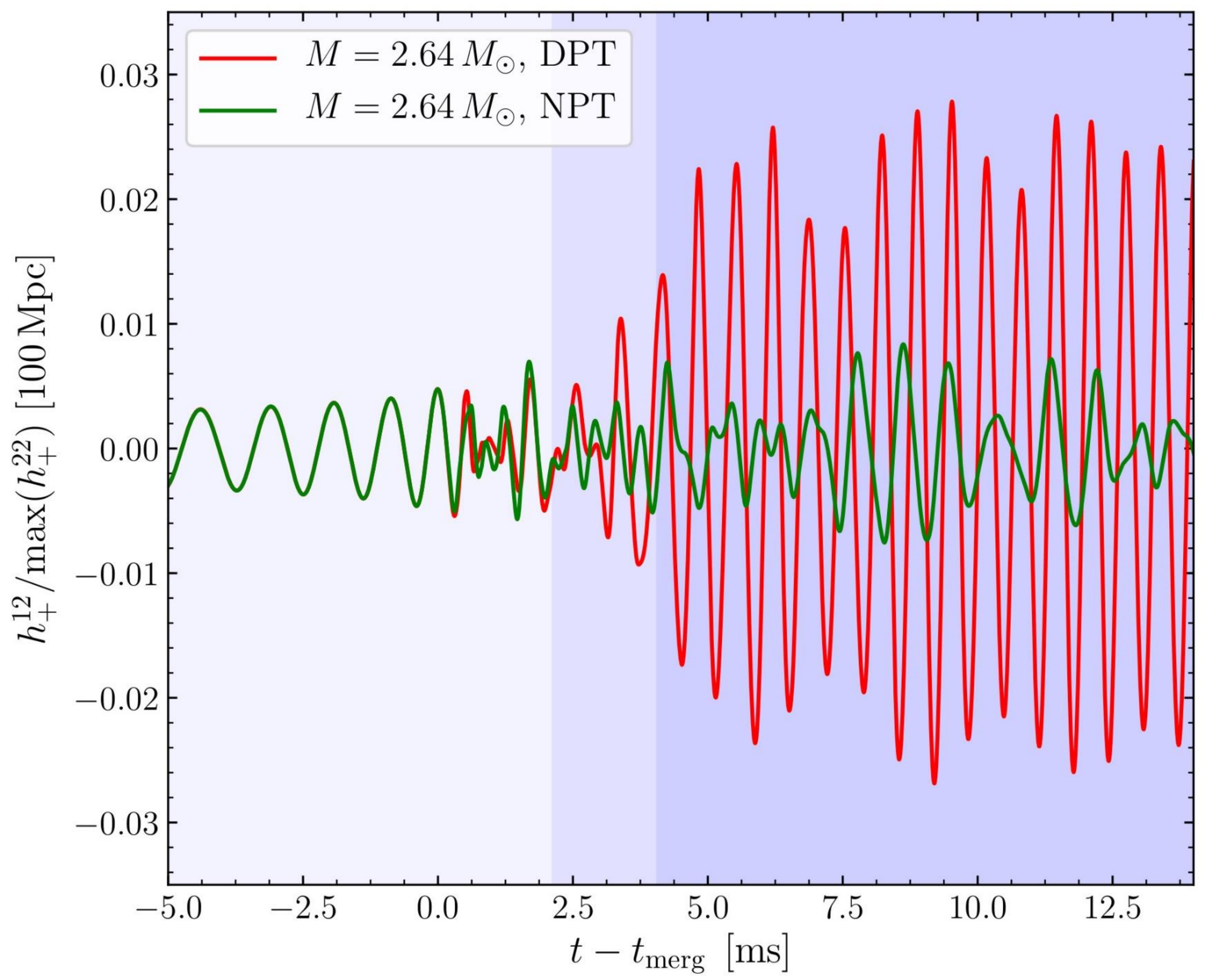

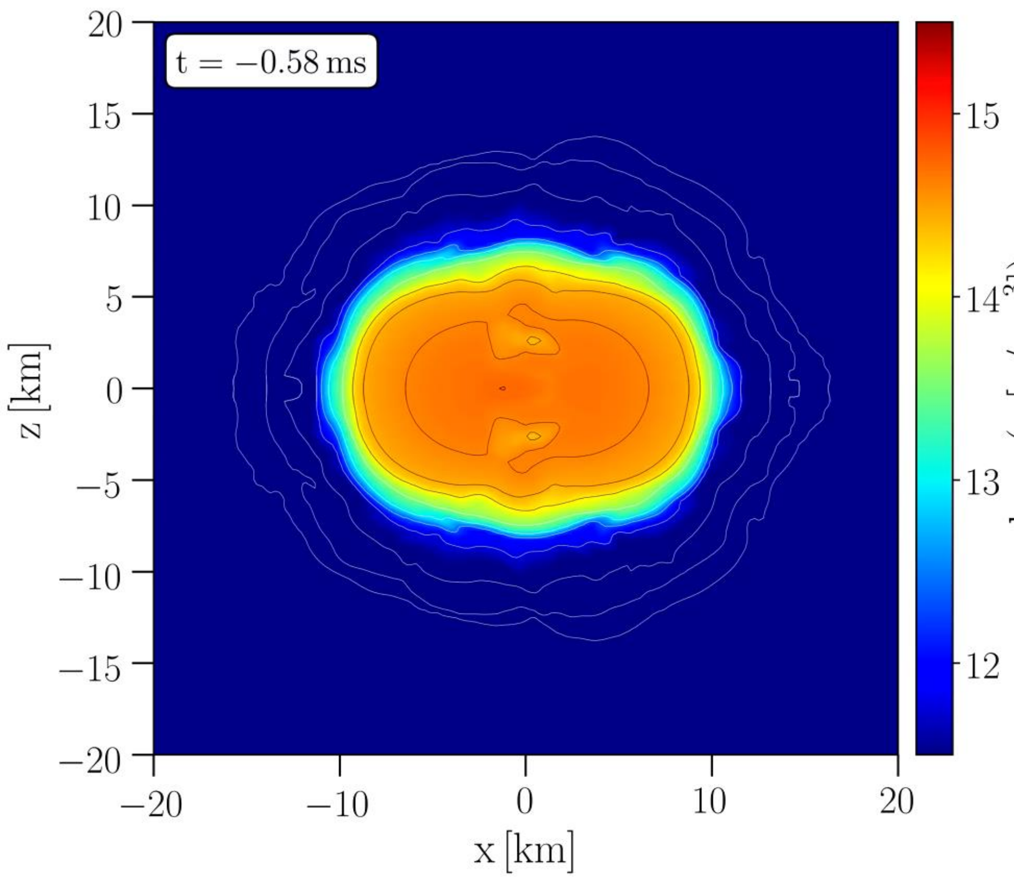

Due to the large m=1 mode of the emitted gravitational wave in the DPT case, a qualitative difference to the NPT scenario might be observable in future by focusing on the h_+^{12} − gravitational wave mode during the post-merger evolution.

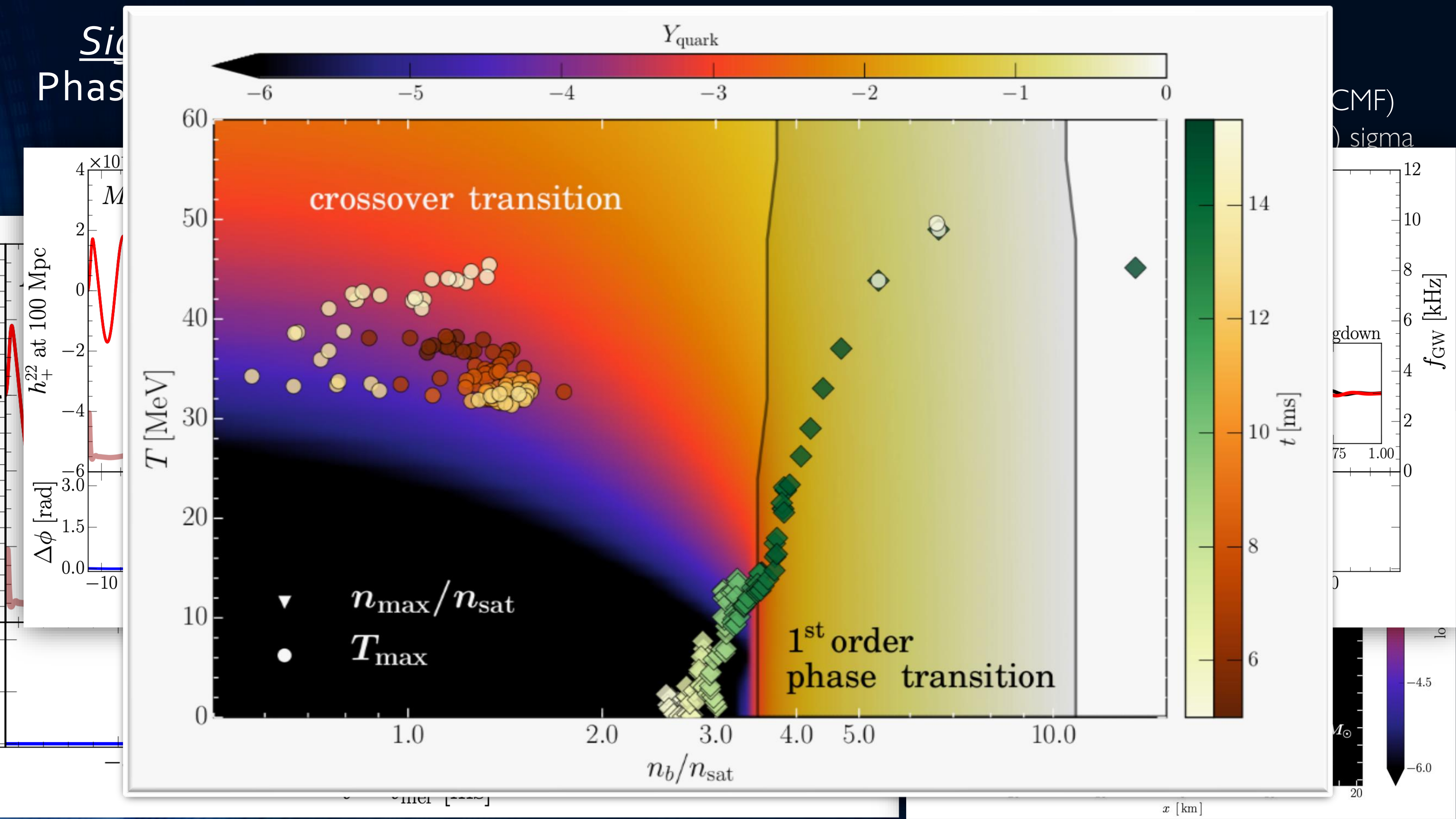

$Y_{\rm quark}$
−6 −5 −4 −3 −2 −1 0
crossover transition
1st order phase transition
$n_{\rm max}/n_{\rm sat}$
$T_{\rm max}$
T [MeV]
$n_b/n_{\rm sat}$
t [ms]
1.0 2.0 3.0 4.0 5.0 10.0
0 10 20 30 40 50 60
6 8 10 12 14
h_+^{22} at 100 Mpc
$\Delta\phi$ [rad]
$f_{\rm GW}$ [kHz]
x [km]

Phase-transition triggered collapse scenario

Signatures of quark-hadron phase transitions in general-relativistic neutron-star mergers

ER Most, LJ Papenfort, V Dexheimer, M Hanauske, S Schramm, H Stöcker and L. Rezzolla

Physical review letters 122 (6), 061101 (2019)

Density-Temperature-Composition dependent EOS within the CMFQ model.

Details see talk by V. Dexheimer (Sat. 9 am)

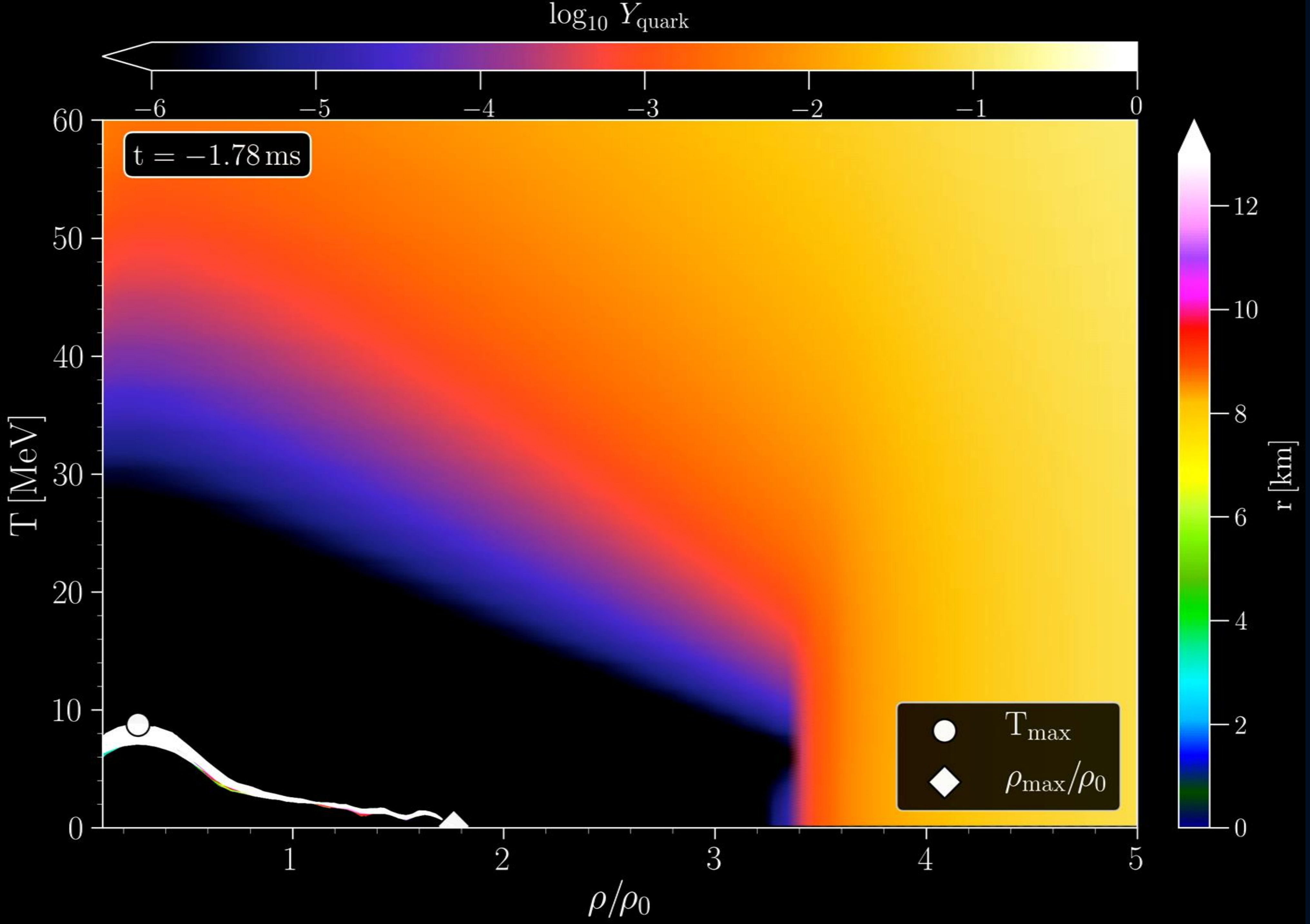

The last sim... r (HMHS)

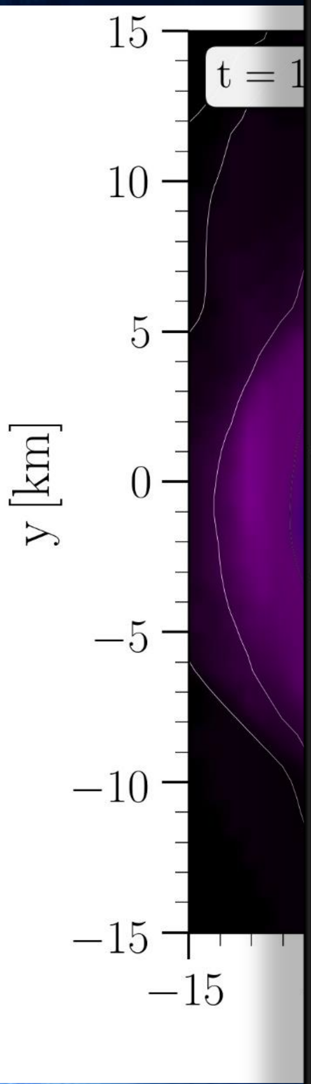

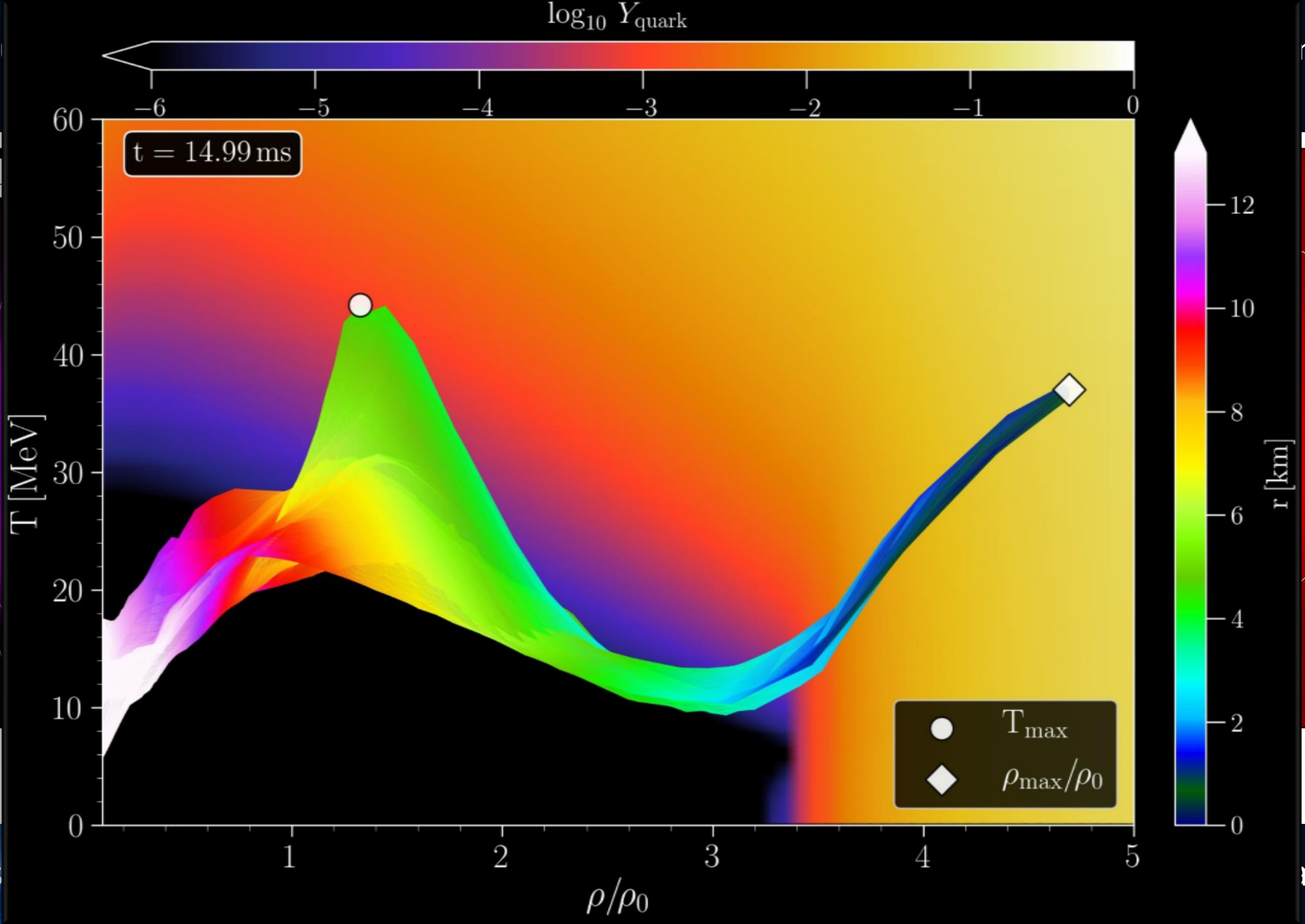

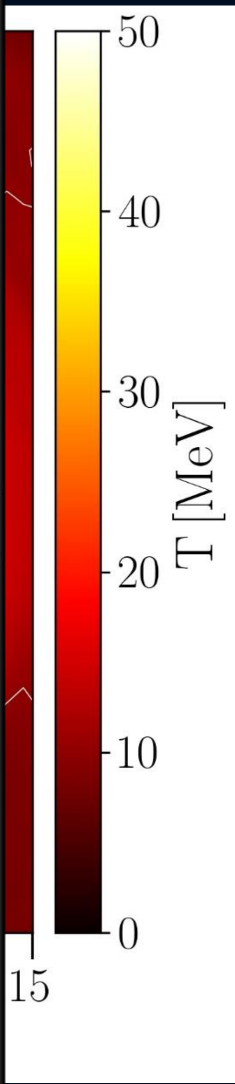

Rest mas... ane

The last sim … (HMHS)

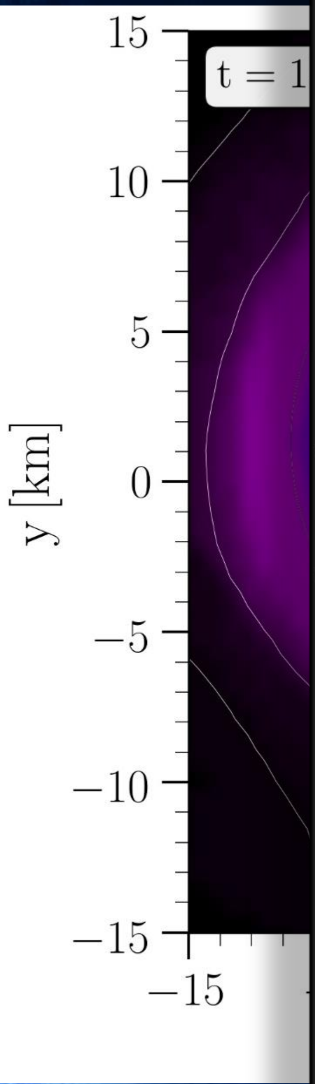

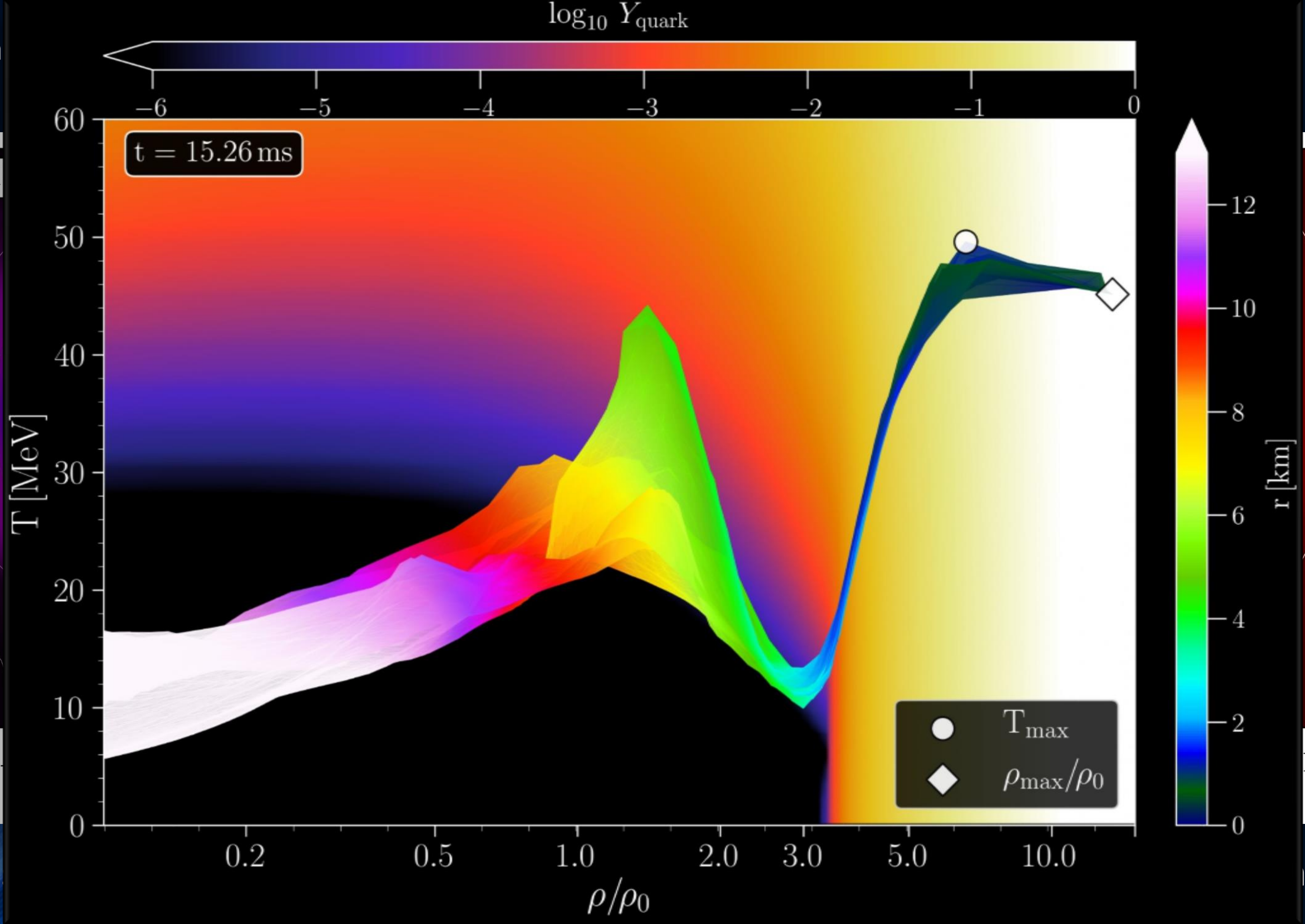

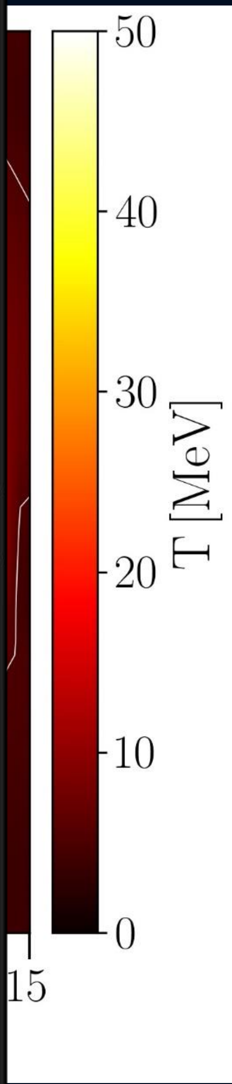

Rest mas… ne

The Strange Bird Plot

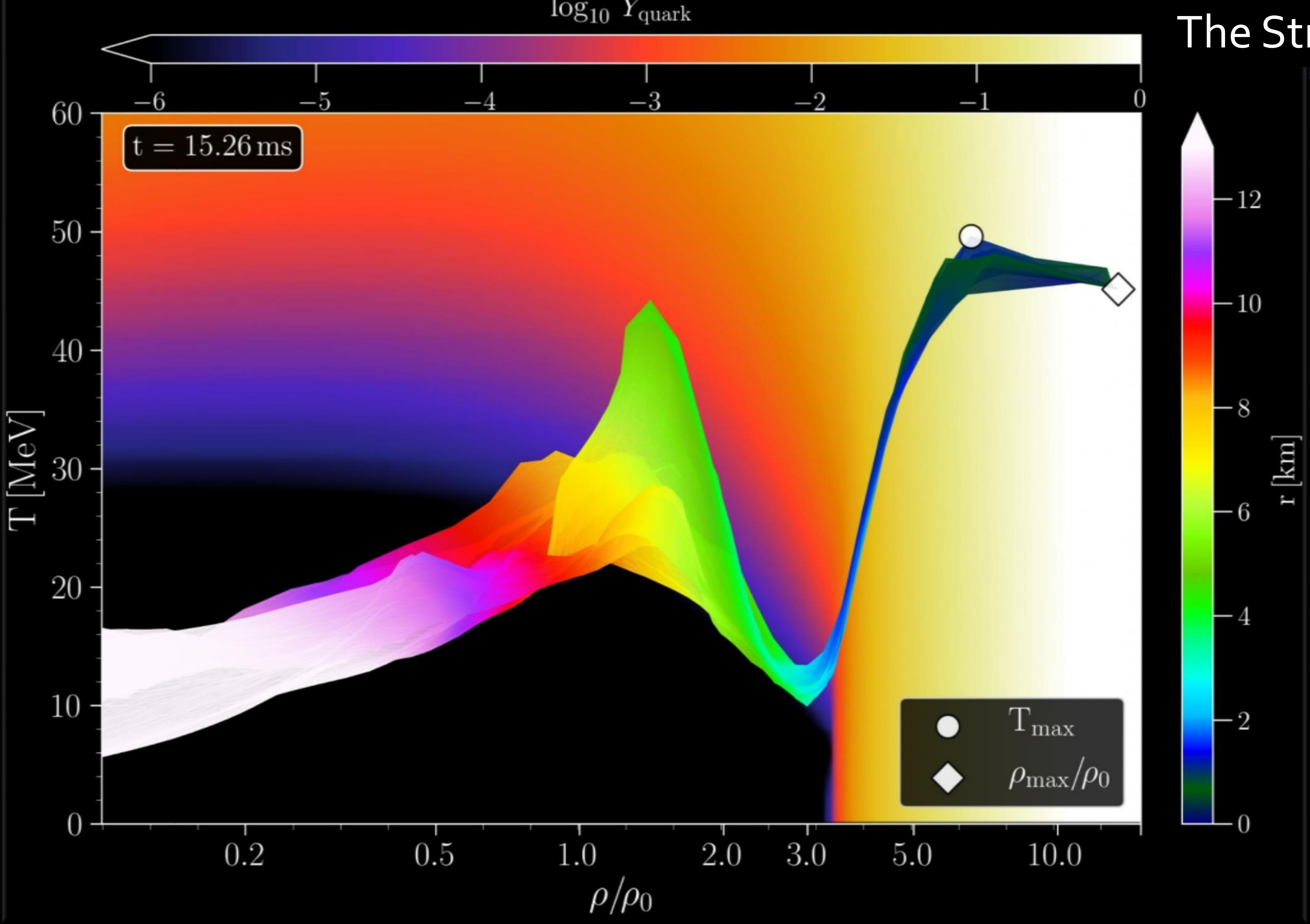

While the quarks in the pelican's head have already rescued themselves from their confinement cage, his body still largely consists of hadronic particles. It is precisely at this point in time that the apparent horizon is formed around the dense and hot head of the strange bird and the free strange quark matter is macroscopically confined by the formation of the black hole.

- Additional Slides

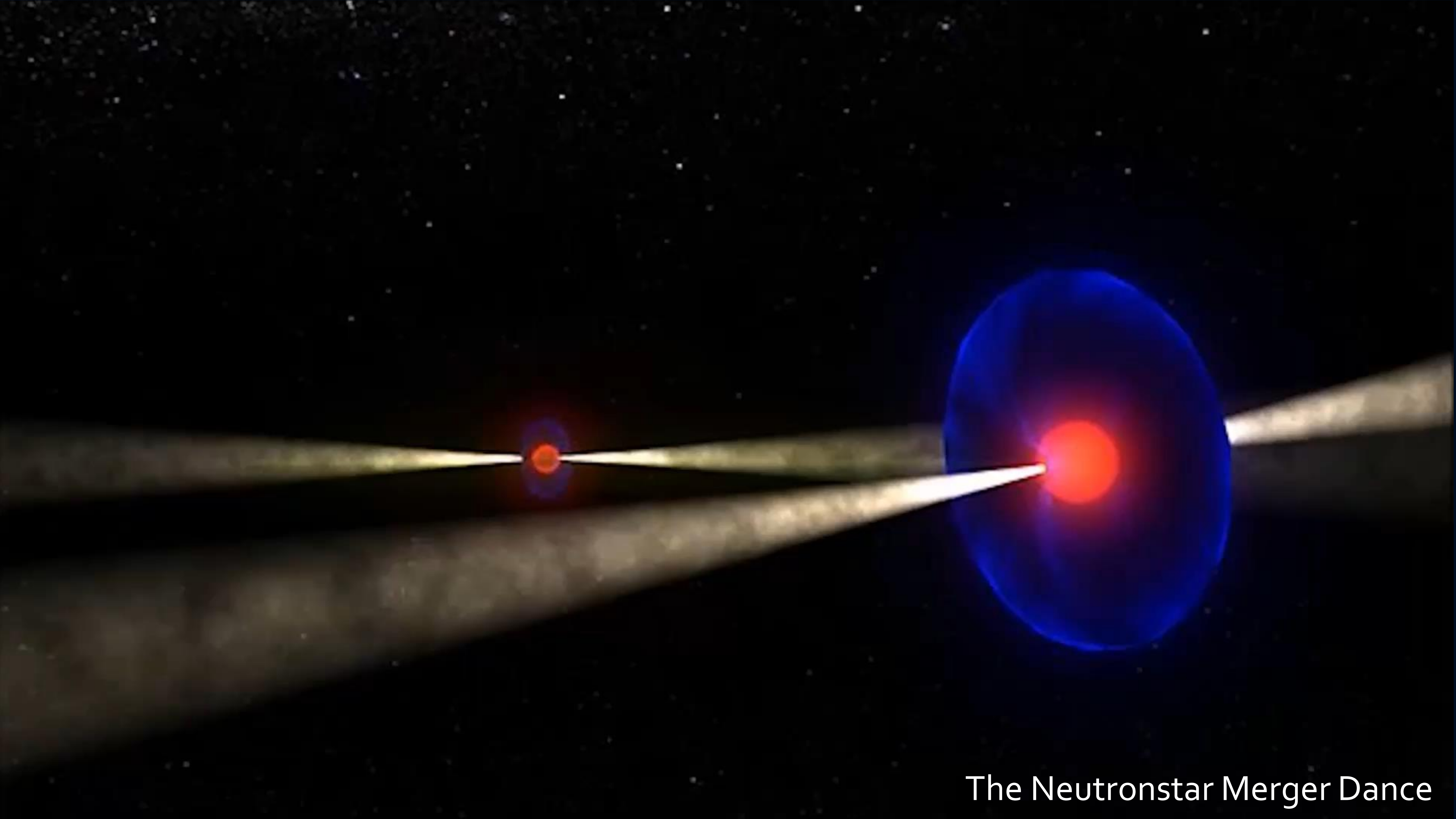

The Neutronstar Merger Dance

arXiv:1912.09340v1

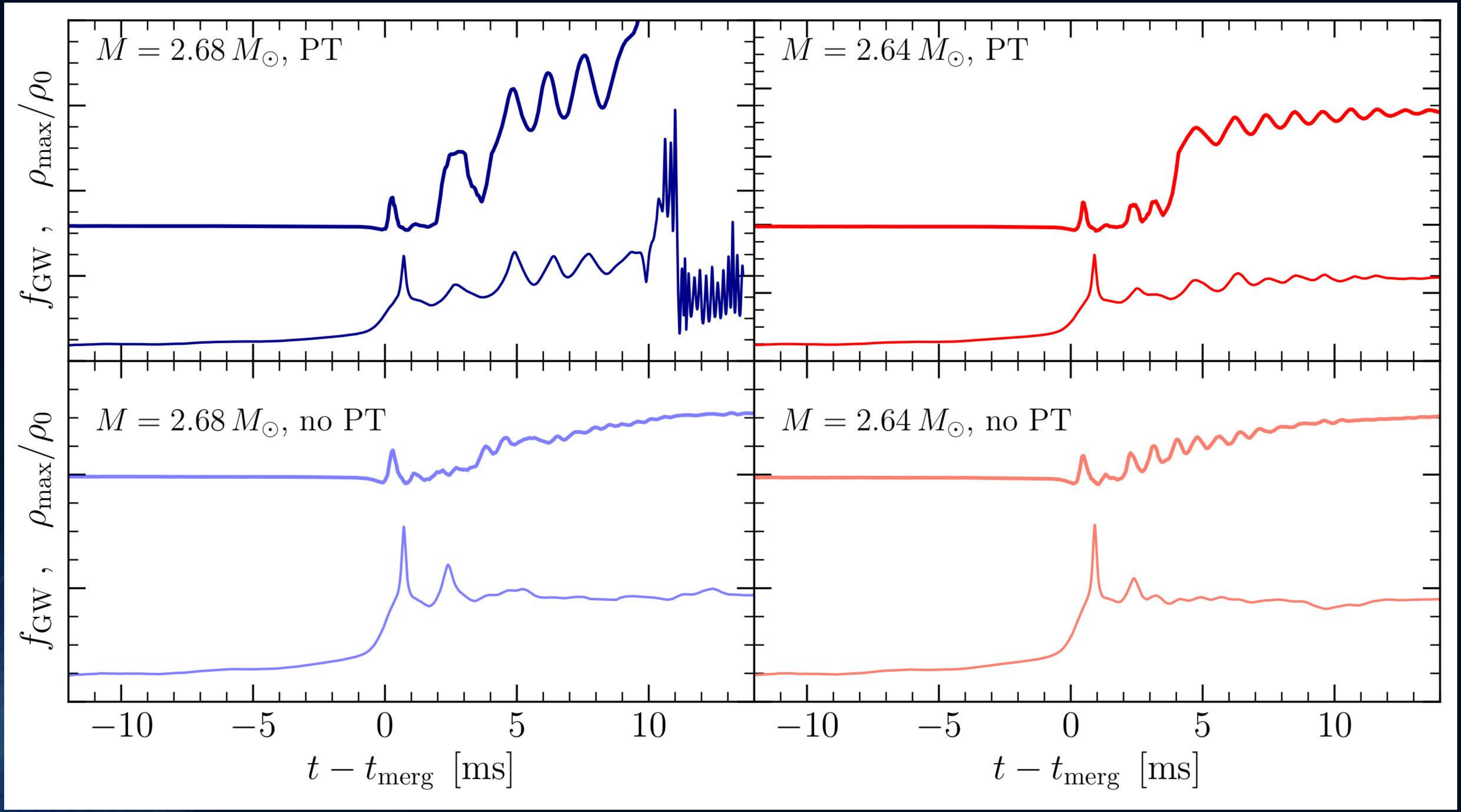

Evolution of the central rest-mass density (top) and instantaneous gravitational wave frequency (bottom).

arXiv:1912.09340v1

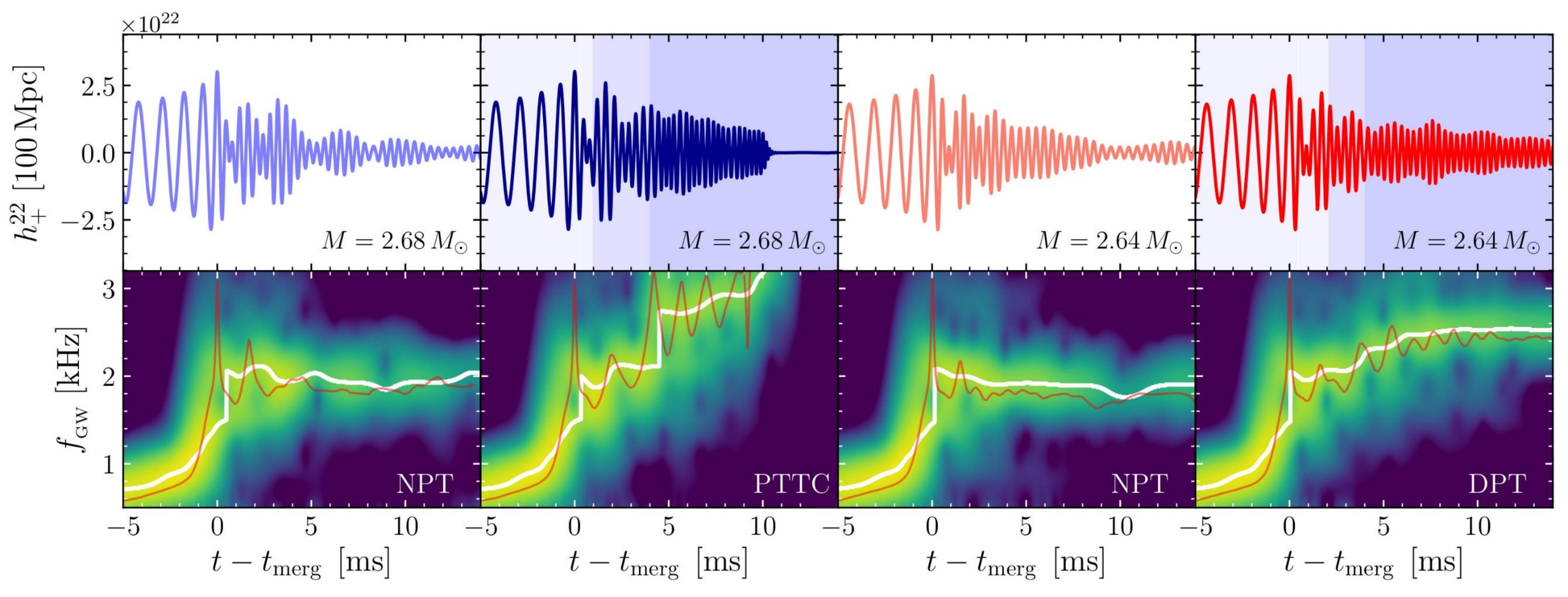

Strain h+ (top) and its spectrogram (bottom) for the four BNSs considered. In the top panels the different shadings mark the times when the HMNS core enters the mixed and quark phases the NPT models are always purely hadronic. In the bottom panels, the white lines trace the maximum of the spectrograms, while the red lines show the instantaneous gravitational-wave frequency.

The different Phases during the Postmergerphase of the HMNS

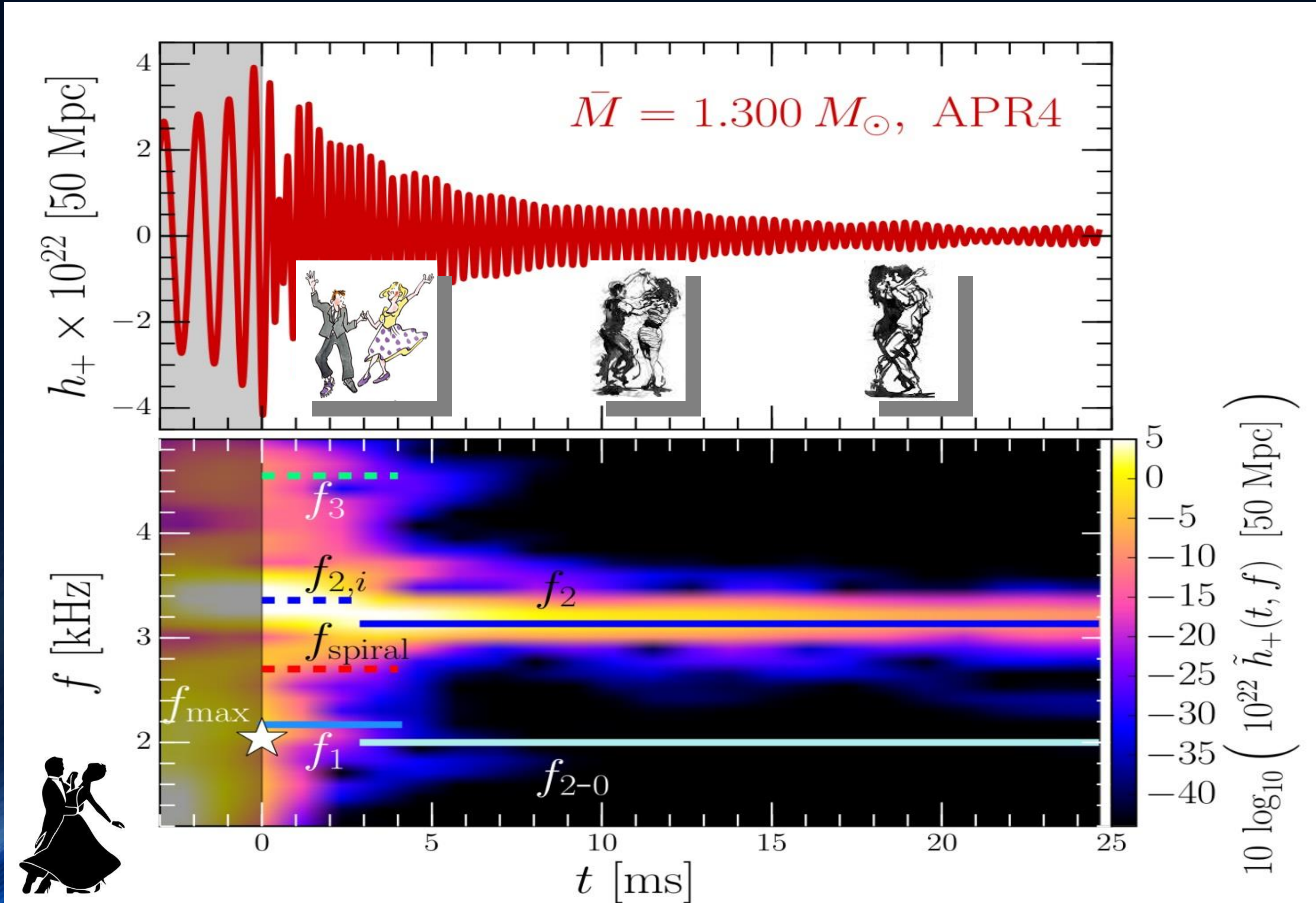

Time Evolution of the GW-Spectrum

The power spectral density profile of the post-merger emission is characterized by several distinct frequencies. Approximately 5 ms after merger, the only remaining dominant frequency is the f_2-frequency (see e.g. L.Rezzolla and K.Takami, PRD, 93(12), 124051 (2016))

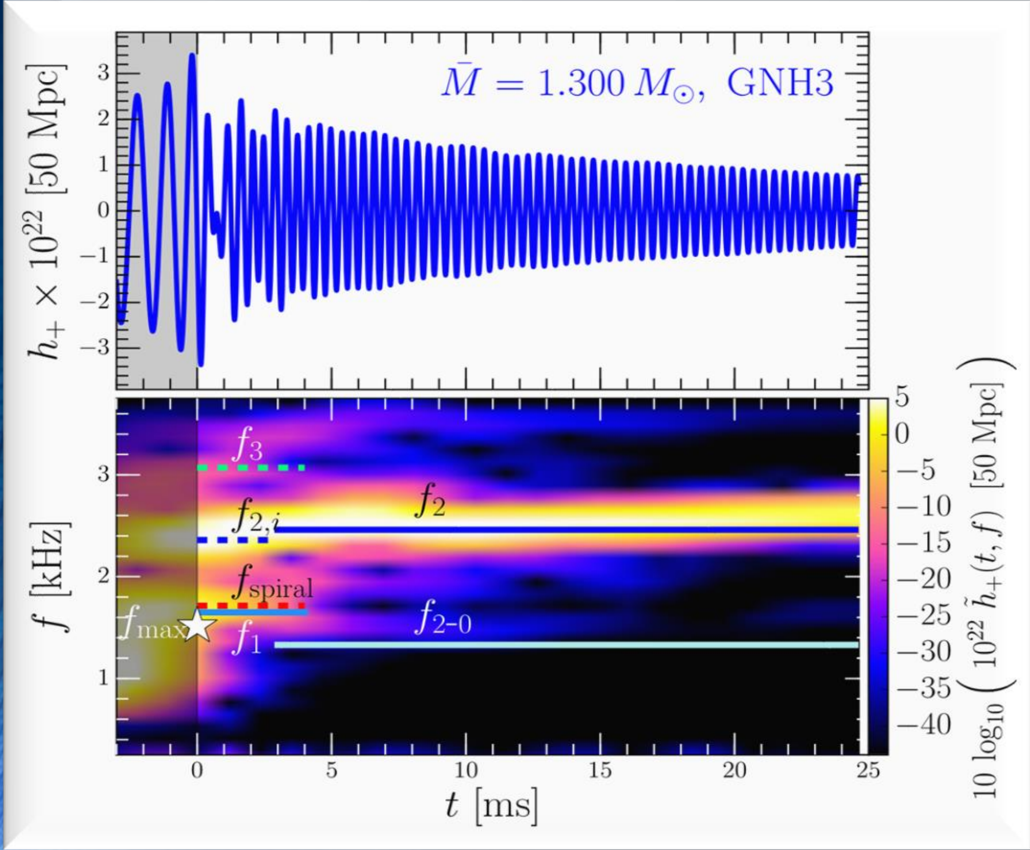

Stiff EOS

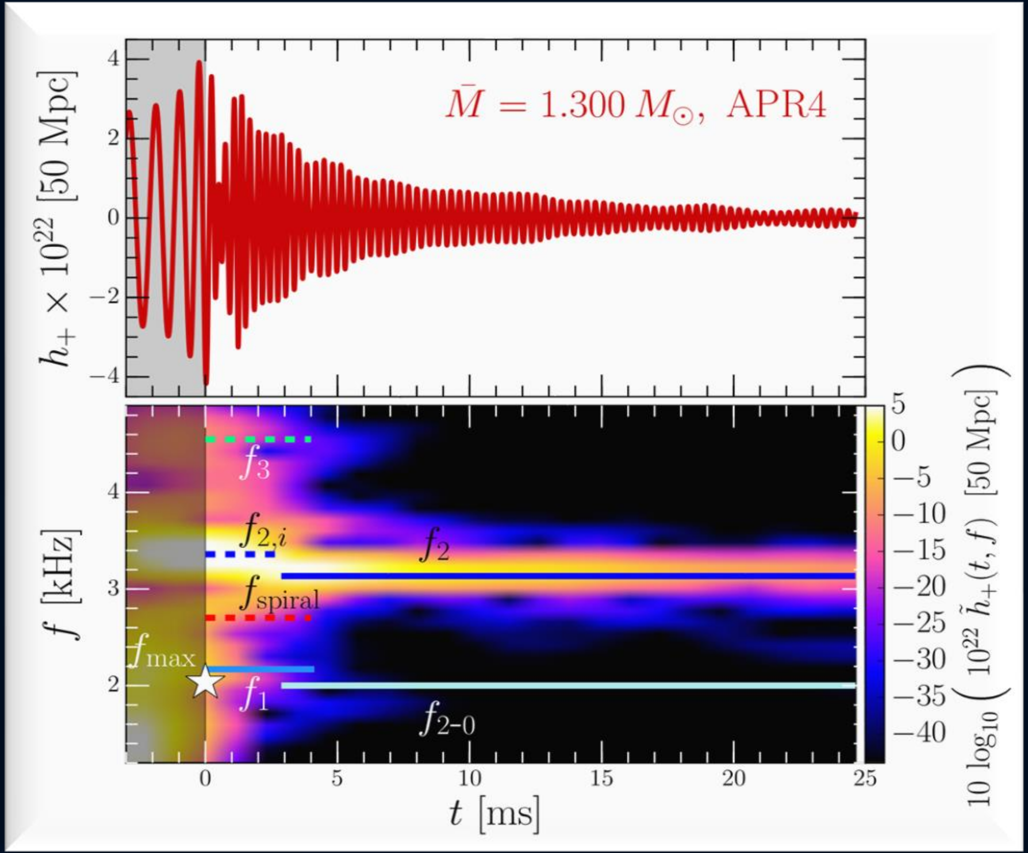

Soft EOS

Unfortunately, clow sensitivity at high gravitational wave frequencies, no post-merger signal has been found in GW170817.

But advanced detectors / next-generation detectors might be able to detect!!?

Evolution of the frequency spectrum of the emitted gravitational waves for the stiff GNH3 (left) and soft APR4 (right) EOS.

A new approach to constrain the EOS

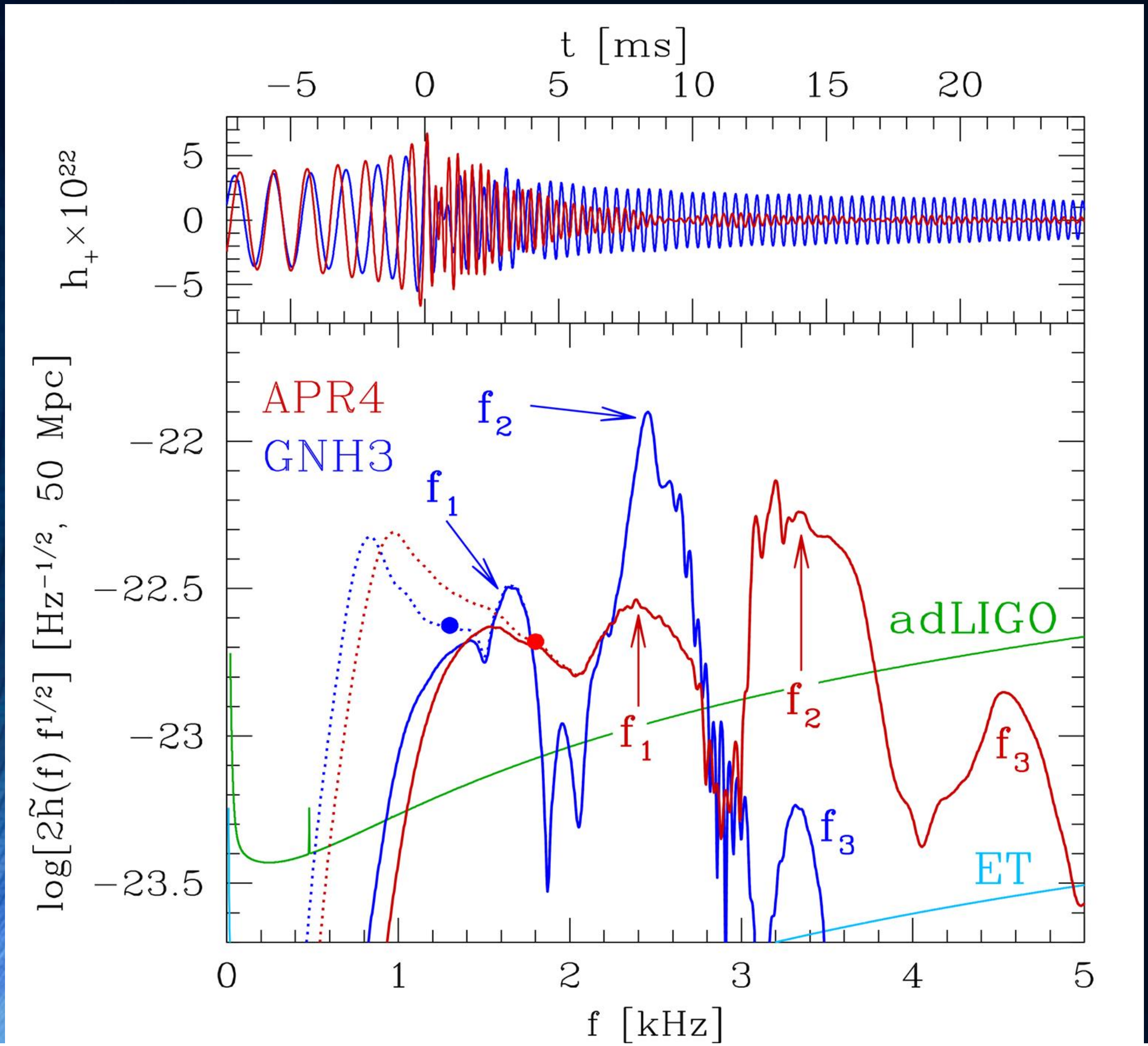

Kentaro Takami, Luciano Rezzolla, and Luca Baiotti, Physical Review D 91, 064001 (2015)

Hotokezaka, K., Kiuchi, K., Kyutoku, K., Muranushi, T., Sekiguchi, Y. I., Shibata, M., & Taniguchi, K. (2013). Physical Review D, 88(4), 044026.

Bauswein, A., & Janka, H. T. (2012). Physical review letters, 108(1), 011101.

Clark, J. A., Bauswein, A., Stergioulas, N., & Shoemaker, D. (2015). arXiv:1509.08522.

Bernuzzi, S., Dietrich, T., & Nagar, A. (2015). Physical review letters, 115(9), 091101.

Oechslin+2007, Baiotti+2008, Bauswein+ 2011, 2012, Stergioulas+ 2011, Hotokezaka+ 2013, Takami 2014, 2015, Bernuzzi 2014, 2015, Bauswein+ 2015, Clark+ 2016, Rezzolla+2016, de Pietri+ 2016, Feo+ 2017, Bose+ 2017 …

Post-merger gravitational-wave signatures of phase transitions in binary compact star mergers

PRL 124, 171103 (2020)

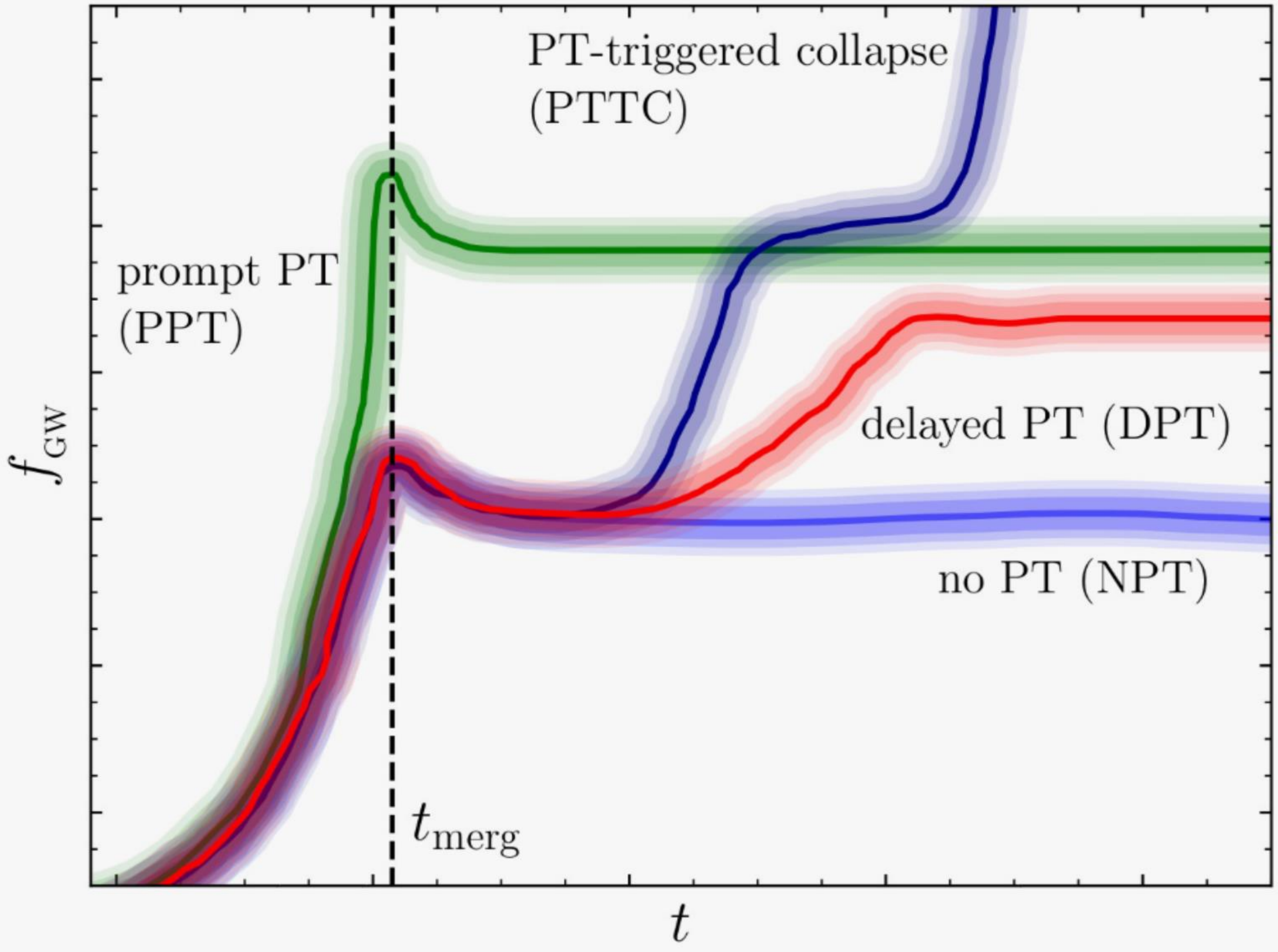

Schematic overview of the instantaneous gravitational wave frequency and how its evolution can be used to classify the different scenarios associated with a hadron-quark phase transition.

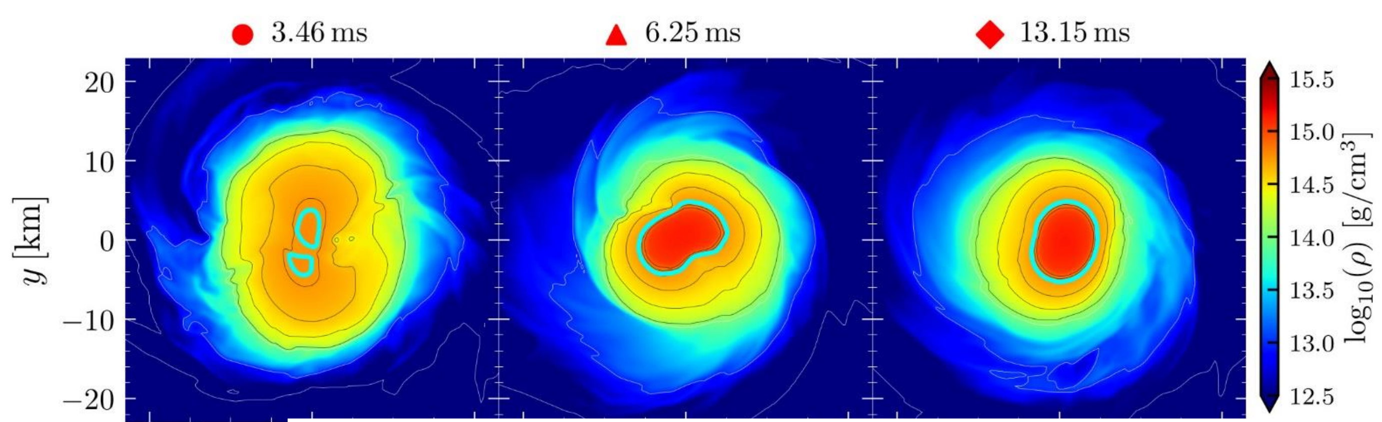

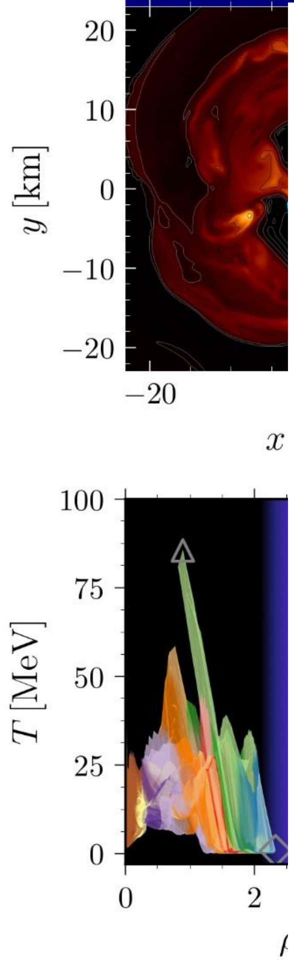

Article submitted (under review)

EPJ Special Topics on "Nuclear Astrophysics in Our Time: Supernovae, Neutron Stars and Binary Neutron Star Mergers"

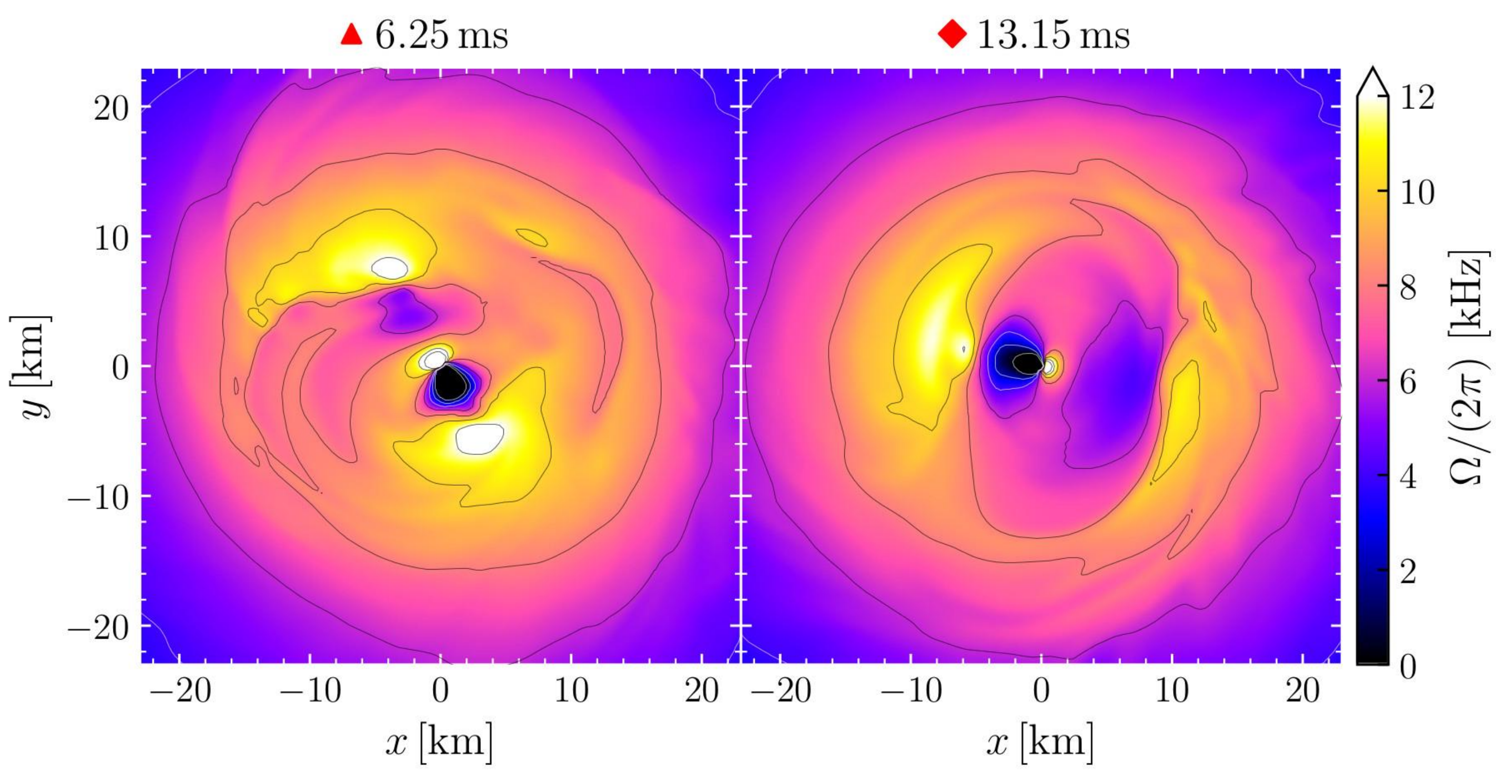

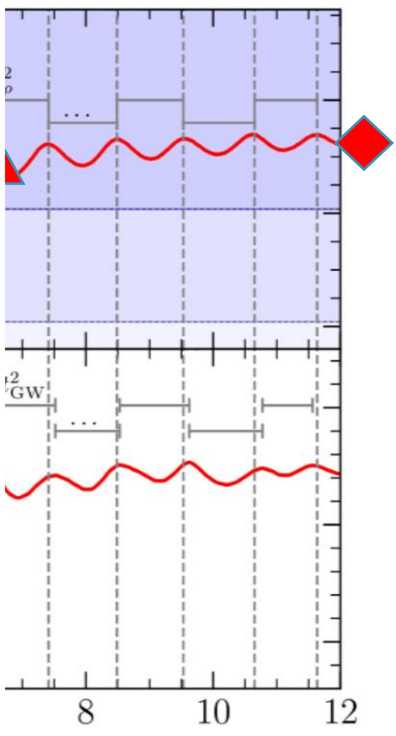

Fig. 4. Angular velocity for two representative times. Contours are drawn for $\Omega \in [0, 2, 4]$ kHz (white) and $\Omega \in [6, 8, 10, 12, 14]$ kHz (black).

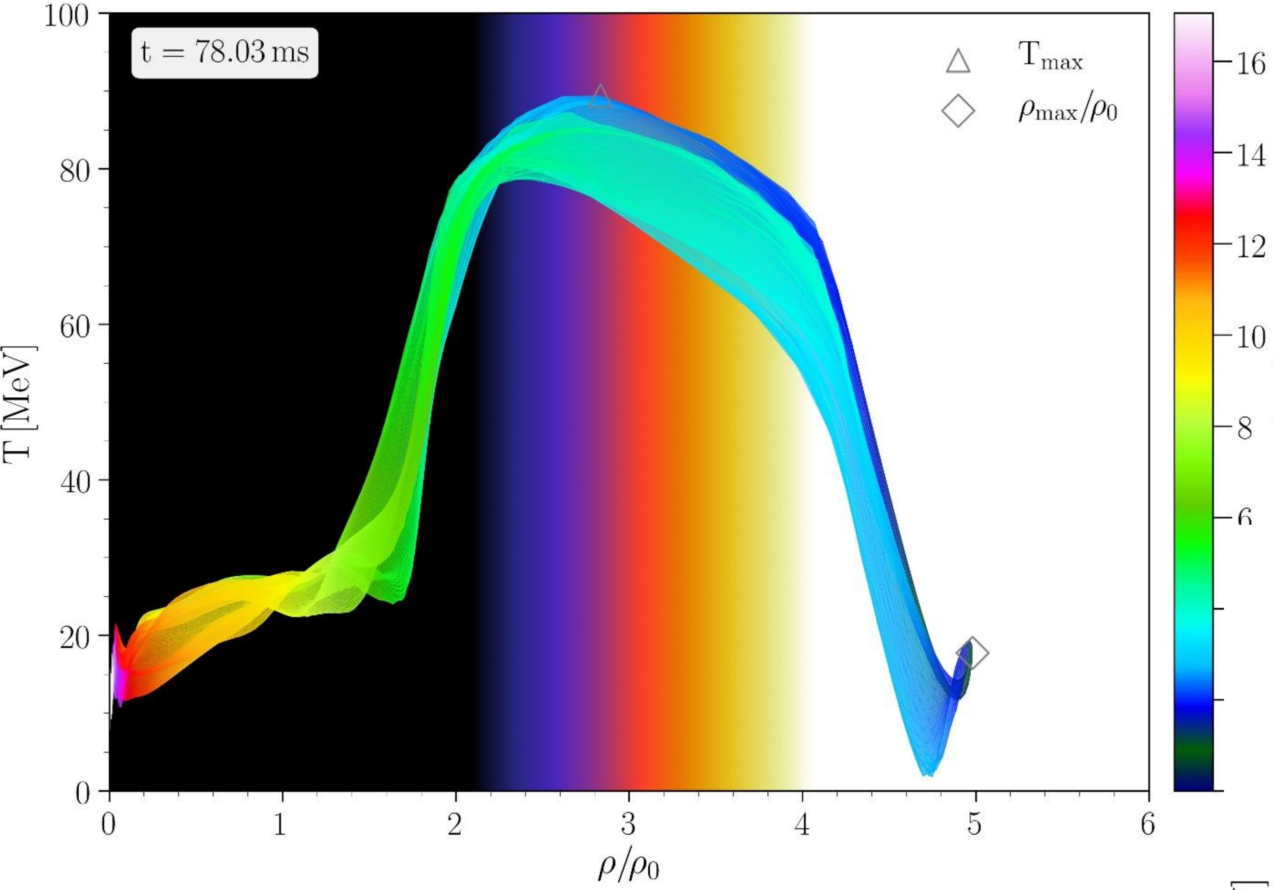
t = 78.03 ms
T_{max}
ρ_{max}/ρ_0
T [MeV]
ρ/ρ_0

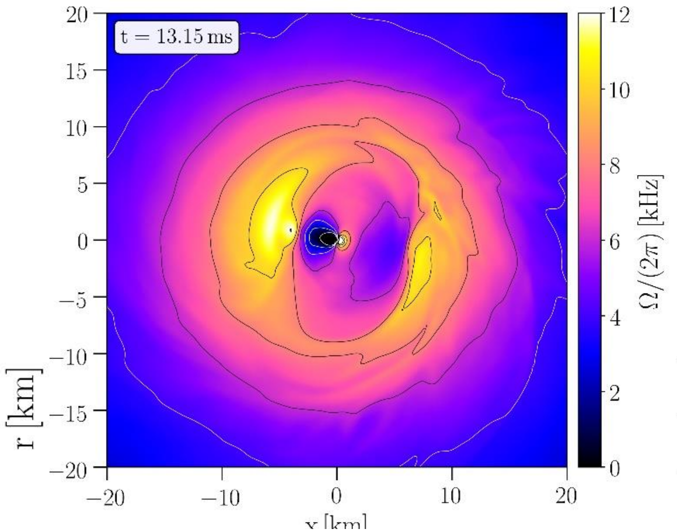
t = 13.15 ms
$\Omega/(2\pi)$ [kHz]
r [km]

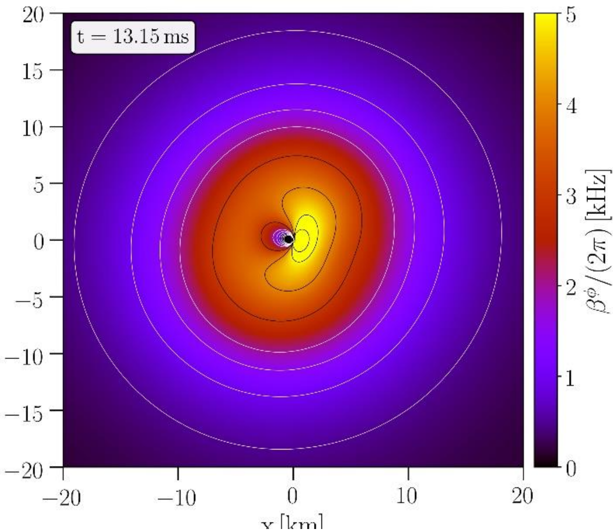
t = 13.15 ms
$\beta^\phi/(2\pi)$ [kHz]

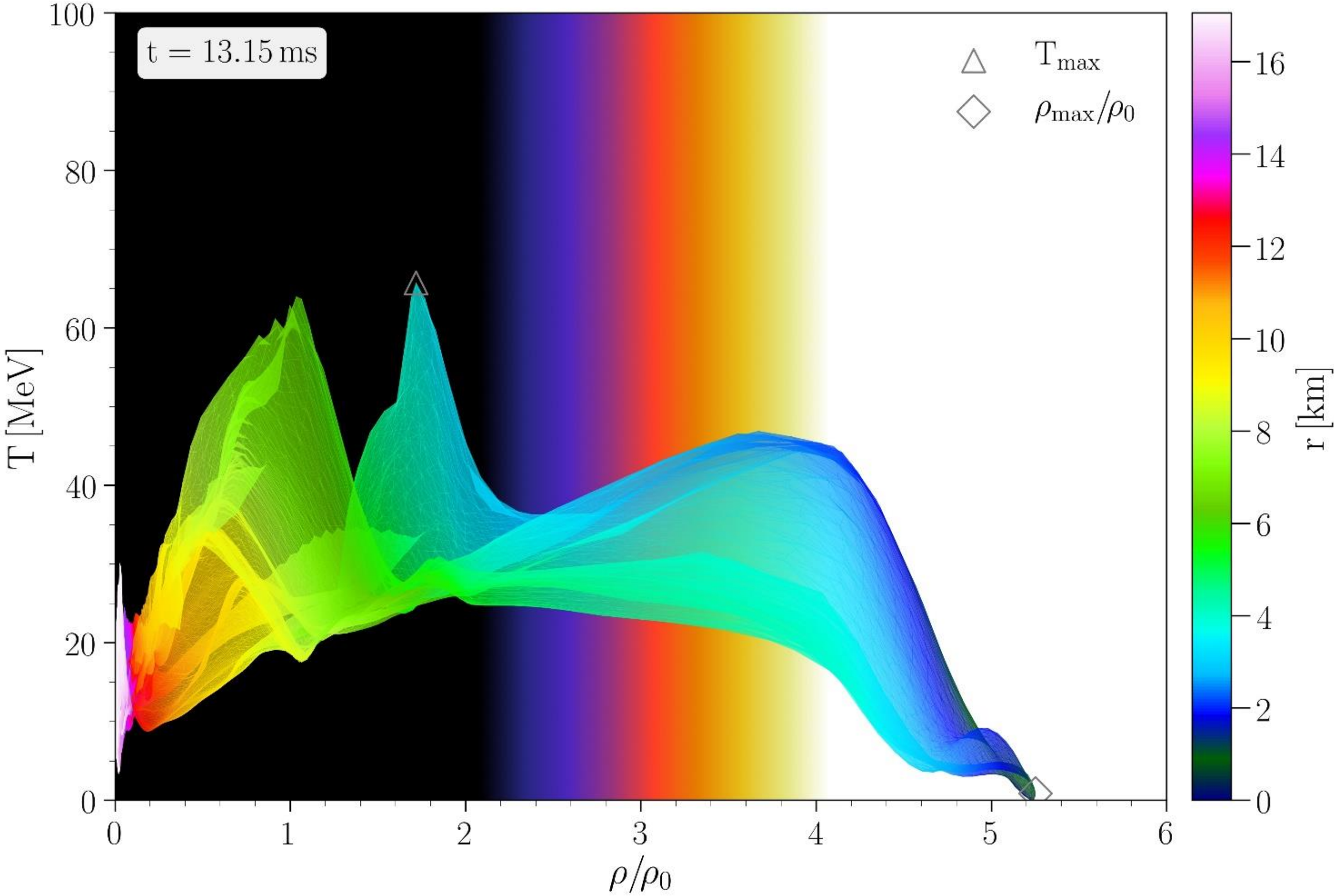
t = 13.15 ms
T_{max}
ρ_{max}/ρ_0
T [MeV]
ρ/ρ_0
r [km]

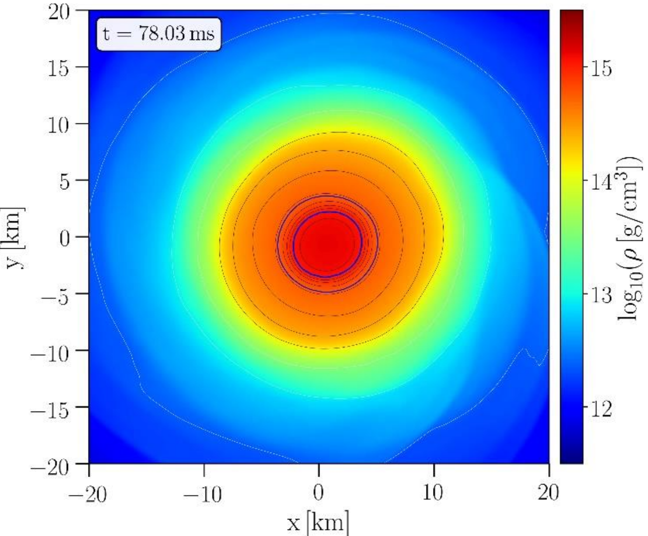
t = 78.03 ms
y [km]
x [km]
$\log_{10}(\rho\,[\mathrm{g/cm^3}])$

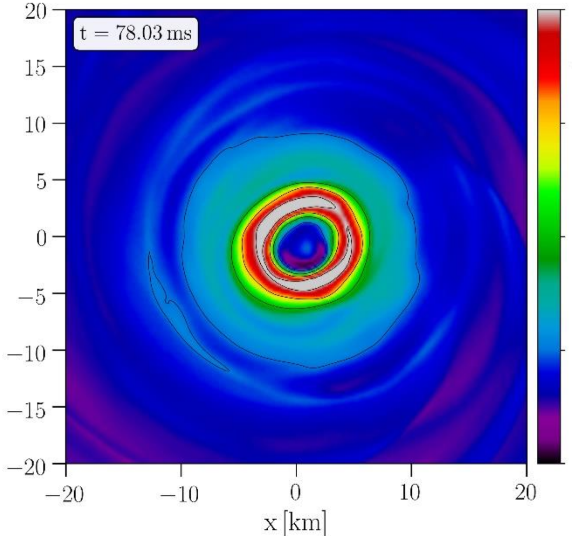
t = 78.03 ms
x [km]

The Angular Velocity in the (3+1)-Split

The angular velocity Ω in the (3+1)-Split is a combination of the lapse function α , the ϕ-component of the shift vector β^{ϕ} and the 3-velocity v^{ϕ} of the fluid (spatial projection of the 4-velocity **u**):

$$\Omega(x, y, z, t) = \frac{u^{\phi}}{u^{t}} = \alpha\, v^{\phi} - \beta^{\phi}$$

Angular velocity Ω

Lapse function α

Φ-component of 3-velocity v^{φ}

Frame-dragging β^{φ}

(3+1)-decomposition of spacetime:

$$g_{\mu\nu} = \begin{pmatrix} -\alpha^2 + \beta_i \beta^i & \beta_i \\ \beta_i & \gamma_{ij} \end{pmatrix}$$

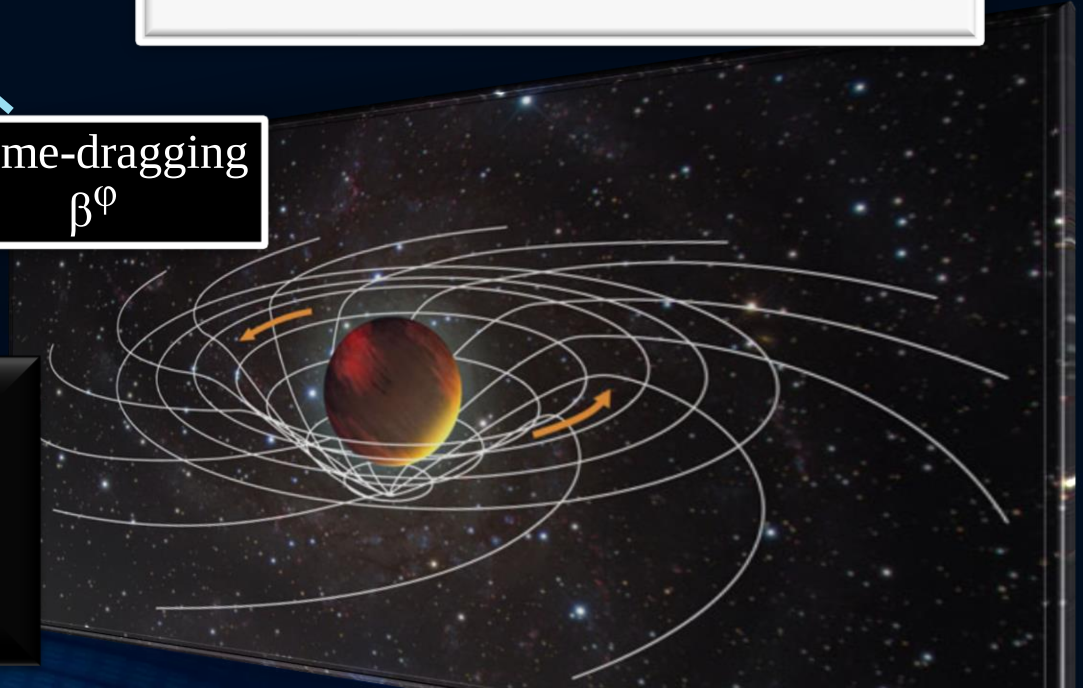

Focus: Inner core of the differentially rotating HMNS

M. Shibata, K. Taniguchi, and K. Uryu, Phys. Rev. D 71, 084021 (2005)
M. Shibata and K. Taniguchi, Phys. Rev. D 73, 064027 (2006)
F. Galeazzi, S. Yoshida and Y. Eriguchi, A&A 541, p. A156 (2012)
W. Kastaun and F. Galeazzi, Phys. Rev. D 91, p. 064027 (2015)

Time-averaged Rotation Profiles of the HMNSs

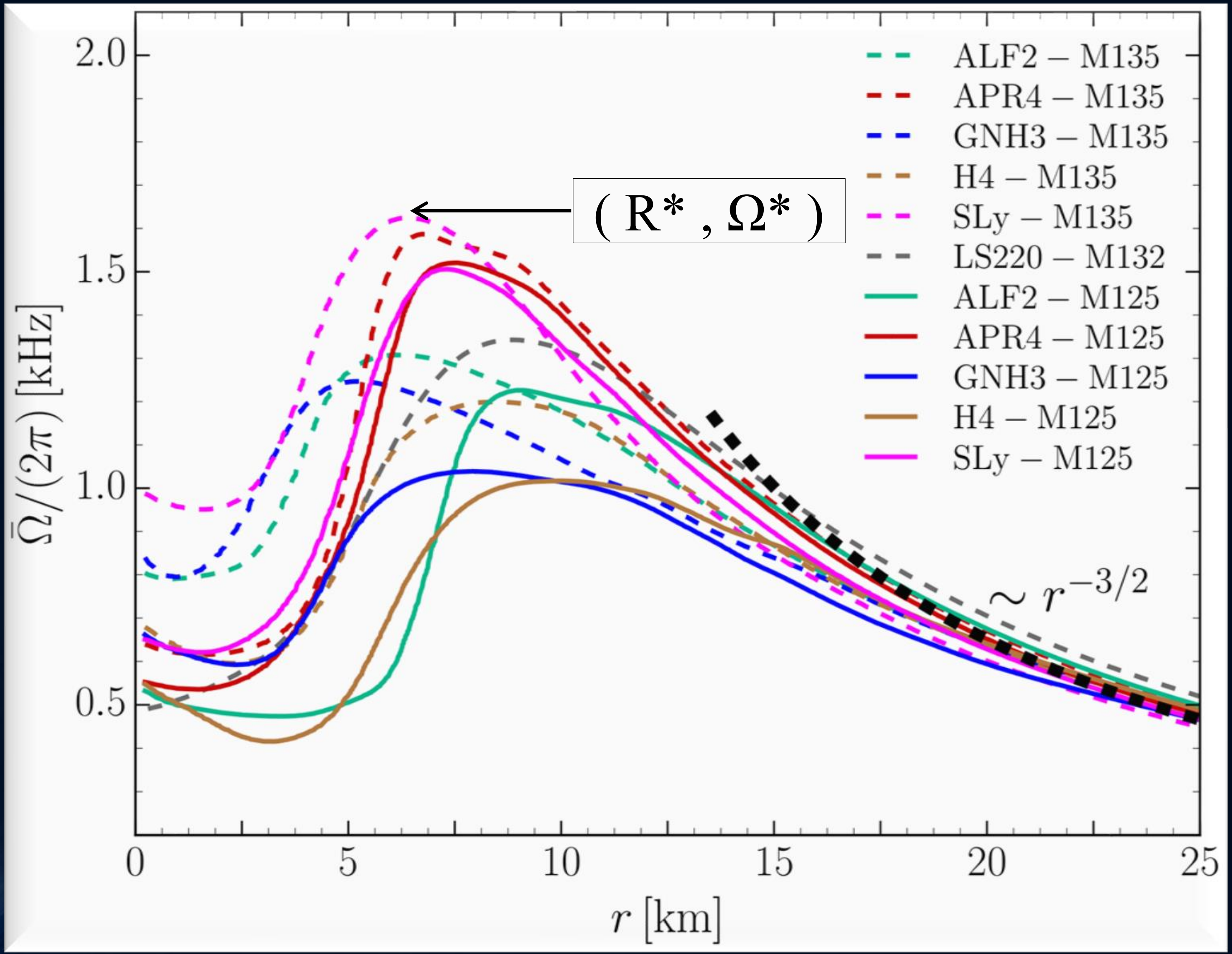

Soft EoSs:
Sly
APR4

Stiff EoSs:
GNH3
H4

Time-averaged rotation profiles for different EoS
Low mass runs (solid curves), high mass runs (dashed curves).

Hanauske, et.al. PRD, 96(4), 043004 (2017)

How to detect the hadron-quark phase transition with gravitational waves

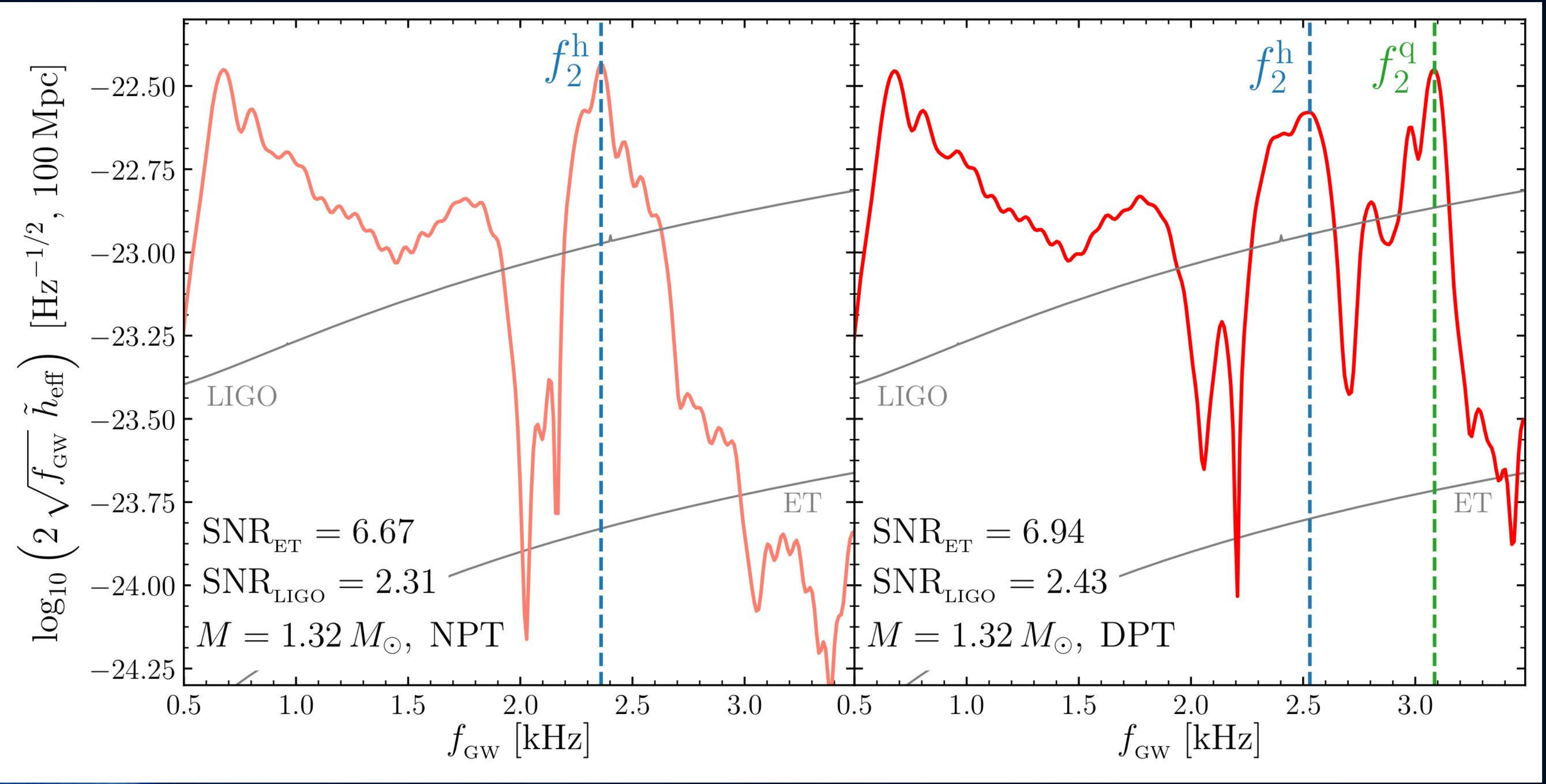

Total gravitational wave spectrum (left NPT, right DPT), PRL 124, 171103 (2020)